10-1-2010

The Human in 3D: Advanced Morphometric Analysis of High-Resolution Anatomically Accurate Computed Models

Summer J. Decker
University of South Florida

The Human in 3D: Advanced Morphometric Analysis of High-Resolution Anatomically Accurate Computed Models

by

Summer J. Decker

A dissertation in partial fulfillment
of the requirements for the degree of
Doctor of Philosophy
Department of Pathology and Cell Biology
College of Medicine
University of South Florida

Major Professor: Don Hilbelink, Ph.D.
Jacqueline Lee, M.D.
Karl Muffly, Ph.D.
Sudeep Sarkar, Ph.D.

Date of Approval:
October 1, 2010

Keywords: three dimensional, medical imaging, virtual anatomy, morphometrics

DEDICATION

I would like to dedicate this dissertation to my parents, Gary and Diana Decker of Jacksonville, Florida who have always believed in me, especially when I didn't. You have always been there to pick me up when I got knocked down. I am who I am, and where I am because of you. This year has been a whirlwind of momentous events. I am most happy and proud to end the year with functioning kidneys, your room full of books, advanced nursing degrees, a hidden Hammock and another Dr. Decker in the family. I would also like to dedicate this work to my partner in crime, Jonathan. I am forever in your debt for so many reasons. I look forward to our team's next adventure with a twinkle in my eye.

ACKNOWLEDGMENTS

I would first like to thank my mentor, Dr. Don Hilbelink for his unwavering support and enthusiasm over the past 4 years. You took an anthropologist and helped me become a professional anatomist. I finish this work because of your backing, guidance and friendship. I can't wait to see what's next. Additionally, I would like to thank Dr. Karl Muffly for being a great Devil's Advocate and sounding board. I am grateful to my other dissertation committee members, Dr. Jacqueline Lee, Dr. Anshuman Razdan, and Dr. Sudeep Sarkar for their time and patience throughout this entire process. This was a better project with all of your input. I would also like to thank Dr. Patricia Kruk for her encouragement throughout the program. I would also like to thank the entire Hilbelink family (Dr. Amy Hilbelink, Garrett and Hannah) for adopting our lab and treating us like family. I would like to thank all my family and friends for their encouragement and patience while listening to me ramble on about 3D models throughout graduate school. A special thank you to Vegas for her patience during all the late nights and weekends with me hunched over a computer. Those puppy kisses got me through. Lastly, I would like to thank Dr. Stephanie Davy-Jow, our research partner, teammate, and my dear friend for all her invaluable input and for all the morning rant sessions online. Our team is going to set the world on fire.

TABLE OF CONTENTS

LIST OF FIGURES iv

LIST OF TABLES vi

ABSTRACT viii

CHAPTER 1: INTRODUCTION 1
- Anatomy 2
- Descriptive Anatomy 2
- Traditional Metric Methodologies 3
- Landmark Data and Morphometric Analyses 6
- 3D Volumetric Data 9
- Quantitative Anatomy 12
- Specific Aims this Dissertation 13
- Poster, Podium Presentations, Journal Articles and Book Chapter 14
- Dissertation Outline 14

CHAPTER 2: ARTICLE I: VALIDATION OF VIRTUAL ANATOMY 17
- Abstract 17
- Introduction 18
- Materials and Methods 19
  - Medical Imaging 19
  - 3D Computer Reconstruction 20
  - Mimics 20
  - Osirix 23
  - Rapid Prototyping 26
  - Anthropological Measurements 27
  - Anthropology Skulls 29
  - Statistical Analysis 30
- Results 31
  - Image quality 31
  - 3D Computer Reconstruction Software 33
  - Anthropological Measurements 34
  - Cadaver Head Results 34
  - Anthropology Skulls Results 36
- Discussion and Conclusions 36
- Acknowledgments 38

CHAPTER 3: ARTICLE II: VIRTUAL DETERMINATION OF SEX: METRIC AND NON-METRIC TRAITS OF THE ADULT PELVIS FROM 3D COMPUTED TOMOGRAPHY (CT) MODELS 39
Abstract .....
Introduction 42
Materials and Methods 42
Clinical Pelves Radiological Scans 42
3D Computer Reconstruction 44
Virtual Sex Estimation: Osteological Measurements 46
Statistical Analysis 51
Fordisc 3.0 Analysis 54
Results 54
3D Modeling and Virtual Measurements 54
Sex Assessment 55
Discussion and Conclusions 58
Acknowledgments 63

CHAPTER 4: ARTICLE III: 3D MODELING AND MORPHOMETRIC ANALYSIS OF VIRTUAL CRANIAL ANATOMY 65
Abstract 65
Introduction 66
Materials and Methods 68
Cadaveric Head Radiological Scans 68
Increasing the Scan Resolution 68
Clinical Head Radiological Scans 69
Three-Dimensional (3D) Computer Reconstruction 70
Virtual Sex Estimation: Osteological Measurements 71
Statistical Analysis 77
Fordisc 3.0 Analysis 79
Results 80
3D Modeling and Virtual Measurements 80
Sex Assessment 80
Discussion and Conclusions 83
Acknowledgments 86

CHAPTER 5: ARTICLE IV: MAKING FACES: 3D MODELING OF CRANIOFACIAL ANATOMY 87
Abstract 87
Introduction 88
Phase I: Facial Approximation Challenge 89
Materials and Methods 91
Study Results 93
Clay Modeling 93
Visualization Specialist Wesley Neville 93
Sculptor Philippe Faraut 95
Virtual Modeling 96

FaceIT 96
FBI Virtual Method 99
Final Results 101
Phase II: Creating Virtual Faces 103
Materials and Methods 103
Cadaveric Soft Tissue Depth Measurements 103
Cadaveric and Clinical Radiological Scans 104
3D Computer Models of the Skull and Face 107
Virtual Soft Tissue Depth Measurements 109
Statistical Analysis 112
Results 113
3D Modeling and Virtual Measurements 113
Actual Pin Depths Versus Virtual Depth Measurements 114
Cadaveric Versus Clinical Facial Data 117
Discussion and Conclusions 119
Acknowledgments 124

CHAPTER 6: APPLICATIONS, RECOMMENDATIONS FOR FUTURE STUDY, AND CONCLUSIONS 126
Applications of Virtual Anatomy 126
Medicine 126
Forensics 133
Biometrics 134
Anatomical Education 135
Recommendations for Future Study 136
Conclusions 137

REFERENCES 139

APPENDICES 153
Appendix A – Articles 154
Appendix B – Book Chapter 155
Appendix C – Poster and Podium Presentations 156

ABOUT THE AUTHOR ..... End Page

LIST OF FIGURES

FIGURE 1.1: Skull with landmarks indicated 8

FIGURE 1.2: X-Ray image of leg 11

FIGURE 1.3: MRI image of pelvis 11

FIGURE 1.4: CT Image of head 11

FIGURE 2.1: 3D reconstruction of cadaver head in *Mimics* © 21

FIGURE 2.2: Isolated cadaver skull in *Mimics* © 21

FIGURE 2.3: Actual cadaver skull after defleshing process 22

FIGURE 2.4: 3D skeletal model of cadaver head made in *Osirix* © 23

FIGURE 2.5: 3D soft tissue model of cadaver head made in *Osirix* © 24

FIGURE 2.6: 3D soft tissue model of cadaver head made in *Osirix* © 24

FIGURE 2.7: Skull prototyping using Zcorp 3D Zprinter © 310 Plus 26

FIGURE 2.8: Virtual skull showing measurements taken 27

FIGURE 2.9: Examples of 3D virtual skulls from USF Anthropology 29

FIGURE 2.10: Screen capture of skull in “bone window” 31

FIGURE 2.11: Screen capture of skull in “lung window” 32

FIGURE 2.12: Anthropological measurements (in mm) of prototype, virtual, and actual skull 34

FIGURE 3.1: Images of a pelvic CT scan in the coronal view 43

FIGURE 3.2: Images of a pelvic CT scan in the sagittal view 43

FIGURE 3.3: A virtual image of the pelvis created from CT data in the anterior view 45

FIGURE 3.4: A virtual image of the pelvis created from CT data in the posterior view 46

FIGURE 3.5: *Mimics* user interface highlighting the 35 landmark points used for pelvimetric assessment indicated on the 2D pelvic mask as well as on the 3D model. 50

FIGURE 4.1: 3D model with measurements shown in the frontal view, in Frankfort Horizontal, and mandible. 73

FIGURE 5.1: Virtual facial muscles from the *FaceIT* technique 90

FIGURE 5.2: Frontal, sagittal and ¾ views of unknown living individual 92

FIGURE 5.3: Frontal and sagittal views of the prototype skull of living individual provided to clay reconstruction artists 92

FIGURE 5.4: Frontal, sagittal and ¾ views of Wesley Neville's clay reconstruction 94

FIGURE 5.5: Philippe Faraut's clay reconstruction 96

FIGURE 5.6: Frontal, sagittal and ¾ view of virtual reconstructions using the *FaceIT* technique 98

FIGURE 5.7: Frontal, sagittal, ¾, and obese views of virtual reconstruction using the FBI's virtual facial approximation 100

FIGURE 5.8: Frontal and sagittal views of actual living individual 102

FIGURE 5.9: 3D model of skull and face 108

FIGURE 5.10: 3D model with virtual soft tissue measurements shown 111

FIGURE 5.11: Error rates between actual and virtual depth measurements 116

FIGURE 5.12: Histogram of gray scale values of a cadaver scan 122

FIGURE 5.13: Histogram of gray scale values of a clinical scan 122

LIST OF TABLES

TABLE 2.1: List of 25 cranial measurements used in the study 28

TABLE 3.1: List of landmarks with definitions 48

TABLE 3.2: Measurement descriptions 49

TABLE 3.3: Measures of central tendencies 52

TABLE 3.4: Measurement error 53

TABLE 3.5: Four-variable model for sex estimation 56

TABLE 3.6: Accuracy of four-variable method 56

TABLE 3.7: Four-variable cross validation test 57

TABLE 3.8: Accuracy of *Fordisc 3.0* method 58

TABLE 4.1: List of landmarks with definitions 74

TABLE 4.2: Measurement descriptions 76

TABLE 4.3: Measures of central tendencies 78

TABLE 4.4: Seven-variable model for sex estimation 81

TABLE 4.5: Accuracy of seven-variable method 81

TABLE 4.6: Seven-variable cross validation test 82

TABLE 4.7: Accuracy of *Fordisc 3.0* method 82

TABLE 5.1: List of depth measurements and angles 110

TABLE 5.2: Measures of central tendencies (virtual male vs virtual female) 113

TABLE 5.3: Measures of central tendencies (actual pin depth vs virtual depth) 115

TABLE 5.4: Error rates between actual and virtual 116

TABLE 5.5: Measures of central tendencies (clinical vs cadaver)..... 118

TABLE 5.6: Four-variable cross validation test 119

The Human in 3D: Advanced Morphometric Analysis of High-Resolution Anatomically Accurate Computed Models

Summer J. Decker

ABSTRACT

Computed virtual models of anatomical structures are proving to be of increasing value in clinical medicine, education and research. With a variety of fields focused on craniofacial and pelvic anatomy there is a need for accurate anatomical models. Recent technological advancements in computer and medical imaging technologies have provided the tools necessary to develop three-dimensional (3D) functional models of human anatomy for use in medicine (surgical planning and education), forensics and engineering (computer-aided design (CAD) and finite element analysis).

Traditionally caliper methodologies are used in the quantitative analysis of human anatomy. In order for experts in anatomy and morphometrics to accept a transition to 3D volumetric data, it must be first validated as anatomically accurate. The purpose of this project was to create anatomically accurate models of modern human anatomy through the use of 3D medical imaging, such as multislice computed tomography (CT), and 3D computer modeling and

reconstruction. This dissertation attempts to validate the models and address current morphometric methodologies with four separate studies. The important results found in these studies were:

1) Medical image data such as computed tomography scans can be used to create high-resolution anatomically accurate 3D models for education and research purposes. These models can be used in morphometric studies through virtual quantitative analyses.
2) 3D virtual models of the human pelvis are 100% accurate in the estimation of sex in the pelvis, which represents an increase in accuracy over current field methods.
3) 3D virtual models of the human skull are 95.1% accurate in estimating sex in the skull, which represents an increase in accuracy over current field methods.
4) 3D models of craniofacial anatomy can be used for soft tissue depth analysis studies and clinical image data is more representative of living individuals.

By testing the imaging and 3D modeling technologies at several levels, we developed new methods for accurately analyzing virtual anatomy for an array of disciplines.

CHAPTER 1

INTRODUCTION

Computed virtual models of anatomical structures are proving to be of increasing value in clinical medicine (1), education (2) and research (3-4). With a variety of fields focused on craniofacial (5) and pelvic anatomy (6) there is a need for accurate anatomical models. Recent technological advancements in computer and medical imaging technologies have provided the tools necessary to develop three-dimensional (3D) functional models of human anatomy for use in medicine (surgical planning and education) (7) and engineering (computer-aided design (CAD) and finite element analysis) (8).

In order for experts in anatomy and morphometrics to accept a transition to 3D volumetric data, it must be first validated as anatomically accurate. The purpose of this project was to create anatomically accurate models of modern human anatomy through the use of 3D medical imaging, such as multislice computed tomography (CT) and magnetic resonance imaging (MRI), and 3D computer modeling and reconstruction. By testing the technology at several

levels, we hope to develop new methods for accurately analyzing virtual anatomy for an array of disciplines.

Anatomy

The field of anatomy is one of the oldest disciplines in medicine. From its origins in early medical schools around 300 B.C., scholars have dedicated themselves to the study of human body in its form. While the field has undergone many transitions over thousands of years, anatomists remain focused on determining the best method for the understanding of the body's structure and function (9).

Descriptive Anatomy

It is thought that the origin of anatomy goes back to ancient Egypt and China who had an in depth understanding of the body for their mummification practices. From Hippocrates (460-370 BC) to Galen (130-200 AD), the fathers of medicine wrote extensively on the nature of the human body without fully examining the actual anatomy of the human body. It was not until Andreas Vesalius (1514-1564) that anatomists and medical scholars began to use descriptive narratives with accompanying images to document the exact nature of anatomy (9-10).

From Vesalius' elaborately drawn plates to Dr. Frank Netter's modern day exhaustive CIBA Collection of Medical Illustrations (11), the field has remained focused on descriptive narratives and two-dimensional (2D) drawings to represent anatomy. Even with all the three-dimensional (3D) imaging technology available to medical professionals today, most professionals, even radiologists (12), resort back to static 2D imagery or illustrations for diagnoses and training. While some fields, like physical anthropology (13) or orthodontia (1), have developed their own measurement methodologies the problem remains that the trend of linear metric and 2D data continues.

Traditional Metric Methodologies

The human skull is a 3D geometric structure that is so unique that an individual can be identified solely by the form that the 28 bones create. The geometry of the human pelvis is less complex than that of the skull, being compromised of only 4 major bones, but together the skull and pelvis are the 2 most critical regions for personal identification. Their unique anatomy is also the basis of many medical and scientific fields such as neurosurgery, plastic surgery, craniofacial surgery, otolaryngology, dentistry, colo-rectal surgery, obstetrics and gynecology, uro-gynecological surgery, and physical and forensic anthropology.

Traditionally, it has been the field of physical anthropology that was dedicated to comprehensively measuring and recording statistical patterns in the

human skeleton (14). However, despite advances in computer technology, the field continues to rely on traditional caliper measurement methodologies that were established hundreds of years ago (15; 6).

Metric measurements are the crux of any analysis of skeletal remains by anatomists and physical anthropologists. Metric data are a series of set measurements that capture a great deal of information about skeletal remains by quantifying specific biological traits such as size, shape, stature and even the 'race' of a skeleton (14). For example, the skull is measured manually by sliding and spreading calipers that record distances from one point on the skull to another. They are the focus of most physical anthropology studies because they are by far the most universally accepted method since any analysis can be repeated by other scientists. (16) Early anatomists defined specific measurements based on biological landmarks that could be easily duplicated (17). A standard set of measurements was compiled from each part of the skeleton (18 - 19; 16; 20).

W.W. Howells was one of the pioneers in the advancement of osteometric and, in particular, craniometric analyses. Howells used physical measurements to determine populational distances and relationships. He was one of the first anthropologists to use quantitative methods to answer and solve morphological problems. His seminal work, "*Cranial Variation in Man: A Study by Multivariate Analysis of Patterns of Difference Among Recent Human Populations*" (21),

measured 17 different world populations craniometrically and became the model for all future studies in human skull identification. Howells was especially interested in determining “ethnicity” (or ancestry) from skulls using quantitative metric methods (22 - 23). Two subsequent works “*Skull shapes and the map: craniometric analyses in the dispersion of modern Homo*” (23) and “*Who’s Who in Skulls: Ethnic Identification of Crania from Measurements”* (24) continued to build on Howells’ previous attempts to establish a database of human craniometric measurements. Numerous attempts at metric classification of the pelvis have been published, but none with the comprehensive depth of the Howells studies for the skull (25 - 26).

Subsequent studies helped produce new methods of human analysis and identification based on metric measurements. One technological advancement was the introduction of *FORDISC* (27); a software program that allows metric measurements of an ‘unknown’ individual to be compared with the same measurements from a large database of different populations in order to determine the sex and stature along with which population group the individual is most likely affiliated. However, no consideration is given to the skeleton’s 3D shape other than a suggested series of subjective non-metric characteristics such as the shape of the orbit (round or squared), the angle of the zygomatic (retreating, vertical, or projecting) or in the pelvis, the width of the greater sciatic notch.

The benefit of using metric methodologies in anatomical study is that they are not as subjective and are more substantive than other methods of analysis (i.e. non-metric traits). However, a drawback to using only metric methods is that they often do not take many identifying traits into account because they are limited to standard landmarks and measurements. Most metric studies conducted on the skull and pelvis continue to disregard their 3D geometry or nature, and consequently lose much of the potential data that it holds. With recent developments in 3D capture devices like 3D digitizers and laser scanners, a portion of the field has begun to examine more quantitative analyses of the anatomy over the traditional descriptive analyses that are currently used (28 - 29).

Landmark Data and Morphometric Analyses

These traditional morphometric studies of anatomy only began in the past few decades. These methods used multivariate statistics to observe variables taken from linear distances on an organism (30). These variables were measured in lengths, widths, and the distances between the landmarks (13). However, it was not possible to visualize the exact geometric form of the object from such measurements which led to weaker results (31 - 32). Over the past 20 years, geometric morphometrics, the study of “covariances of biological form” that is based on the collection of 3D coordinate data from anatomical landmarks (31), has overcome some of the limitations of linear metric data, which have led to

ambiguous or generalized results. Geometric morphometric studies have proven to increase precision and control error in the interpretation of biological data over those using traditional metric measurements. Data are recorded in the form of landmark points, whose location is recorded as x, y, z coordinates in 3D space, which together represent the geometric form of an object; where form= size + shape.

Geometric morphometric analyses, in particular, can use coordinate data to give a more comprehensive depiction of the object by capturing the relationships between the landmarks. Landmarks are “samplings of the map of homologies” that are biologically determined by the geometric features of a specimen (33). The landmarks themselves must be clearly defined and be reproducible from specimen to specimen with great accuracy by different researchers (31; 33 - 34). While traditional distance measurements can be generated from these data, geometric morphometric methods allow the researcher to better visualize the data in 3D space. Many of the conventional morphometric landmarks used in anatomy and physical anthropology correspond with traditional anatomical landmarks like ectoconchion, zygion, and jugale (Figure 1.1).

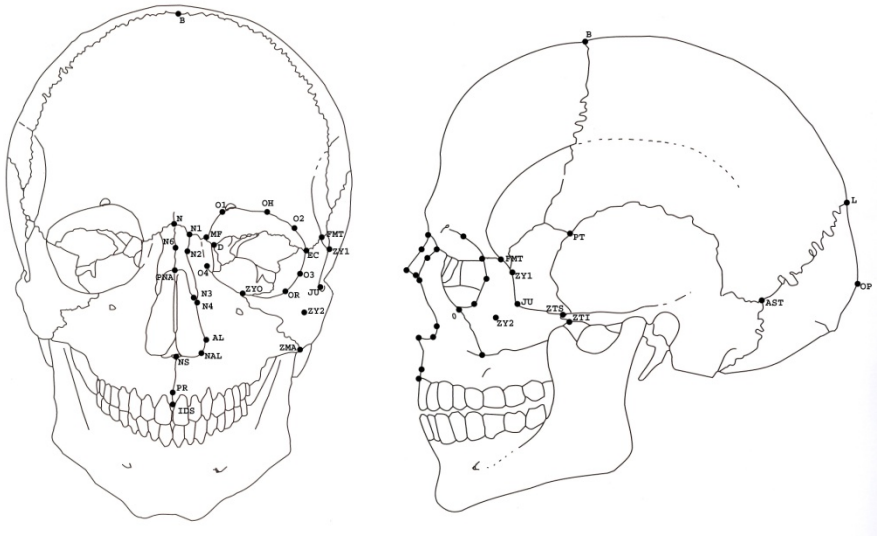

FIGURE 1.1: Skull with landmarks indicated (Anterior view left, Lateral view right) (Modified from Buikstra and Ubleaker, 1994)

However, conventional landmarks often do not give the most complete picture of the object being studied (26). Additional craniometric and pelvimetric markers can be designed to complete this gap and give an added dimension that would not otherwise have been captured, thus better representing the form of the trait being studied. The problem that has arisen with coordinate data is that it is only as reliable as the replicability of the anatomical landmarks (28). Often landmarks are difficult to reproduce because of their ambiguity. These “Fuzzy Landmarks” (34) present a serious hurdle to morphometric studies where reproducibility is key in being able to establish cross-populational patterns. Morphometric studies for medicine, forensics and biometrics are in need of more robust data.

3D Volumetric Data

"3D volumetric data" is the type of data that is the standard output of current 3D image acquisition devices used in medical imaging modalities like Magnetic Resonance Imaging (MRI) and Computed Tomography (CT). Commonly referred to as DICOM images, this volumetric data is embedded with an abundant amount of information that is not fully utilized by modern medical practitioners (35). From X-Ray to CT, each imaging method has provided an insight into the internal structure and function of the human body.

Imaging of anatomy for medicine began with the discovery of x-radiation by Wilhelm Roentgen in 1895 and W.D. Coolidge's x-ray tube in 1903. For the first time, images of the internal body could be taken of living individuals (36 - 37). X-ray imaging involves taking a piece of film in a cassette and placing it between the object being imaged (body part) and the x-ray emission device or source. The film (or image capture receptor) detects the X-ray's waves and creates an image of the anatomy that it passed through. X-ray images are known to be effective at capturing bone and other dense structures but are less useful in distinguishing soft tissue (38). X-rays were the gold standard for 2D imagery until 1973 when the first 2D magnetic resonance images (MRI) were released. (Figure 1.2)

With the introduction of Magnetic Resonance Imaging (MRI), medical imagery was finally able to capture much of the soft tissue that had been elusive in x-ray imagery. In MRI, the nuclei of the hydrogen atoms in the body are polarized via an extremely strong magnet that creates a gradient or magnet field over the body. The stronger the magnetic field is, the higher the resolution of the image will be. The data is captured by reconstruction algorithms that sense the proportions in voltage between the nuclei's polarized and relaxed states (Enderle et al. 2005: 956) and create a grey-scale image. (Figure 1.3) MRI is seen as one of the safest medical imaging techniques because it does not emit any ionizing radiation like x-ray (38).

In 1967, Sir Godfrey Hounsfield developed the first computed axial tomography (CAT) imaging device on the concept that large series of x-ray images could be grouped at angles around an axis and reconstructed with an algorithm to create a more in depth image than the standard X-Ray. CT images are based on algorithms (mostly Fourier transforms) (38) that depend on speed and accuracy of the scanner itself for the quality of the image. In a CT scan, x-rays are absorbed by the body so that an overall "mean attenuation" images result along the directed path. CT differs from MRI in that it captures the scatter from tissues in the body from the X-ray rather than the wavelength. Radioactive agents, like contrast, can enhance this scatter resulting in higher quality images and definition (38). CTs are best at capturing bone, lungs, and more dense organs, as well as foreign bodies like surgical implants. Each CT scanner has a

series of convolution kernels that are included by the manufacturer which assist in maximizing specific types of tissue like bone and the lungs (39 - 40). (Figure 1.4) Due to the use of large series X-Ray, CT scans have more ionizing radiation than any of the other medical imaging modalities.

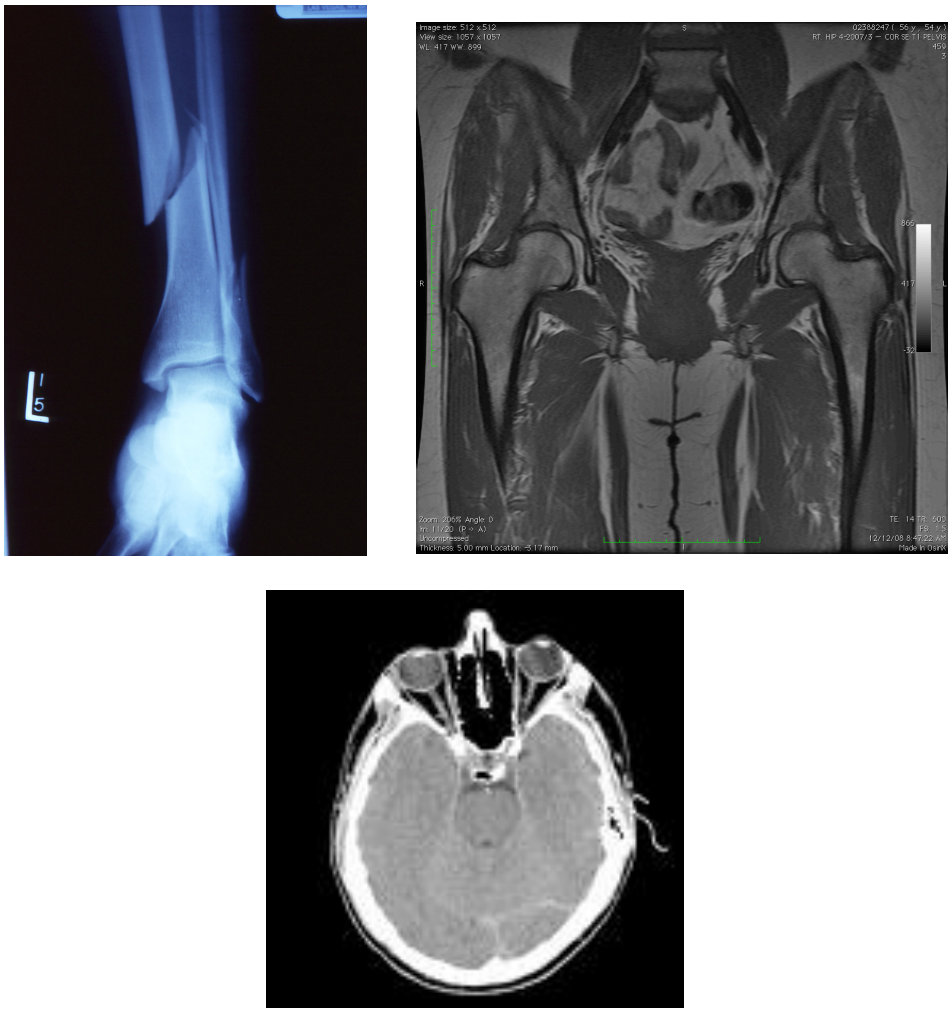

FIGURE 1.2-1.4 a) X-Ray image of leg; b) MRI image of pelvis; c) CT image of head

3D images from MRI and CT are created from tiny cubes called voxels (Voxel = $\Delta x \Delta y \Delta z$) which are reconstructed to create 3D models of the 2D and 3D images taken from the scanner (38). However, technological restrictions such as computer processor speed and scanner resolution have limited the 3D applications of the data until recently. With advances in computer and imaging technologies, higher resolution images and models are now possible and a trend towards using the extracted 3D volumetric data and models to create more quantitative 3D anatomy is emerging (29; 41).

Quantitative Anatomy

In the early 1990's, advances in medical imaging and computer technology allowed researchers from around the country to join with the National Library of Medicine for one of the most comprehensive anatomical studies ever undertaken. The Visible Human Project (42 - 43) used a donated human cadaver to image, segment and section in order to extract 3D volumetric data from medical images for 3D reconstructions. The Visible Human Project sparked a myriad of studies on anatomy, 3D visualization, and quantitative measurement tools for 3D data (44 - 45).

For the first time since the Visible Human Project, anatomists and medical professionals are able to capture the true nature of an anatomical structure or complex through 3D volumetric data and visualization. This data is allowing

anatomy to be three-dimensionally measured and quantified. The quantified anatomy provides the opportunity to establish populational trends and patterns that have never been captured before (44 - 45). There is even the potential to observe one's individual anatomy over time. Current projects are focusing on the registration of this 3D volumetric data for more accurate quantitative measures between specimens or within the same individual over time (41). However, the validation of 3D volumetric data as a truly accurate representation of human anatomy will be critical in continuing the current 3D data volume trend.

Specific Aims of this Dissertation

The goal of this project was to create anatomically accurate models of modern human anatomy through the use of medical imaging, 3D computer modeling and reconstruction. By analyzing the 3D models' geometry quantitatively, we hope to develop new methods for accurately defining virtual anatomy that can be applied to various scientific and medical disciplines.

To accomplish the phases of this project, four specific aims were proposed:

1. **Scanning Protocol:** Determine a medical imaging scan protocol that optimizes key anatomical features and can be used universally.

2. **Accurate Computer Model:** Validate the computer modeling technology and create accurate models that are representative of human anatomy.

3. **Morphometric Analyses:** Conduct a series of morphometric analyses on models to determine any populational statistical patterns in the anatomy and see how that data relates to current field standards.

4. **Clinical Application or Relevance:** Apply the datasets to different fields (e.g. forensics, pathology, facial reconstruction, and obstetrics and gynecology).

Poster, Platform Presentations, Journal Articles, and Book Chapter

This work and other portions of this study not included in this document have been presented through posters, platform presentations, journal articles and a book chapter. Please see Appendix A, B, and C for a listing.

Dissertation Outline

The format of this dissertation includes a series of journal articles based on the different phases of the research project. There may be information that is redundant from chapter to chapter but this format is hopefully the most efficient way to convey the project at each phase.

Chapter 2 explains the initial pilot study and techniques that were undertaken to validate the accuracy of the virtual and rapid prototyped anatomical models. Chapter 3 details the process of making a large series of 3D virtual pelves that were measured and analyzed to test the accuracy of current forensic sex determination standards.

Chapter 4 investigates the complexities of 3D modeling of human crania from cadaveric and clinical medical scans for morphometric analyses.

Chapter 5 examines 3D modeling of soft tissue of the face. Traditional techniques of soft tissue depth measurements were tested from the actual cadaveric specimens to the virtual models. Clinical medical scans are also utilized here to improve the quality of facial data

Chapter 6 concludes with recommendations, a description of the variety of applications the datasets are being applied to, the current state of the research project and future directions.

CHAPTER 2

A VALIDATION STUDY OF 3D ANATOMICAL MODELS

Abstract

Computed virtual models of anatomical structures are proving to be of increasing value in medical education and research. In this study, morphometric measurement was conducted to validate the accuracy of technologies now available to produce virtual as well as printed three-dimensional (3D) replicas of actual human skulls. A human cadaveric head was medically imaged via computed tomography (CT) and a virtual model of the skull was constructed from the volumetric CT data using a suite of different visualization software packages. A full size prototype of the skull was then produced from the digital model using a 3D ZPrinter 310 (ZCorp ©) printer. The cadaver head was processed and the skull recovered and cleaned. A series of classic anthropological measurements were made on all three versions of the skull (virtual, printed solid model and actual) and the resulting data was statistically analyzed. To further test the accuracy of the virtual models, a series of skulls from the University of South Florida's Anthropology Department were CT scanned, reconstructed in 3D and measured both virtually and physically.

The data demonstrates that anatomically accurate virtual and prototypic representations can be made of actual anatomical structures using state-of-the-art medical imaging and computer technology. We are confident that expansion of this pilot study will confirm that anatomically accurate virtual and/or prototypic anatomical models can be produced for use in a wide range of anatomical structures for use in medicine, biological anthropology and the forensic sciences.

Introduction

The advent of new forms of imaging technology has allowed anatomists new ways to visualize their specimens. Medical imaging modalities, such as Computed Tomography (CT), are providing unique data sources for examining modern human variation in a more quantitative manner while extending osteological resources to researchers beyond actual contact. The newer virtual methodologies have shown an increase in accuracy and reproducibility over traditional methods (1 - 2).

Virtual 3D models of anatomical specimens can be made either by laser surface scanning or by medical scanning. Both methodologies are non-invasive and do not damage the specimen. The two-dimensional (2D) images from the scans can be imported into 3D modeling packages like *Mimics* or *ScanIP*, or any medical image rendering software package. In the software, the images can be reconstructed to form 3D models of the anatomy. Measurements and

observations can be made from these 3D computer models in a similar manner to those taken from the actual specimen.

In 2007, the Center for Human Morpho-Informatics Research began a project to simply find a software package or suite of packages to validate the accuracy of the virtual anatomical models. A pilot study was devised to test strengths and weaknesses of each package in our research. Our pilot study looked to answer how 3D computed virtual models compared to an actual specimen with such unique geometry as the human skull. The goal of this study was to specifically compare the accuracy of measurements made using computed 3D imaging technology to data obtained by traditional caliper measurement methodologies of both an actual skull and a prototype of a skull made on a 3D rapid prototype printer.

Materials and Methods

Medical Imaging

The pilot study began by utilizing a randomly selected intact human cadaver head for use in computed tomography (CT) scans, virtual reconstruction, and rapid prototyping. The cadaver was CT scanned at H. Lee Moffitt Cancer Center's Radiology Services. The scan had a pixel spacing of 0.49609375/0.49609375 mm and was acquired at a slice thickness of 1 mm. The specimen was scanned on a 3D multi-slice Computed Tomography (CT)

Siemens SOMATOM Sensation 16 scanner. Several convolution kernels or windows pre-sets were tested such as standard (B30), bone (B40), and lung (B50) to determine which kernels adjusted the sharpness of the images to optimize the boney anatomical features (3). The raw data was extracted as DICOM images and the different convolutions series compared visually in the laboratory.

3D Computer Reconstruction

Prior to the start of the project, several commercial and open source medical visualization software packages were tested by the researchers: *Analyze, ScanIP, 3DSlicer, Mimics,* and *Osirix*. Only two packages were selected for testing based on their robusticity, visualizations, reliability and ease of use.

Mimics ©

Mimics © by Materialise is an advanced engineering software package used for the visualization of 3D image data for Computer Aided Design (CAD) and Finite Element Analysis (FEA). *Mimics* accepts most image file types like DICOM, TIFF, and JPEG for import. Its main purpose is for the segmentation of the 2D images and reconstruction into 3D exportable models such as stereolithographic files (STL). A STL file describes the surface geometry of an object in a series the tessellated triangular meshes that correspond to a 3D coordinate system. These files can be exported into CAD and FEA engineering software packages like *COMSOL* or *Abaqus* for further analysis in biomechanical

studies. One benefit of *Mimics Innovation Suite* is the ability to capture the complete volumetric data, meaning the internal anatomy along with the external surface anatomy. This makes it possible to run analyses on structures not normally captured in other packages.

For the purposes of our study the volumetric data from the scan was taken into *Mimics* © (version 11.1). Using a lower pixel threshold of 150 and upper of 255, a FloodFill method of seeding the image was done to select only the soft tissue (Figure 2.1) and the bone (Figure 2.2) pixels in the data set. This 3D volumetric pixel grouping was then filtered of artifact holes and closed to create one unsegmented structure. The resultant pixel masks from the transverse (axial), coronal, and sagittal planes were converted to voxels by the software to produce a 3D model of the selected region(s) of the head (face and skull). The dataset was then exported as a Stereolithographic file (STL).

Once the initial 3D modeling of the intact cadaveric head was complete, the actual skull was isolated from the soft tissue (Figure 2.3) using a defleshing process that cleaned the skull of all facial tissues. The remaining skull was CT scanned again for comparison to the original scan series and to document any modifications made in the defleshing process.

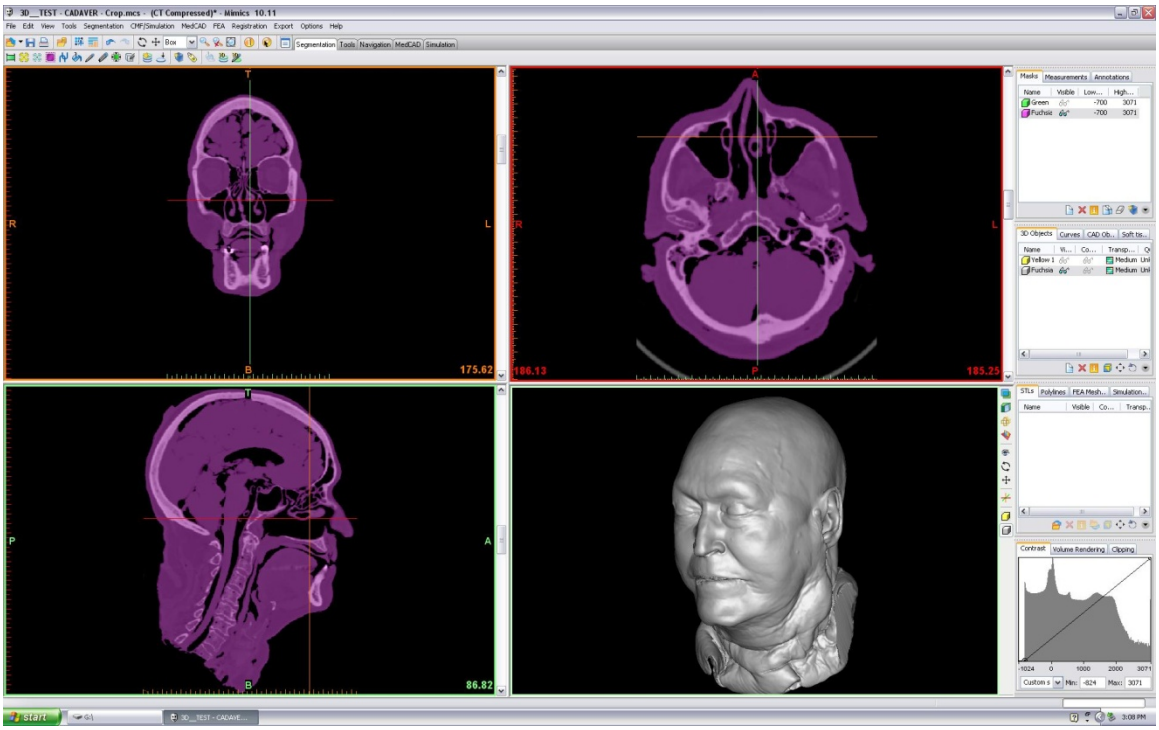

FIGURE 2.1: 3D reconstruction of cadaver head in *Mimics* ©.

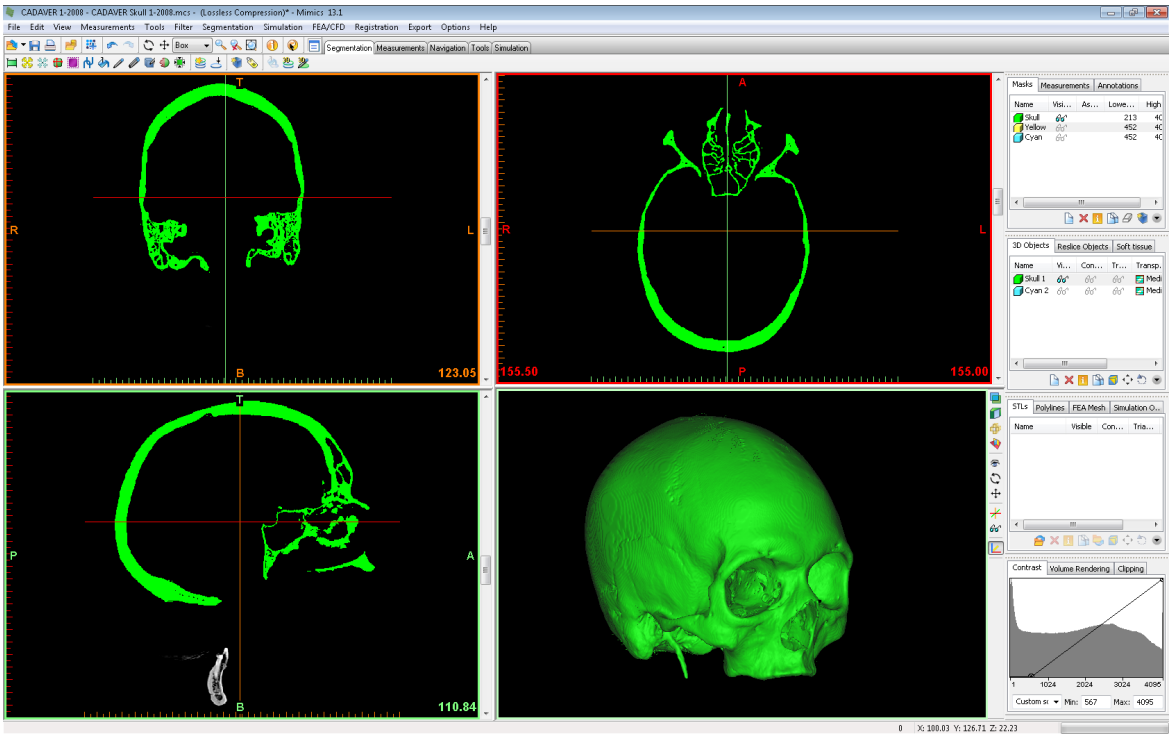

FIGURE 2.2: Isolated cadaver skull in *Mimics* ©

FIGURE 2.3: Actual cadaver skull after defleshing process.

OsiriX

Additional 3D models of the data set were rendered in the radiological software package, *Osirix* © version 2.1. *Osirix* is an open source DICOM viewer and visualization workstation developed by researchers at University of California, Los Angeles Medical Center and the University Hospital of Geneva, Switzerland. Once the DICOM images are imported into the software's database, 2D and 3D volume visualization is possible through a series of tissue presets or through a 8-bit or 16-bit Color Look-Up Table (CLUT) editor.

The raw DICOM data set of the intact cadaveric head was imported into *Osirix* and 3D volume rendered. The 3D reconstructions were maximized to isolate only the boney features of the scan. A glossy texture was applied to the rendered skull to replicate a life-like appearance (Figure 2.4). Next, 3D volumetric reconstructions of the cadaveric soft tissue were made and the opacity adjusted to visualize the individual tissue layers in the specimen seen in Figures 2.5 - 2.6. Unfortunately while very good at 3D high-end visualizations, at this time *Osirix* only allows for 3D surface exportation. Once the 3D models were complete, stereolithographic models of the surface renderings were exported.

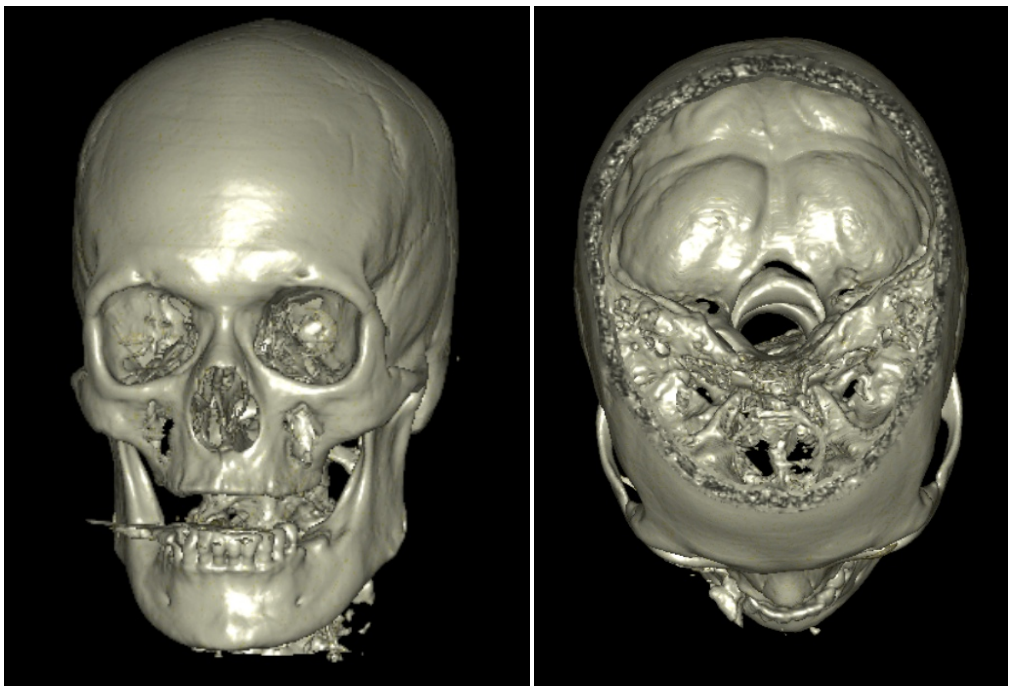

FIGURE 2.4: 3D skeletal model of cadaver head made in *Osirix* ©

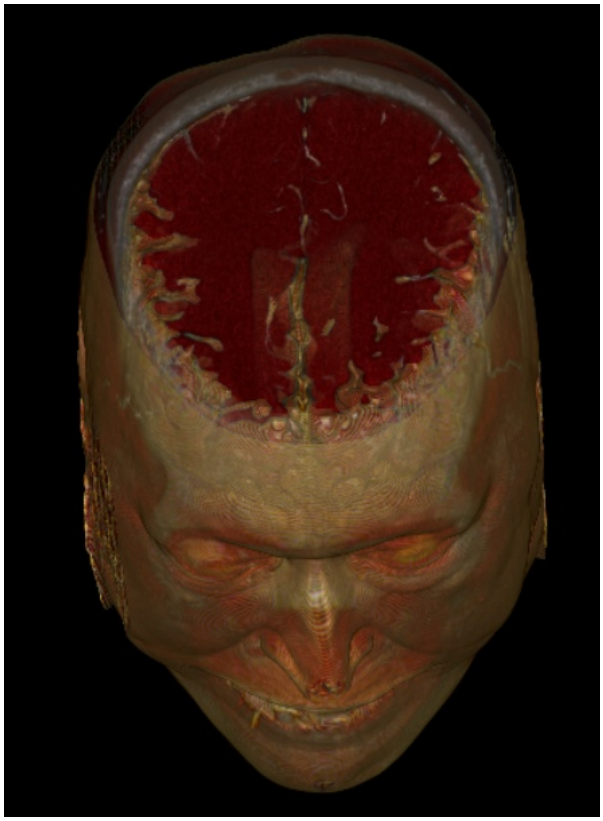

FIGURES 2.5-2.6: 3D soft tissue model of cadaver head made in *Osirix*

Rapid Prototyping

Rapid Prototyping (RP) is an additive manufacturing technology commonly used in industrial and biomedical engineering that uses 3D models of objects and constructs physical copies of that model using powders, liquids, and specific glues. RP is used for the physical testing of the ergonomics of commercial devices such as cell phones or tools as well as in art and architecture for the designing of sculptures or structures. Medical researchers use RP for the designing of orthopedic implants, surgical tools, and temporary anatomical implants such as cranial plates.

After the volumetric 3D models of the cadaveric skull were complete in *Mimics*, the stereolithographic files were exported for use in RP. A 3D prototype was then generated using a Zcorp 3D ZPrinter© 310 Plus (Figure 2.7). In the 3D printing, layer upon layer of fine ZP 102 Powder was pressed until it formed a prototype of the cadaver skull. After printing, Z-Bond TM 101 Medium Strength Cyanoacrylate Binder glue was used to fix the specimen for handling. The printed model contains all external and internal anatomy of the actual skull including the frontal sinuses.

FIGURE 2.7: Skull prototyping using Zcorp 3D Zprinter © 310 Plus

Anthropological Measurements

For quantifying the variation between the actual, virtual, and prototype skulls, 25 anthropometric measurements were selected from Buikstra and Ubelaker's (4) index of standard cranial landmarks based on their effectiveness in establishing a biological profile in skeletal analysis. Measurements of the physical skulls were measured using traditional spreading and sliding calipers. An osteometric toolkit was designed for landmark placement on the 3D virtual skulls in the *Mimics* software package that allowed the researcher to examine the midline and bilateral variables. The toolkit assists the observer in the analysis

since they simply need to place a landmark at a location-defined toolkit itself. The software then calculates linear distances, angles, and indices between specified points. This data is output in a format ready for use in statistical analysis packages.

For this study, the measurements for the validation were chosen to meet the criteria of commonly used measurements reported in the literature for capturing true skeletal geometry. The selected measurements included: Maximum Cranial Length & Breadth, Upper Facial Height & Breadth, Nasal Height & Breadth, Orbital Height & Breadth, as well as Foramen Magnum Length & Breadth. See Table 2.1 for complete listing and definitions.

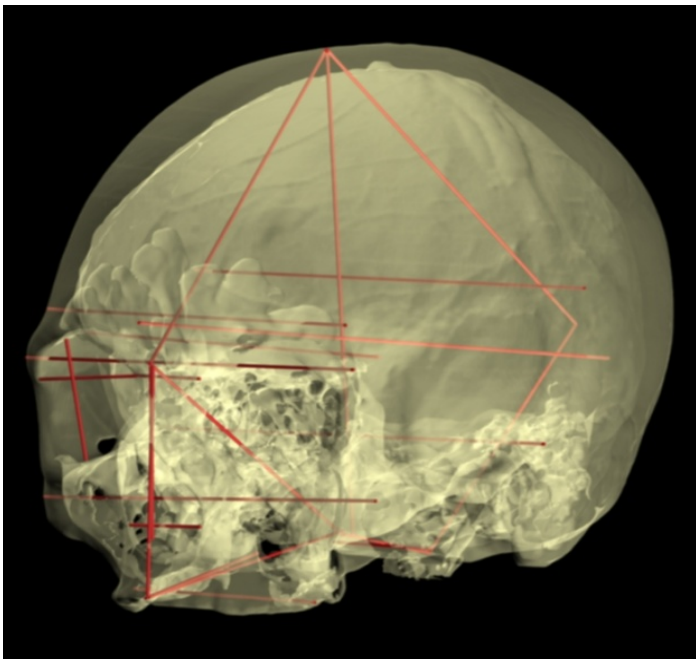

FIGURE 2.8: Virtual skull showing measurements taken

TABLE 2.1: List of 25 cranial measurements used in the study

Number	Measurement	Definition
1	GOL	Max Cranial Length
2	XCB	Max Cranial Breadth
3	ZYB	Bizygomatic Diameter
4	BBH	Basion-Bregma Height
5	BNL	Cranial Base Length
6	BPL	Basion-Prosthion Length
7	MAB	Maxillo-Alveolar Breadth
8	MAL	Maxillo-Alveolar Length
9	AUB	Biauricular Breadth
10	NAH	Upper Facial Height
11	WFB	Minimum Frontal Breadth
12	XFB	Max Frontal Breadth
13	FMT	Upper Facial Breadth
14	NHH	Nasal Height
15	NLB	Nasal Breadth
16	OBB	Orbital Breadth
17	OBH	Orbital Height
18	BOB	Biorbital Breadth
19	IOB	Interorbital Breadth
20	FC	Frontal Chord
21	PC	Parietal Chord
22	OC	Occipital Chord
23	FML	Foramen Magnum Length
24	FMB	Foramen Magnum Breadth
25	MDH	Mastoid Height

Anthropology Skulls

In order to further test the accuracy of virtual 3D models from medical image scans, a collection of 8 skulls were obtained from the University of South Florida's Department of Anthropology. The specimens were photographed and scanned at H. Lee Moffitt Cancer Center's Radiology Services on a 3D multi-slice Computed Tomography (CT) Siemens SOMATOM Sensation 16 scanner.

Several convolution kernels or windows pre-sets were tested such as standard (B30), bone (B40), and lung (B50) to determine which kernels adjusted the sharpness of the images to optimize the boney anatomical features (3). The image data was 3D reconstructed in *Mimics*, and virtually measured using the same osteometric toolkit developed for the cadaver head in the software. Examples of the 3D anthropological skulls are shown in Figure 2.9.

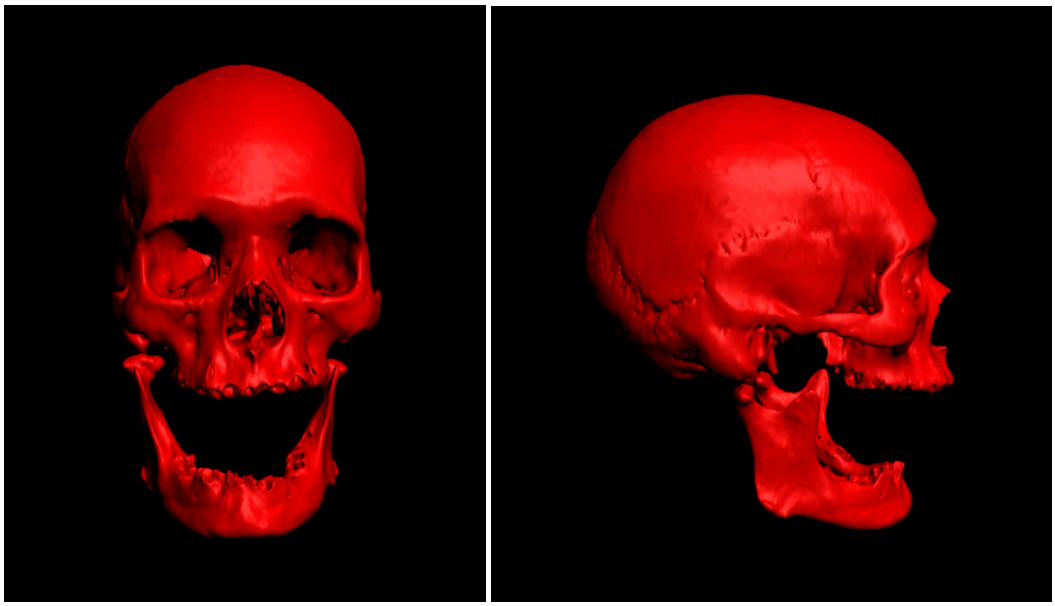

FIGURE 2.9: Examples of 3D virtual skulls from USF Anthropology

Statistical Analysis

All data from both the cadaver head (actual, virtual and prototype) and the anthropology skulls (actual and virtual) were subjected to statistical analysis of the measures of central tendency. Standard deviations and p-values were also calculated to determine the significance of the differences between the

measurements. Data collected for this study was analyzed in the software package, *SPSS* version 16.0.

Results

Image Quality

Overall the image quality was very good from the high-resolution CT scans. This can be attributed to the low slice thickness (1mm) and specific convolution kernels or window levels that were used by the CT technologists. Interestingly, it was not the bone window (B40) but rather the lung window (B50) that best captured the bone pixels. In Figure 2.10, the bone window shows the bone pixels have been visualized towards the highest end of the gray scale making fine details difficult to visualize.

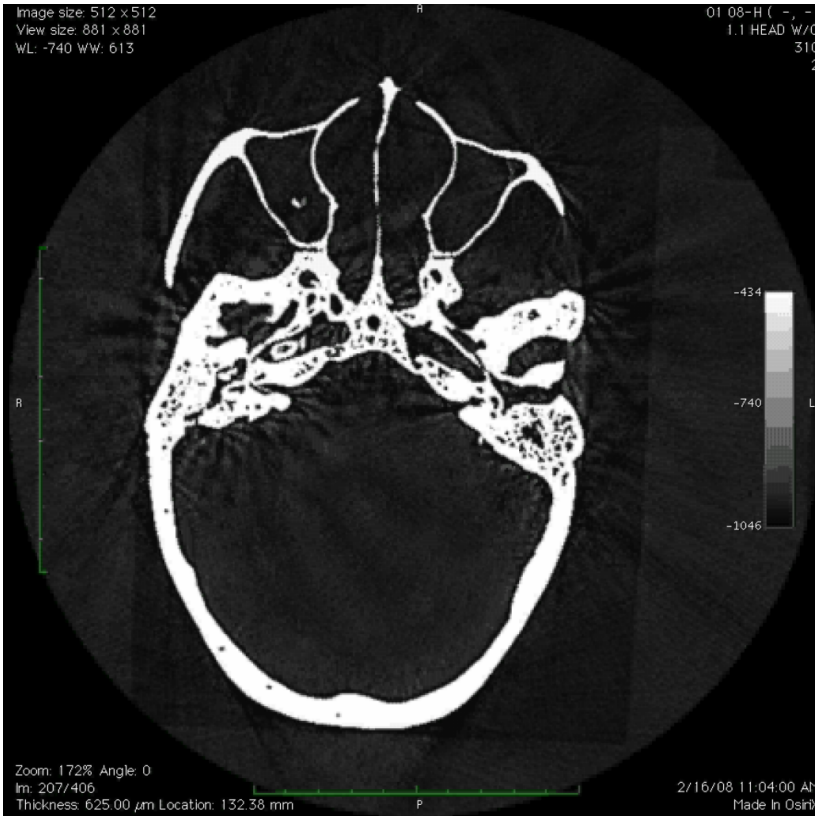

FIGURE 2.10: Screen capture of skull in “bone window”

While in Figure 2.11, the same skull is displayed in the lung window with much higher clarity of fine details such as suture lines.

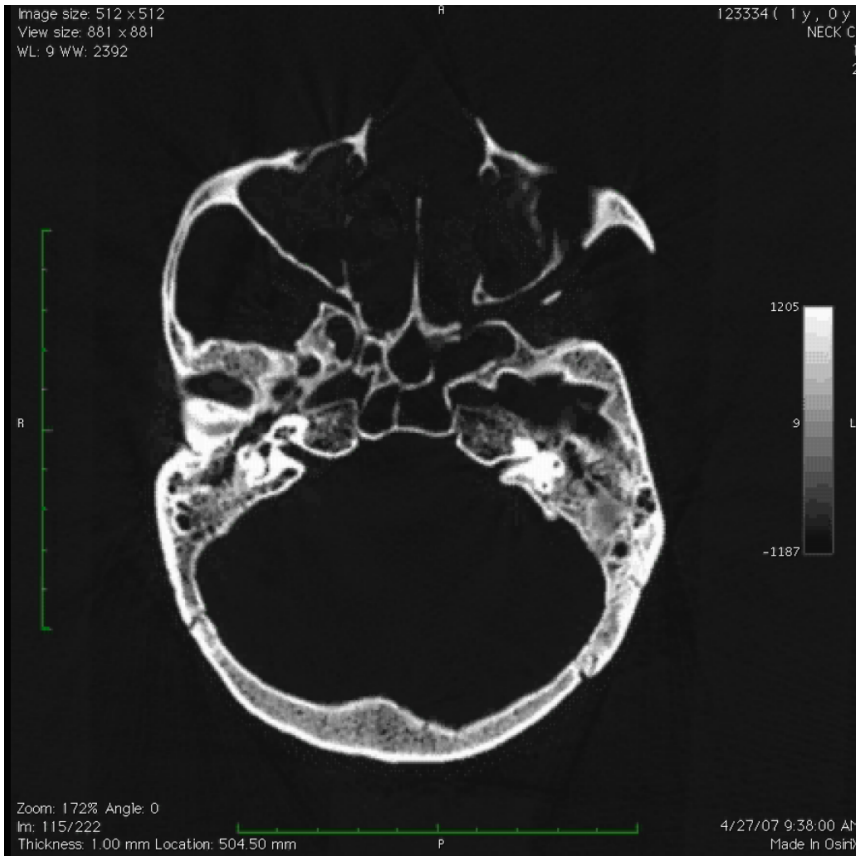

FIGURE 2.11: Screen capture of skull in "lung window"

3D Computer Reconstruction Software

We found in our pilot study that the most complete software package for our research out of the box was the *Mimics Innovations Suite*. The *Osirix* software works as a wonderful quick visualization tool and database management system of medical scans, however, its measurement capabilities were limited for what was required in this study without extensive computer programming of a plug-in. While the *Mimics* software package is costly, it does provide the most comprehensive research tool for image analysis, segmentation, 3D modeling and export for CAD- and FEA-ready models of any package tested

at the laboratory. The ability to build specific measurement toolkits for this research project was an added bonus.

Anthropological Measurements

In the study, the actual measurements of the virtual skulls were found to be consistent with those taken from the 8 actual skulls even considering intra-observer error. Previous studies (5 - 7) have suggested that normal measurement variation amongst experts in traditional caliper methodologies is on average approximately 0.52 - 1mm. Our overall statistical analysis of virtual versus actual skull measurements indicated an average variation of approximately + 0.4 mm, less than 1mm.

Cadaver Head Results

Statistical analysis of the measurements data comparing all of the samples (actual, virtual and prototype), confirmed the accuracy of the computer modeling and measurement technologies (Figure 2.12). The majority of the measurements demonstrated little to no variation between specimens. Others showed some variation but no more than is accepted in the field of anthropology as normal inter-and intra-observer error. Additionally, we found the prototypes to be a valuable reproduction of the original skulls, even taking into consideration artifacts from the printing process such as faint sutures lines.

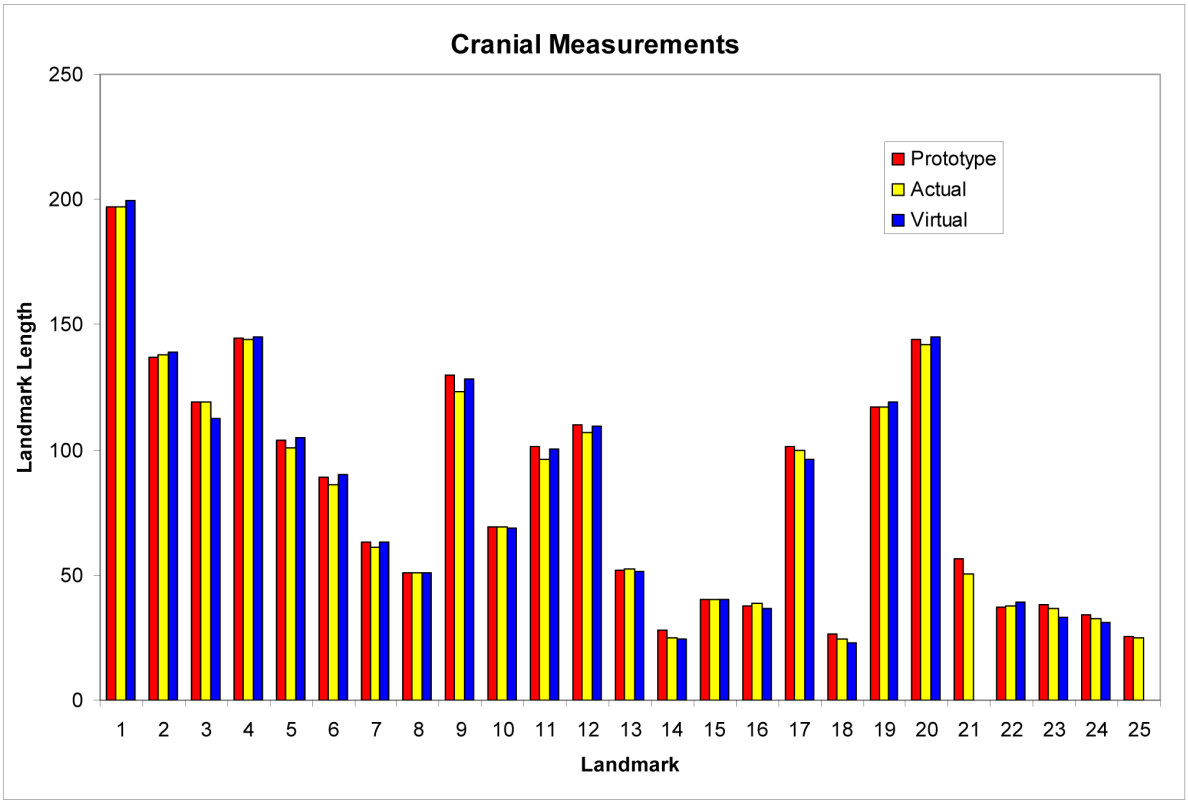

FIGURE 2.12: Anthropological measurements (in mm) of prototype, virtual and actual skull.

Of the measurements, the most reliable and consistent between the 3 types of skulls measured were basion-bregma height, maximum alveolar length, upper facial height, and nasal breadth. This consistency is likely due to the fact that several of these measurements are taken from clearly defined landmarks like the intersection of the frontal and parietal sutures on basion-bregma height.

The least consistent measurements were found to be biauricular breadth, orbital height, the parietal chord and mastoid height. The biauricular breadth, defined as the least breadth across the roots of the zygomatic, and the mastoid height are notoriously difficult for measurement in anthropology due to the lack of

defined landmarks from which to take the measurements.

Anthropology Skulls Results

The results of the measurement comparison between the actual and virtual skulls showed were found to be consistent with that of the initial cadaveric study. Between the virtual and actual skull measurements there was a less than 5% (4.93%) rate of error. It is generally held in anthropology that error rates of less than 10% are accepted as beyond chance and considered accurate (8). This study demonstrates that virtual replicas of actual skulls can be produced with precision and should be considered as accurate replicas.

Discussion and Conclusions

With the methodology of making 3D virtual anatomical models from medical imaging validated, the benefits of such models can be explored. Computer-generated anatomical models provide the added benefit of allowing anatomists or anthropologists to not have to handle fragile 'real' specimens. Often in forensic cases, there is residual soft tissue attached to the bone specimen that cannot be removed or defleshed. This soft tissue can obscure critical landmarks and features used in establishing the biological profile or evidence of trauma. With the virtual 3D models, this soft tissue can be virtually removed or made transparent for analysis. Fragmentary remains are another common issue in anthropology. Remains can often be disturbed, destroyed or

even missing from a site. Virtual models of bones allow for partial remains to be duplicated or “filled in” in order to continue with analysis.

In an era of limited access to osteological resources, large collections of virtual anatomical models can be provided to researchers to augment their research studies. Instead of having to travel to the site of the major collections such as the Smithsonian Institute, accurate 3D virtual specimens allow for osteometric analysis to be conducted remotely using specialized toolkits, like the ones that have been developed by our lab.

Most importantly, virtual forensic analysis of bone allows for more objective results. Non-metric or subjective traits such as the angle of the zygomatic bone (cheek) or the shape of the orbit can be “metricized” (9 - 10) to quantify biological variation rather than scale it. This has inevitably added to the reliability and reproducibility of current osteometric methods. While physical anthropology will continue to rely on metric analyses, more computerized methods will be developed to further our understanding of populational pattern recognition for the assessment of unknown human remains.

By using methodologies developed and validated in this pilot study, the researchers are now confident that anatomically accurate virtual and/or prototypic anatomical models can be produced using state of the art medical imaging and computer software like *Mimics* for use in a wide range of anatomical

structures for use in medicine, biological anthropology and the forensic sciences. This study demonstrates that 3D datasets are useful and accurate tools to the study of human anatomy for both clinical and forensic purposes. Through virtual anatomy we are provided the opportunity to reevaluate current methods of analysis and create new ones, which in turn, will increase the accuracy of results and expand the accessibility to anatomical specimens beyond actual contact.

Acknowledgements

The researchers would like to thank the H. Lee Moffitt Cancer Center, Radiology Services for their assistance in the medical imaging portions of this study. We would also like to acknowledge Wesley Frusher, MS, of the Department of Mechanical Engineering in USF's College of Engineering for his invaluable input and efforts in the rapid prototyping section of this study. We would finally like to thank the developers and staff at Materialise and the *Osirix* Research Team for their assistance and input during the different stages of this project.

Travel support for the presentation of this project was sponsored in part by the NSF IGERT Program Grant DGE 0221681.

CHAPTER 3

VIRTUAL DETERMINATION OF SEX: METRIC AND NON-METRIC TRAITS OF THE ADULT PELVIS FROM 3D COMPUTED TOMOGRAPHY (CT) MODELS

Abstract

Examination of the adult os coxae and sacrum is one of the most common methods of sex estimation from bone. Medical imaging, such as computed tomography (CT), provides the opportunity for three-dimensional (3D) imaging of the skeleton from clinical scans of known individuals *in situ*. In this study, a randomly selected subset of abdominopelvic CT derived models were used to evaluate simple, repeatable metric methods of sex estimation based on a combination of obstetric measurements and the traditionally non-metric Phenice-derived traits. A four-variable discriminant function for sex estimation was developed based on statistical analyses. Overall, the cross-validated accuracy of this method was 100%, with interobserver error showing an average of only 2.2%. Comparative analysis was run on the data set using *Fordisc 3.0*. This study shows that current sex determination standards from the pelvis should be

updated to include more *in vivo* data in order to increase accuracy of identification.

Introduction

The importance of developing accurate and reliable techniques for establishing the biological profile from human skeletal remains that meet the *Daubert* guidelines has been well documented (1 - 2). However recently, with an increased spotlight on the field of forensic sciences, there has been an international initiative towards developing higher standards through more quantitative, reproducible methodologies. In 2009, a Congressionally mandated review of the forensic sciences undertaken by the US National Research Council and US National Academy of Sciences found severe deficiencies in the many of the subdisciplines and immediately issued a call for standardization of methods and reform of current practices (3).

Modern, documented skeletal collections are needed to supplement and improve upon the existing body of knowledge of both global and population-specific methods for sex discrimination. There are few skeletal collections that are comprised primarily of individuals that were deceased in the last decade or even century. Notable exemptions include but are not limited to the Bass Collection, Maxwell Collection, Pretoria Collection, Athens Collection and the Wichita State Cadaver Collection (4 - 8). Numerous studies have discussed the

value of current reference samples (9 - 12). Without quantifiable data, there are obvious implications for the certainty with which even the most highly trained anthropologists can support their assessments in court. Recent studies have introduced novel methods for assessing sex in the pelvis but have focused on existing archaeological osteology collections (13 - 15). Only by introducing additional data sets that are representative of living subjects can we begin to improve the application of identification techniques.

Traditionally, anthropologists rely on established metric and non-metric, observational analyses of the actual bone (4;16 - 17). Medical imaging modalities, like computed tomography (CT), are providing unique data sources for examining modern human variation in a more quantitative manner while extending osteological resources to researchers beyond actual contact (18). In the last decade, there has been a growing trend towards computerized (19) or virtual methodologies. These studies have shown an increase in accuracy and reproducibility over traditional linear methods in establishing a biological profile (20 - 22).

For purposes of sex discrimination, it is widely noted that morphological techniques are simple and accurate above chance in correct classifications of most males and females; however, this is highly reliant on the experience level of the observer (23). Numerous attempts at metric classification have been published, but often require complex or time-consuming measurements (24 - 30).

In non-metric sex estimation of the pelvis, the evaluation is focused on Phenice-defined traits of specific regions of the innominate: ventral arc, sub-pubic concavity, and ischio-pubic ramus (23; 31 - 36) and may include additional scored traits as well as the morphology of the greater sciatic notch. However, while non-metric methods are a quick means of assessment, they tend to be extremely subjective. Attempts have been made to 'metricize' or quantify non-metric traits with success (37) in other regions of the body. By 'metricizing' specific non-metric traits in the pelvis, more objective data for sex estimation should be possible and repeatability should increase. Other pelvic indices such as those used in clinical medicine can be used to supplement measurements in the anthropological literature. Medical fields like obstetrics and gynecology regularly use metric measurements of the pelvis in their assessment and treatment of patients (38 - 40).

This study was undertaken to investigate whether three-dimensional volumetric virtual models can be used in the estimation of sex from the pelvis and if they can, whether 'metricizing' non-metric sex estimation traits in the pelvis and utilizing current medicine indices will increase the accuracy and reliability of the data over current methods. A sample of pelves from one hundred modern, living individuals was evaluated for sex using standard and novel measurements. The study was comprised of a number of elements: 1) landmarking and measurement of the sample; 2) metric evaluation of interobserver landmarking error; 3) interobserver error using traditional Phenice-derived sex estimation techniques;

4) discriminant function analysis to predict sex; 5) comparison of sex estimation results from FORDISC 3.0 (41) and this study; and 6) a preliminary evaluation of untrained observer accuracy.

In light of the recent NAS report (3), it is important to scrutinize current and future practices to ensure that they are robust. By studying individuals contemporaneous with those likely to end up on the anthropologist's examination table, this study attempts to provide data that can lead to more accurate biological profiles of unknown decedents.

Materials and Methods

Clinical Pelves Radiological Scans

For the purposes of this study, a random selection of abdominal CT scans taken of patients (FIGS 3.1 & 3.2) at the University of South Florida College of Medicine were used per institutional approval. The clinical data was anonymized

at the source and collected with informed patient consent.

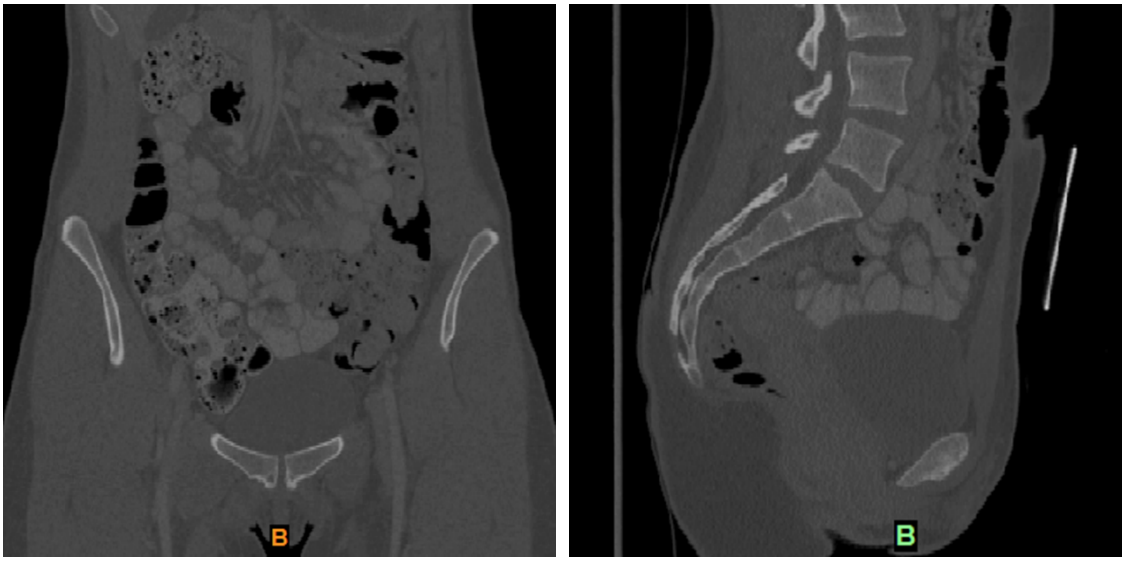

FIGURES 3.1 and 3.2: Images of a pelvic CT scan in the coronal and sagittal view.

A total of 100 individuals with known demographics and complete os coxae and sacra were evaluated to test the virtual determination of sex. The age range was 19 - 83, with a mean age of 49.7 (median 50). The sex distribution for the calibration sample was 40 males and 60 females. The average age of the males is 52.8 (range 19-80) and the average age of the females is 47.6 (range 20-83). When selecting the study participants, individuals with large surgical prosthesis, such as hip replacements, were excluded from the study as the implants cause artifacts or “flares” to appear on the DICOM images that occlude the acetabulum and distort other portions of the pelvis. The age and sex information was withheld from the observers during the measurement phase.

Three-dimensional (3D) Computer Reconstruction

Detailed 3D skeletal models were visualized from the DICOM slice data using *Mimics* v 13.1 (Materialise) (FIGS 3.3 & 3.4). The original DICOM data was set at a slice thickness of 1.25 mm. A mask was created to select for the bone pixels, and thresholding was adjusted to account for individual variation in bone density. The resultant pixel masks from the transverse (axial), coronal, and sagittal planes were converted to voxels by the software to produce a 3D bone model of the selected region(s) of the skeleton. For older individuals with marked osteoporosis, the threshold was manually entered in order to account for individual variation in bone density. Pixels from the femora were not selected to allow for observation of the acetabulum. These models can then be measured in *Mimics* or exported into most other 3D packages for further analyses. Accuracy of the virtual models has been verified in previous studies by the authors and other researchers (20).

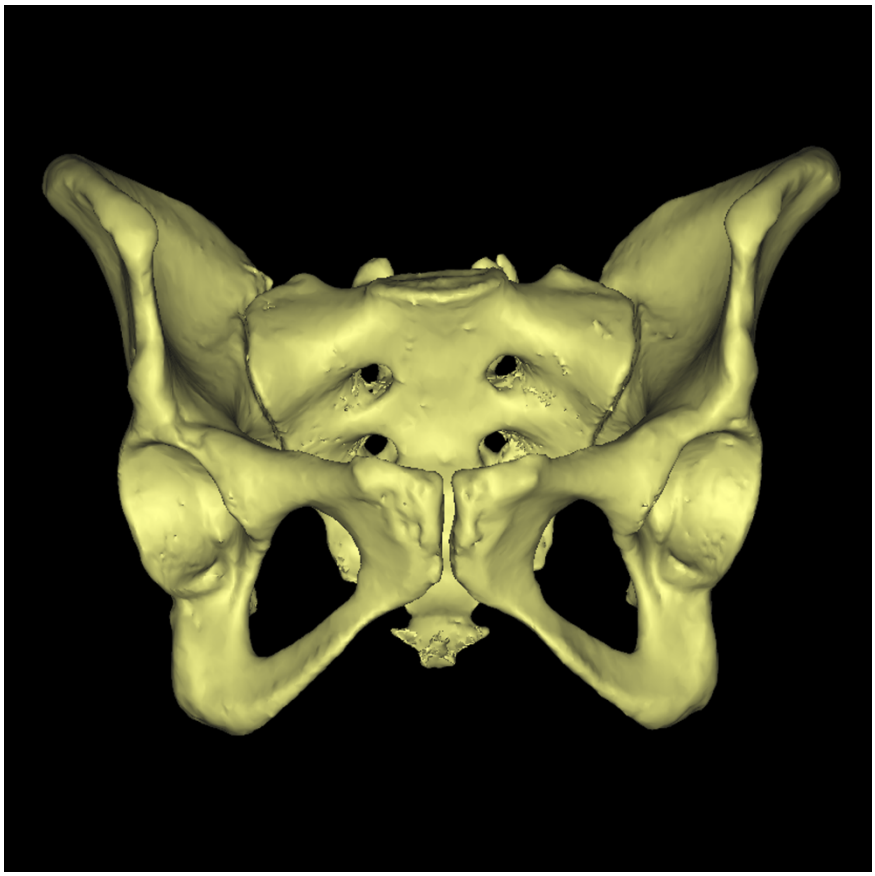

FIGURE 3.3: A virtual image of the pelvis created from CT data in the anterior view.

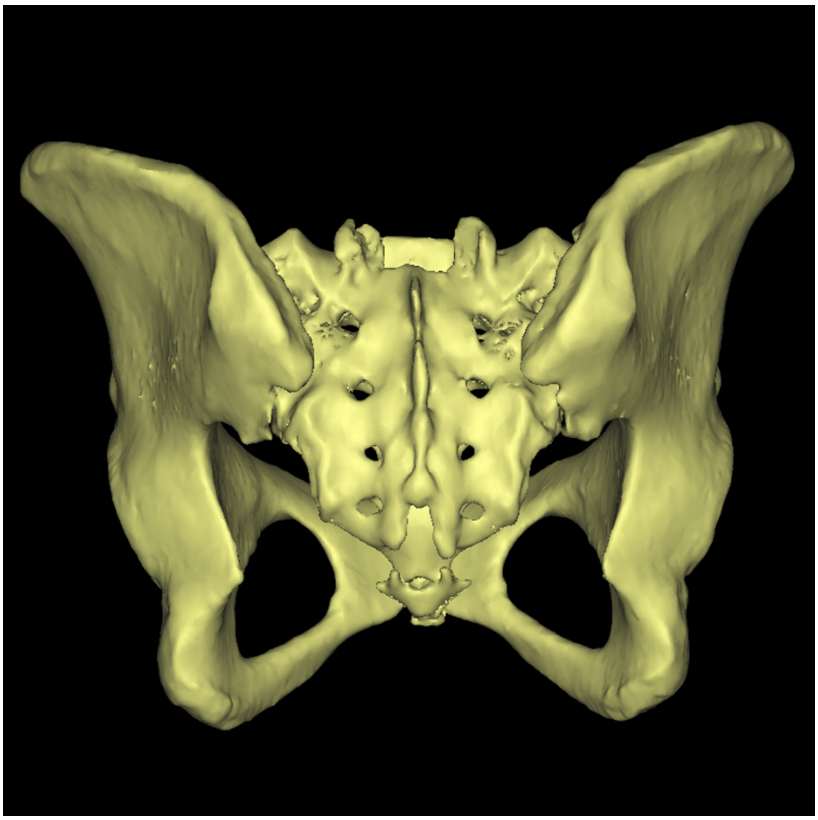

FIGURE 3.4: A virtual image of the pelvis created from CT data in the posterior view.

Virtual Sex Estimation: Osteological Measurements

A selection of both traditional and novel measurements were chosen for use in establishing sex in the pelvis. Decades of literature have demonstrated that features of pelvic morphology such as ventral pubic arc, subpubic concavity, width of the greater sciatic notch, presence/absence of the preauricular sulcus and ischiopubic ramus are highly successful in correct sex classification by trained observers (13; 14; 23; 32 - 34). However, correct classification suffers using less experienced observers. For this study, the measurements for the calibration sample were chosen to meet one or more of the following criteria: a commonly used measurement reported in the literature (e.g. ischium-pubic

index); a ‘metricized’ version of a traditional non-metric trait (e.g. greater sciatic notch, subpubic angle); or medical indices not traditionally applied to anthropology (e.g. conjugate inlet of true pelvis). A total of 35 landmarks (5 midline and 15 bilateral) were placed on each pelvis. Landmarks were located and marked by two trained anthropologists. Definitions are listed in Table 3.1, below. From these, 20 distances, angles, and anthropological and medical indices were calculated. The 20 variables listed in Table 3.2 were tested for their effectiveness in sex estimation.

An osteometric toolkit was designed for landmark placement in the *Mimics* software package (FIG 3.5) that allowed the researchers to examine the 20 variables. The observer would simply need to place a landmark at a location defined both in the handbook and in the toolkit itself. The software then calculates linear distances, angles, and indices between specified points. This data is output in a format ready for use in statistical analysis packages.

TABLE 3.1: List of landmarks with definitions

Landmark	**Definition**
Midline Points	
Coccyx	Most extreme tip of the coccyx
S Pubic Symphysis	Point at the most superior portion between both pubic symphyses (mark on left – this will be a near duplicate of AS left Pubic symphysis)
SCB	Mid Sagittal Point on Sacral/Coccyx Border
Sacral Promontory	Most superior, anterior point on the mid-sagittal plane
I Pubic Symphysis	Point at the most inferior portion between both pubic symphyses – *place on the left pubic symphysis*
Bilateral Points	
AS Pubic Symphysis	Most anterior superior point on the symphyseal surface
ASIS	Anterior Superior Iliac Spine
Acetabulum Junction	Junction of ilium, pubis, and ischium in the acetabulum
Greater Sciatic Notch	Deepest point in the GSN
Ischial Spine	Ischial spine (base of Greater Sciatic Notch)
Ischial Tuberosity	Most inferior point on the ischial tuberosity
Ischiopubic Ramus	Lowermost point on the left ischiopubic ramus
Lower Pubic Symphysis	Most inferior point on the symphyseal surface
PI Iliac Spine	Most inferior spine on the ilium at the Greater Sciatic Notch
PSIS	Posterior Superior Iliac Spine
Sacral Width	The superior portion of the sacrum at its widest point
Sacro-Lumbar Articular Surface	Most lateral point on the superior articular surface between the sacrum and lumbar vertebrae
Sup Iliac Crest	The most superior point on the iliac crest
Pelvic Inlet	Most mediolateral point of the ischium, looking superior to inferior. *The most lateral points on the interior of the pelvic brim*
Pelvic Outlet	Most mediolateral point of the ischium, looking inferior to superior

TABLE 3.2: Measurement descriptions

Measurement	Type	Landmark calculation
Anterior Breadth of the Sacrum	Distance (mm)	Maximum transverse projection of the sacrum at the anterior projection of the auricular surface
Anterior Height of Sacrum	Distance (mm)	Distance between the sacral promontory and SCB
Anteroposterior Pelvic Outlet Diameter	Distance (mm)	Distance from coccyx to inferior pubic symphysis
Conjugate Pelvic Inlet Diameter	Distance (mm)	Distance between sacral promontory and superior pubic symphysis
Pubic Symphysis Length	Distance (mm)	Distance between the most superior and inferior points of the pubic symphysis (taken at left side)
Sub Pubic Angle	Angle (degrees)	Angle between the iliac spine, deepest portion of the GSN and the ischial spine
Transverse Diameter of Sacral Segment 1	Distance (mm)	Distance between the 2 most lateral points of the 1st sacral segment
Transverse Pelvic Inlet	Distance (mm)	Widest medio-lateral points on the plane created by the sacral promontory and the most superior point of the pubic symphysis
Transverse Pelvic Outlet	Distance (mm)	Widest medio-lateral points on the plane created by the coccyx and the most inferior point of the pubic symphysis
Bilateral Measurements		
Illiac Breadth	Distance (mm)	Distance from ASIS to PSIS
Ischium Length	Distance (mm)	Distance from the acetabulum junction to the deepest point on the ischial tuberosity
Pubis Length	Distance (mm)	Distance from the point on the acetabulum junction to the superior point on the pubic symphysis
Width of Greater Sciatic Notch	Angle (degrees)	Angle between the iliac spine, deepest portion of the GSN and the ischial spine
Innominate Height	Distance (mm)	Distance from the most superior point on the iliac crest to the most inferior point on the ischial tuberosity

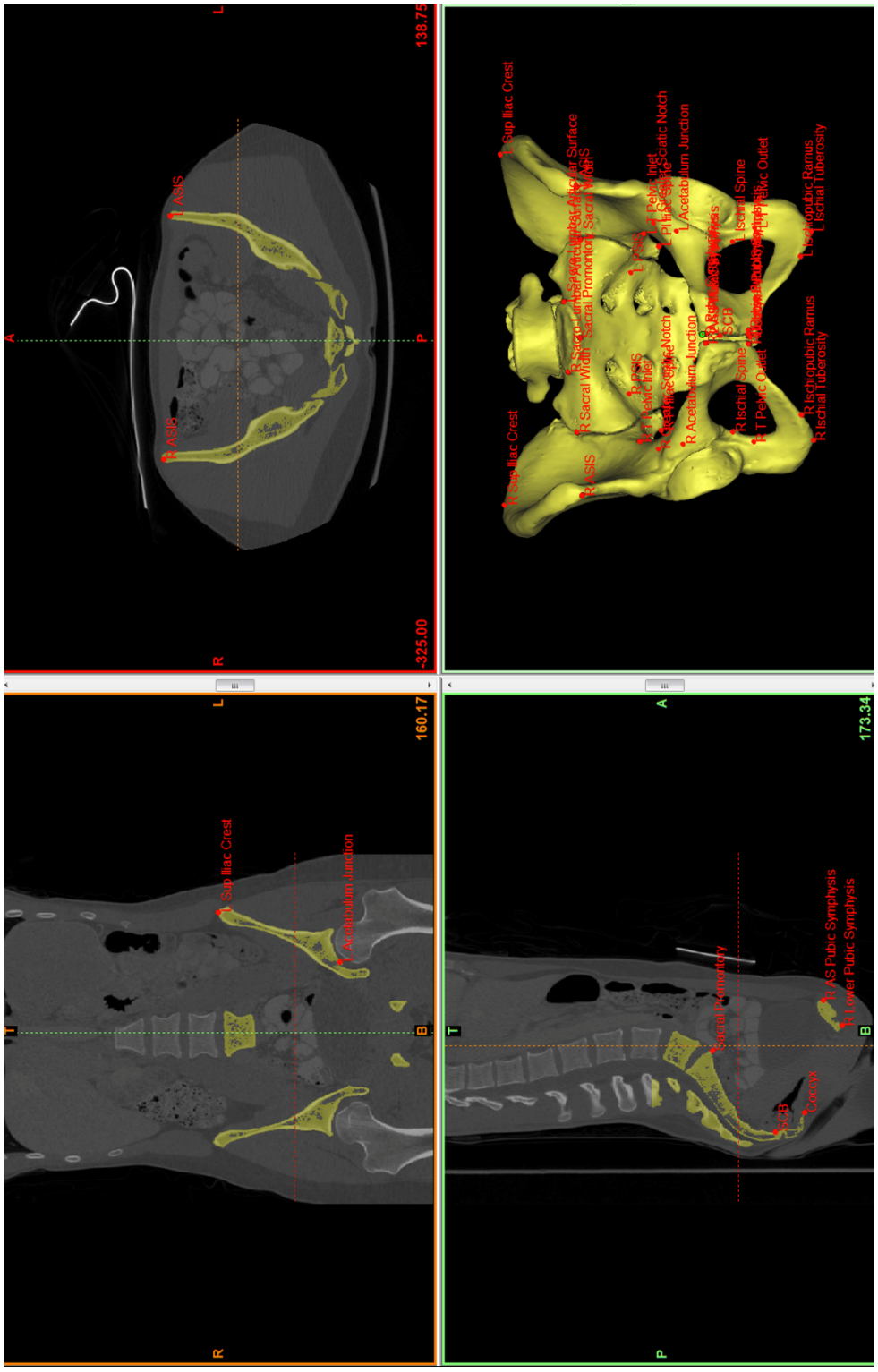

FIGURE 3.5: ***Mimics*** **user interface highlighting the 35 landmark points used for pelvimetric assessment indicated on the 2D pelvic mask as well as on the 3D model.**

Statistical Analysis

Data collected for this study was analyzed in the software package, *SPSS* version 18.0. To begin the analysis, measures of central tendency and descriptive statistics (mean, median, standard deviation, etc) were run to check for any errors in the data. Table 3.3 provides the mean values and standard deviations for all 20 variables across the sample of 100 individuals. A test of interobserver error was conducted to verify the repeatability and accuracy of the landmark placement and definitions of the novel measurements. A subset of 10 pelves from the original calibration sample were landmarked by two trained anthropologists (authors SJD and SDJ). The two observers were in separate locations at the time of landmarking and did not confer during the landmarking sessions. A Cohen's Kappa coefficient was also calculated to determine the level of agreement between observers (Table 3.4).

TABLE 3.3: Measures of central tendencies

Variable	Measurement Name	Male (Mean)	Male (SD)	Female (Mean)	Female (SD)
ABS	Anterior Breadth of the Sacrum	116.7	8.9	115.6	7.2
AHS	Anterior Height of Sacrum	114.2	16.2	109.8	11.2
APOD	Anteroposterior Pelvic Outlet Diameter	104.8	13.1	108.0	11.3
CPID	Conjugate Pelvic Inlet Diameter	119.6	11.7	126.8	8.7
LIB	L Iliac Breadth	164.9	11.6	155.3	8.6
LIL	L Ischium Length	95.6	7.6	83.3	5.8
LPL	L Pubis Length	91.6	8.2	90.7	7.2
LGSN	L Width of Greater Sciatic Notch	69.7	8.2	80.7	6.0
LIH	Left Innominate Height	220.1	13.6	193.0	12.0
PSL	Pubic Symphysis Length	35.4	4.9	29.9	4.2
RIL	R Ischium Length	96.5	7.3	83.4	4.8
RPL	R Pubis Length	89.7	8.8	89.3	8.4
RGSN	R Width of Greater Sciatic Notch	68.1	8.0	80.3	7.0
RIB	Right Illiac Breadth	164.9	12.0	155.5	8.9
RIH	Right Innominate Height	220.2	14.1	193.2	10.7
SPA	Sub Pubic Angle	71.4	7.8	82.9	5.7
TDSS	Transverse Diameter of Sacral Segment 1	55.7	6.3	48.8	6.1
TPI	Transverse Pelvic Inlet	122.3	8.7	130.1	9.3
TPO	Transverse Pelvic Outlet	100.8	7.1	118.4	9.1

All measurements in mm or degrees

TABLE 3.4: Measurement error

Variable	Measurement Name	Error (Mean)	Error (SD)
ABS	Anterior Breadth of the Sacrum	1.6%	1.6%
AHS	Anterior Height of Sacrum	1.6%	2.3%
APOD	Anteroposterior Pelvic Outlet Diameter	3.1%	2.0%
CPID	Conjugate Pelvic Inlet Diameter	0.9%	0.7%
LIB	L Iliac Breadth	1.1%	1.4%
LIL	L Ischium Length	3.9%	2.2%
LPL	L Pubis Length	4.2%	2.5%
LGSN	L Width of Greater Sciatic Notch	1.9%	1.7%
LIH	Left Innominate Height	2.2%	1.3%
PSL	Pubic Symphysis Length	3.5%	2.3%
RIL	R Ischium Length	3.1%	2.3%
RPL	R Pubis Length	2.9%	1.8%
RGSN	R Width of Greater Sciatic Notch	2.1%	1.7%
RIB	Right Illiac Breadth	0.5%	0.4%
RIH	Right Innominate Height	2.2%	1.8%
SPA	Sub Pubic Angle	3.5%	2.4%
TDSS	Transverse Diameter of Sacral Segment 1	2.0%	1.3%
TPI	Transverse Pelvic Inlet	0.8%	0.6%
TPO	Transverse Pelvic Outlet	1.2%	1.1%
Average		**2.2%**	
N = 10			

A Pearson's Correlation test was performed to determine which of the variables were the highest predictors of sex. From the correlation study, the four variables with the highest influence were: innominate height, greater sciatic notch angle, subpubic angle and transverse pelvic outlet. These four represented a combination of both anthropological and medical variables. A binary logistic regression was performed using these four variables with male coded as 0 and female coded as 1. This regression was used to develop the four-variable formula for sex estimation. Once the variables were identified, a discriminant

function was performed on the four variables to establish cross-validated classification results.

A group of further individuals not included in the calibration sample was landmarked to verify the robustness of the calibration sample findings. This test group consisted of 2 males and 3 females, with an age range of 37-54 (mean 48.6). A leave one out cross-validation test was run to determine the robusticity of the results on a holdout sample.

Fordisc 3.0 Analysis

In order to compare our results to the current field standard, the data was run through the software package, *Fordisc version 3.0* (41). In *Fordisc*, there are seven variables measured on the os coxae and sacrum with published levels of accuracy. They are: sacral length, sacral breadth, sacral breadth at segment 1, innominate height, iliac breadth, pubic length, and ischial length. Results for this portion of the study were compared back to the formula established in the previous portion.

Results

3D modeling and virtual measurements

From the import of the DICOM images to output of the data, the time taken for each specimen was dependent on the type of computer used and the

observer's experience and familiarity with the software. The import of the images and the making of the model took approximately 20 minutes per case. The landmarking and measurements took approximately 10-15 minutes per case.

Sex Assessment

In order to establish which measurements were best in assessing sex in the pelvis, averages for the measurements were calculated for each sex. Table 3.3 displays the averages of each variable used in the study broken down by sex.

In the interobserver error test, the results of 10 measured specimens from each anthropologist were compared. The error rates ranged from 0.51% to 4.21%. The overall error average between both observers was only 2.22%, which is well below the accepted range of error (23). Table 3.4 demonstrates the error ranges by variable. The calculated Cohen's Kappa coefficient was determined to be 1.0, which indicates an almost perfect agreement between observers that is not a result of chance.

The Pearson correlation test listed which variables indicated the highest influence on sex estimation. 11 variables of the 20 original variables were determined to be statistically significant at the 0.01 level of a two-tailed test. The variables with the highest loadings were selected and narrowed down to: innominate height, greater sciatic notch angle, subpubic angle and transverse pelvic outlet. The Pearson's test demonstrated strong correlations between

measurements that were bilateral. Comparisons were made between both left and right innominates and the variation was found to be negligible. Therefore, only the left side of the pelvis was used for the statistical model to prevent any duplication or artificial inflation of the results.

The binary logistic regression provided a four-variable formula that was useful for calculating sex from pelvis. For this formula, each sex was coded as males = 0 and females = 1. The formula for estimating sex from the pelvis in this study is listed in Table 3.5. For the calibration sample, the accuracy for the formula was 100% in both males and females with a p-value of 0.001 (Table 3.6). The canonical discriminant function run on the calibration dataset had a 100% cross-validated group classification accuracy rate also with a p-value of 0.001. Results are shown in Table 3.7.

TABLE 3.5: Four-variable model for sex estimation

Sex = (0.859 x LGSN) + (-1.799 x LIH) + (3.867 x TPO) + (1.786 x SPA)-244.41

Sex, >0 individual is female, <0 is male.

TABLE 3.6: Accuracy of four-variable method

Accuracy of four-variable method		
Male	40/40	100%
Female	60/60	100%
Total	100/100	100%

TABLE 3.7: Four-variable cross validation test

Classification Results[b,c]					
		Sex	Predicted Group Membership		
			0	1	Total
Original	Count	0	40	0	40
		1	0	60	60
	%	0	100.0	.0	100.0
		1	.0	100.0	100.0
Cross-validated[a]	Count	0	40	2	40
		1	0	60	60
	%	0	100.0	.0	100.0
		1	.0	100.0	100.0

a. Cross validation is done only for those cases in the analysis. In cross validation, each case is classified by the functions derived from all cases other than that case.
b. 100.0% of original grouped cases correctly classified.
c. 100.0% of cross-validated grouped cases correctly classified.

The leave one out cross-validation test was run on the five specimen sample that had not been included in the calibration sample. The method resulted in a 100% accuracy classification rate for the specimens.

For the *Fordisc* portion of the study, all of the specimens in the calibration sample were run in the software for all seven variables that are used in the sacral and os coxae analysis. The results showed that the male specimens were correctly classified 67.50% of the time and the females were classified 98.30% of the time. Overall, the *Fordisc* analysis correctly classified the specimens' sex approximately 86% of the time (Table 3.8).

TABLE 3.8: Accuracy of *Fordisc 3.0* method

Accuracy of Fordisc		
Male	27/40	67.5%
Female	59/60	98.3%
Total	86/100	86.0%

The overall accuracy of our model was 100% and indicates an increase in accuracy over current anthropological methodologies. Further studies are needed to confirm these findings using a larger sample of observers.

Discussion and Conclusion

This study demonstrates that it is possible to estimate sex accurately (100% with a p-value of 0.001) in three-dimensional (3D) virtual pelvic models derived from computed tomography (CT) scans. Medical image data provides the opportunity for high-end forensic analysis to be conducted outside the usual confines of traditional anthropological procedures. Imaging modalities such as CT are extensively used in the diagnosis and treatment of patients in a clinical setting. Their reliability has been well-documented for years through radiological research. 3D imaging has tremendously expanded in the past few years with increases in scanner technology. This study utilized medical image data from state-of-the-art 64-slice CT scanners which are quickly becoming the field standard. These scanners are capable of scanning a full body in less than one

minute at a high-resolution slice (0.625 mm). With CT's speed and its ability to capture high-level detail of boney features without having to remove soft tissue, it becomes an ideal tool to save time and to protect remains from physical manipulation. Remains can be examined without the need for defleshing.

Additionally, current studies are showing that medical imaging and modeling are allowing for remote analyses without assuming chain of custody of the evidence (18). This permits local and federal law enforcement agencies to securely transfer data and have access to experts beyond their geographic location. Forensic pathologists are now using medical imaging, 3D modeling, and specialized biopsies to supplement the traditional autopsy in a process called "Virtopsy". These methods also allow for the archiving of case-related data that can be used long past when the remains have been buried (42).

The speed with which the virtual bone models and measurements were generated (20-30 minutes per case) in this study makes the method a practical alternative to traditional analyses. Our interobserver error test results illustrate the accuracy and repeatability of the method by trained anthropologists. However beyond accuracy, it is important for new methods of analyses to be accessible enough to be used by practitioners at different levels of training. To investigate this, a preliminary user friendliness study with student users was conducted with positive initial results. Three upper level undergraduate students at Liverpool John Moores University who had completed a course in Osteology were recruited

to explore the impact of experience on our virtual method. None of the students had ever used the software before the test. Each student was independently provided with the same unknown virtual pelvis and training manual. The students were first asked to assess the pelvis using traditional non-metric traits. The results showed differences between each observer using traditional non-metric observations. For example, the greater sciatic notch was scored by the students between a 2, 3, and 4. Though there were differences in the scorings, each student classified the pelvis correctly. Next, the students were asked to landmark and measure the virtual pelvis using the method outlined in this study. The results could be directly compared and were reasonably accurate with a higher error rate than with the trained observers. While this method was proven to be reproducible for trained practitioners, it is highly recommended that users have training in both forensic anthropological and radiological methods. Future studies may expand the number of observers to test the impact of experience more fully.

This study also highlights the effectiveness of ‘metricizing’ non-metric traits. Phenice traits in the pelvis have been shown to be significant in the estimation of sex. However, in answering the congressional call for more quantifiable methods in forensic science, ‘metricizing’ non-metric traits allows researchers to move away from subjective scored (on a scale of 1-5) analyses towards more objective methodologies. The four variable formula derived in this study illustrates the strength of combining ‘metricized’ traits with medical indices, such as the transverse pelvic outlet. We found that traditional anthropological

literature differed from current medical standards in the areas of sub-pubic angle and pelvic outlets. These discrepancies made a significant difference in the successful classification of sex in our calibration sample. When analyzing the subpubic angle, it is recommended by anthropologists that any pelvis <90° is male (24), however, this study found that a large portion of the females would have been misclassified as males if this standard was followed. The angles in the study for females were found to be closer to 78-83°; this assertion is also reflected in current obstetric literature (38-40).

In *Fordisc 3.0 (41)*, skeletal remains are classified using numerous osteological metric variables. For the innominate and sacral complex, there are 7 variables that the software uses to estimate sex. These variables are based on metric measurements that do not completely characterize the unique three-dimensional geometry of the pelvic anatomy needed to distinguish between the sexes. While overall in our study *Fordisc* correctly classified the specimens' sex approximately 86% of the time, the results showed that the male specimens were only correctly classified 67.50% of the time. It is suggested that this discrepancy in classification rates is due to either too much "noise" introduced by the 7 variables used by *Fordisc 3.0* or the lack of consideration of non-metric variables. By adding 'metricized' non-metric traits and current medical indices into our four variable formula, the authors hypothesize that classification rates for sex in the pelvis will increase.

This subsequently brings into question, how does our dataset differ from traditional skeletal collections and thus, current field data sources? The samples used in this study were a 100% modern population from clinical patients scanned at the University of South Florida College of Medicine. Most anthropological samples are skewed toward older adults due to availability in current collections, however it has been reported that elderly individuals demonstrate less sexual dimorphism (8, 36), so it is theorized that the method for successful sex discrimination in this sample is more robust since they represent a larger sample of younger individuals with wide overall age range (19-83 years). Furthermore, most anthropological osteology collections are archaeological in nature and therefore, do not currently best represent the remains that are most common in forensic cases.

One potential limitation of this study is that we used complete, intact pelves. We acknowledge that unlike our data set, in many cases the remains examined in an anthropological setting may be incomplete or fragmented. By utilizing additional aspects of the 3D software in which the remains are measured, fragmented remains can be reconstructed in virtual space. Additionally, the study reveals that that the most important characteristics in sex discrimination in this population (innominate height, greater sciatic notch angle, subpubic angle and transverse pelvic outlet), require only the presence of one innominate and the sacrum.

To increase the value of datasets like the one utilized in this study, more information should be gathered such as ancestry of the patient. The anonymized patient data did not include the patient's ancestral background so it is unclear at this time what role, if any, race played in the classification of sex of this calibration sample. By collecting more clinical data, we will be able to better understand patterned phenotypic variation in modern human populations.

In summary, the establishment of the biological profile (age, sex, stature and ancestry) from human remains is at the core of the forensic anthropologist's training and practice. This study demonstrates the value of CT data for making detailed virtual models of the pelvis that can be analyzed beyond contact with the actual bone. From these 3D models, a novel, accurate formula for sex estimation was developed using 'metricized' non-metric traits and medical indices. The proposed method in this study represents a quick, reliable alternative to traditional anthropological methodologies used in establishing sex from the pelvis.

Acknowledgements

The authors would like to especially thank our respective institutions, the University of South Florida College of Medicine and Liverpool John Moores University, and our departments for their support of our continued collaboration.

We would also like to recognize the USF Health Imaging Centers (Morsani and South), particularly Melanie O'Brien and Matthew Woods, and Dr. Ren Chen of the USF Health Biostatistics Core for their assistance in different phases of this project. We would like to acknowledge J. Burns, K. Clarke, and C. Armstrong at LJMU for their participation in the study.

This study was supported in part by the University of South Florida Clinical and Translational Science Institute.

CHAPTER 4

3D MODELING AND MORPHOMETRIC ANALYSIS OF VIRTUAL CRANIAL ANATOMY

Abstract

The human skull is the most important region of the body for personal identification from bone. From the skull alone, we can estimate sex, age, ancestry, pathologies and trauma. In this study, a series of cadaveric and clinical craniofacial computed tomography (CT) scans with known demographic information were used to evaluate the ability of three-dimensional (3D) virtual skulls to address the establishment of the biological profile in bone, such as in sex estimation. The skull data was 3D modeled and measured using a combination of traditional and novel landmarks. A seven-variable discriminant function for sex estimation was developed based on statistical analyses. Overall, the cross-validated accuracy of the method was 95.1%. Comparative analysis was run on the virtual data set in *Fordisc 3.0*. This study shows that 3D computed models of skulls can be used as accurate representations of the actual skull and that virtual analyses provide an increase in accuracy over traditional methodologies.

Introduction

From the time of the National Library of Medicine's Visible Human Project (1 - 2), researchers have attempted to use human cadavers to extract three-dimensional (3D) volumetric data from medical images for anatomical studies. Medical imaging advances also are providing an opportunity to use clinical scans to establish virtual databases of normal anatomy. In the first phase of the project, we determined that anatomically accurate models of dry skulls could be made from 3D modeling of volumetric medical images (Chapter 2). In this next phase, the study will be expanded to include computed tomography (CT) scans of fixed cadaveric material as well as clinical patient data for computer modeling and morphometric analyses of the skull.

This study was undertaken to investigate whether 3D volumetric virtual models can be used in the estimation of the sex from the skull and if they can, whether virtual analyses will increase the accuracy and reliability of the data over current methods. A sample of skulls from 81 modern individuals was evaluated for sex using standard and novel measurements. The study was comprised of a number of elements: 1) the extraction of 3D virtual bony models from cadaveric and clinical CT scans 2) landmarking and measurement of the sample; 3) discriminant function analysis to predict sex; and 4) comparison of sex estimation results between FORDISC 3.0 (3) and this study.

Sex estimation is one of the principal components of the biological profile in the human skeleton. Next to the pelvis, the skull is second best region of the body for estimating sex due to its unique sexual dimorphism (4). A combination of traditional metric measurements and non-metric indices are used to document the robusticity of the male skull or the gracile nature of the female skull (5 - 6). Specific regions of the skull like the glabellar, mastoid, and nuchal regions are scored on a scale of 1-5 but are quite subjective. (7). Many of the modern standards for sex estimation have been established on historical or even ancient populations (Smithsonian Terry Collection) and of those, many of the remains are undocumented. Current standards need to be re-addressed with modern documented skeletal collections.

In light of the scarcity of modern human anatomical materials for education and research purposes, it is imperative that anatomically accurate alternative resources be developed. It is the goal of this project to ascertain if 3D computed models of cranial anatomy could serve as substitutes for the handling and analysis of actual human skulls.

Materials and Methods

Cadaveric Head Radiological Scans

In November 2007, all of the cadavers obtained for University of South Florida's Medical Gross Anatomy course were full-body scanned on a GE MSCT 8-slice scanner. In total, 38 cadavers were scanned at a 3mm slice thickness and heads at a 1mm slice thickness.

Increasing Scan Resolution

In 2008, we scanned the cadavers at the highest resolution possible on a GE LightSpeed VCT 64-slice scanner at USF Health's South Campus and USF Health's Morsani Center to bring the total to 64. We increased the scan resolution by decreasing the slice thickness from 3mm to 1mm to a resolution of 0.625 mm. Several cadavers were scanned at multiple resolutions and those scans will be compared to determine the level and quality of anatomical data available at each resolution. The goal of this portion of the project is to increase the "*n*" of the cadaver scans to database of statistical significance. All the DICOM data was stored for evaluation and computer modeling.

A total of 60 adult individuals (38 at 1mm slices and 22 at 0.625mm slices) with known demographics and complete heads were evaluated to test the usability of computed skulls in the virtual determination of sex. The age range was 53 – 96, with a mean age of 79.03 (median 85.5). The sex distribution for the

calibration sample was 24 males and 36 females. The average age of the males is 78.3 (range 62 - 93) and the average age of the females is 79.5 (range 53 - 96). Cadavers that did not have complete heads or were sub-adult were excluded for this study. The age and sex information was withheld from the observer during the measurement phase.

Clinical Head Radiological Scans

In order to compare scanning resolution between fixed cadaveric tissue and living individuals, we examined the imaging and computer-modeling properties of clinical patient scans. For the purposes of this study, a random selection of craniofacial CT scans taken of patients at the University of South Florida College of Medicine were used per institutional approval. The clinical data was anonymized at the source and collected with informed patient consent. Only age, sex, and scan description were documented beyond the technical meta-data (IRB approved). The deidentified medical scans were from the “Cyberknife” pre-operative scan protocol since they include all craniofacial geometry and the scans terminate beneath the mandible. This scan is usually conducted for patients with brain lesions or tumors, which should not interfere with the craniofacial anatomy.

From the clinical sample, a total of 21 individuals with known demographics and complete cranial anatomy were evaluated for our virtual determination of sex study. The age range was 33 - 85, with a mean age of 62.9

(median 70). The sex distribution for calibration sample was 6 males and 15 females. The average age of the males is 59.67 (range 35-80) and the average age of the females is 64.2 (range 33-85). When selecting the study participants, individuals with extensive metallic dental implants such as crowns or partials, were excluded from the study as the implants cause artifacts or “flares” to appear on the DICOM images that occlude portions of the skull and distort other portions of the face. The age and sex information was withheld from the observer during the measurement phase.

In total the complete sample for this project with both cadaveric and clinical data was 81 individual CT scans. There were a total of 30 males and 51 females included. The overall mean age was 74.9 (median 79) with an age range of 33- 96. The mean age for the males was 74.6 (range 35 - 93) and the mean age for the females was 75 (range 33 - 96). The ancestry of the sample population was unknown and therefore, not included in the analysis.

Three-dimensional (3D) Computer Reconstruction

Once the cadaveric and clinical DICOM data is extracted from the scanner, it was imported into the 3D visualization software packages *Mimics* © version 13.1 (Materialise) and *OsiriX* © (Rosset). The computer models were made using protocols previously established by our lab (8). The bone pixels were isolated in the data set in order to extract the skull from the surrounding soft tissue. The facial soft tissue data of both the cadaver and clinical scans were

ignored since this is outside the scope of the current project. The models were cleaned of artifact in the engineering software package 3Matics © version 4.4 (Materialise) and saved as Stereolithographic (stl) files for analysis and/or rapid prototyping. Accuracy of the virtual models has been verified in previous studies by the authors and other researchers (8).

Virtual Sex Estimation: Osteological Measurements

A selection of both traditional and novel measurements were chosen for use in establishing sex in the skull. Years of extensive research have demonstrated the effectiveness of cranial regions such as the glabella, mastoid, and mandible for estimating sex in the skeleton (4; 9 - 10). For this study, the measurements for the calibration sample were chosen to meet one or more of the following criteria: a commonly used measurement reported in the literature (e.g. Cranial Length) or a 'metricized' version of a traditional non-metric trait (e.g. 'robusticity' of the glabella). A total of 71 landmarks were placed on each skull (15 midline and 28 bilateral pairs). Definitions are listed in Table 4.1, below. From these, 35 distances, angles, and anthropological indices were calculated. The 35 variables listed in Table 4.2 were tested for their effectiveness in sex estimation.

An osteometric toolkit was designed for landmark placement in the *Mimics* software package (FIG 4.1) that allowed the researchers to examine the 35 variables. The observer would simply need to place a landmark at a location defined in the toolkit itself. The software then calculates linear distances, angles,

and indices between specified points. This data is output in a format ready for use in statistical analysis packages.

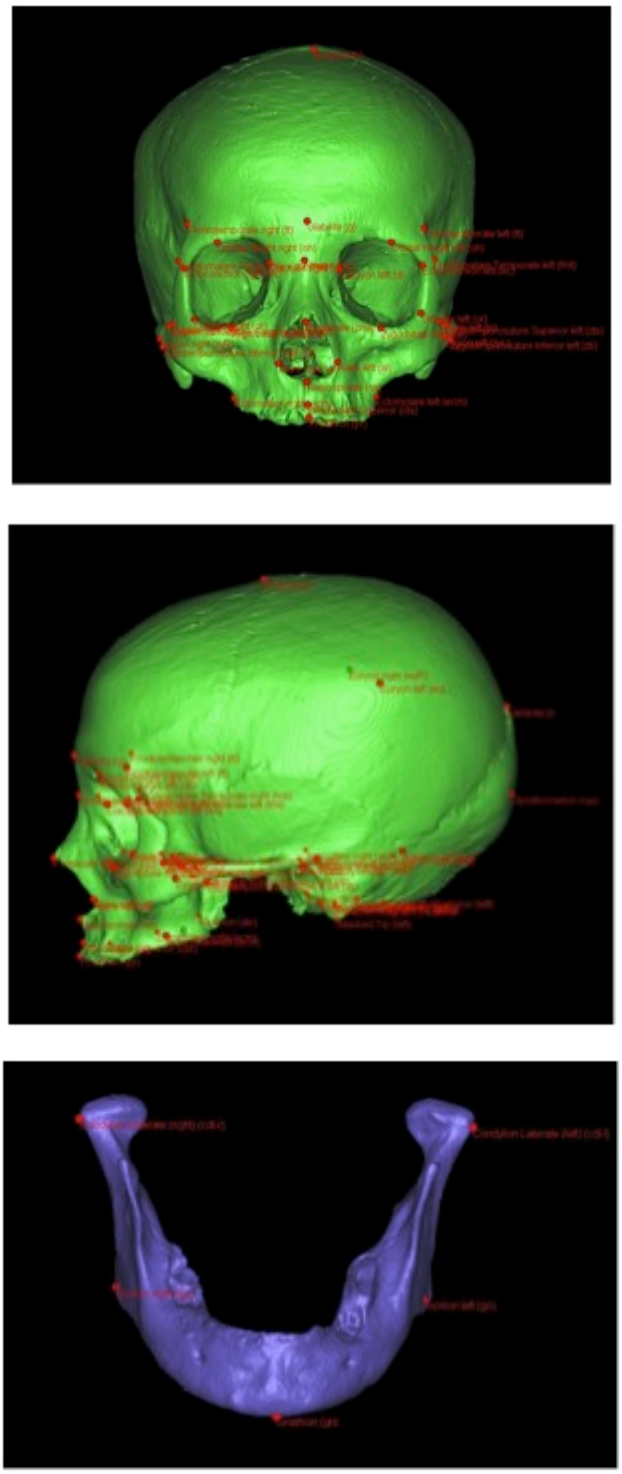

FIGURE 4.1: 3D model with measurements shown in the a) norma frontalis view, b) in norma lateralis aligned to the Frankfort Horizontal Plane, and c) the mandible

TABLE 4.1: List of landmarks with definitions

Landmark	Definition
Midline Points	
Alveolon	The point on the hard palate where a line drawn through the most posterior points of the alveolar ridges crosses the palate
Basion (ba)	The median point of the anterior border of the foramen magnum
Bregma (b)	The midline point where the coronal and sagittal sutures intersect
Gabella (g)	The most anterior midline point on the frontal bone, usually above the frontonasal suture.
Gnathion (gn)	The most inferior midline point on the mandible.
Infradentale Superior (ids)	The upper alveolar point; the apex of the septum between the upper incisors
Lambda (l)	The junction of the sagittal and lambdoid sutures
Nasion (na)	The point of intersection between the frontonasal suture and the midsagittal plane
Nasal 6 (n6)	The deepest point on where the two nasals meet at the midline
Nasiospinale (ns)	The point where a line drawn between the lower margins of the right and left nasal apertures is intersected by the midsagittal plane
Olare (ol)	The most forward point of the intermaxillary suture on the oral surface of the alveolar process
Opisthocranion (op)	The most posterior point of the skull not on the external occipital protuberance
Opisthion (o)	The midline point at the posterior margin of the foramen magnum
Pronasale (pna)	The most projecting point of the nasal tip; the point of the nose
Prosthion (pr)	The most anterior point in the midline on the alveolar processes of the maxillae
Bilateral Points	
Alare (al)	The most lateral point on the nasal aperture taken perpendicular to the nasal height
Asterion (ast)	The junction of the temporoparietal, lambdoid and temporo-occipital sutures
Auriculare (au)	A point on the most lateral aspect of the root of the zygomatic process at the deepest incurvature, whereever it may be.
Condylion Laterale (cl)	The most lateral point on the mandibular condyle
Dacryon (d)	The point on the medial border of the orbit at which the frontal, lacrimal, and maxilla intersect
Ectoconchion (ec)	The point of maximum breadth on the lateral wall of the eye orbit
Ectomolare (ecm)	The most lateral point on the outer surface of the alveolar borders of the maxilla, often opposite the middle of the second molar tooth

External Auditory Meatus (eam)	The upper border of the external auditory meatus
Foramen Magnum Lateral	Most lateral point of the foramen magnum
Frontomalare Temporale (fmt)	The most laterally positioned point on the fronto-malar suture
Frontotemporale (ft)	The point where the temporal line reaches its most anteromedial position on the frontal.
Gonion (go)	A point along the rounded posteroinferior corner of the mandible between the ramus and the body.
Jugale (ju)	The point in the depth of the notch between the temporal and frontal processes of the zygomatic
Mastoid Breadth Anterior	The most anterior portion of the mastoid at the widest point.
Mastoid Breadth Posterior	The most posterior portion of the mastoid at the widest point.
Mastoid Tip	The lower most tip of the mastoid process.
Maxilliofrontale (mf)	The point of intersection of the anterior lacrimal crest (medial edge of the eye orbit)
Nasioalare (nal)	Most inferior nasal border
Orbit Height (oh)	Superior midline point on the upper orbital rim used in craniometric measurement for orbital height
Orbit 2 (o2)	When picturing the orbit as a rectangle, the most superior, lateral point on the upper orbital rim
Orbit 3 (o3)	When picturing the orbit as a rectangle, on the zygomatic, the most inferior, lateral, oblique point on the lower orbital rim (often diagonal from *o1*)
Orbit 4 (o4)	Termination point of the lower orbital ridge on the maxilla; inferior to *d* and *mf*
Orbitale (or)	The lowest point in the margin of the orbit
Zygion	The most lateral point on the zygomatic arch.
Zygomatic 1 (zy1)	Zygomatic tubercle inferior to *fmt*
Zygomatic 2 (zy2)	The most anterior central point on the zygomatic
Zygomaxillare (zma)	The most inferior point on the zygomaticomaxillary suture
Zygorbitale (zyo)	The point where the orbital rim intersects the zygomaticomaxillary suture

TABLE 4.2: Measurement descriptions

Measurement	Type	Landmark calculation
AUB	Distance (mm)	Biauricular Breadth
BBH	Distance (mm)	Basion-Bregma Height
BCB	Distance (mm)	Bicondylar Breadth
BNL	Distance (mm)	Cranial Base Length
BOB	Distance (mm)	Biorbital Breadth
BPL	Angle (degrees)	Basion-Prosthion Length
FC	Distance (mm)	Frontal Chord
FMB	Distance (mm)	Foramen Magnum Breadth
FML	Distance (mm)	Foramen Magnum Length
FMT	Distance (mm)	Upper Facial Breadth
GA	Distance (mm)	Max Cranial Length
GOL	Angle (degrees)	Gabellar Angle
IOB	Distance (mm)	Interorbital Breadth
MAB	Distance (mm)	Maxillo-Alveolar Breadth
MAL	Distance (mm)	Maxillo-Alveolar Length
MBB	Distance (mm)	Mandibular Body Breadth
MBD	Distance (mm)	Mastoid Breadth
MBH	Distance (mm)	Mandibular Body Height
MDH	Distance (mm)	Mastoid Height
MNG	Angle (degrees)	Mandibular Angle
MNL	Distance (mm)	Mandibular Length
MiRB	Distance (mm)	Minimum Ramus Breadth
MxRB	Distance (mm)	Maximum Ramus Breadth
MxRH	Distance (mm)	Minimum Ramus Heigth
NAH	Distance (mm)	Upper Facial Height
NHH	Distance (mm)	Nasal Height
NLB	Distance (mm)	Nasal Breadth
OBB	Distance (mm)	Orbital Breadth
OBH	Distance (mm)	Orbital Height
OC	Distance (mm)	Occipital Chord
PC	Distance (mm)	Parietal Chord
UFA	Angle (degrees)	Upper Facial Angle
WFB	Distance (mm)	Minimum Frontal Breadth
XCB	Distance (mm)	Max Cranial Breadth
ZYB	Distance (mm)	Bizygomatic Diameter

Statistical Analysis

Data collected for this study was analyzed in the software package, *SPSS* version 18.0. To begin the analysis, measures of central tendency and descriptive statistics (mean, median, standard deviation, etc) were run to check for any errors in the data. Table 4.3 provides the mean values and standard deviations for all 35 variables across the sample of 81 individuals.

TABLE 4.3: Measures of central tendencies

Variable	Measurement Name	Male (Mean)	Male (SD)	Female (Mean)	Female (SD)
AUB	Biauricular Breadth	128.9	5.0	121.0	5.2
BBH	Basion-Bregma Height	140.3	5.7	133.2	5.1
BCB	Bicondylar Breadth	124.8	4.6	116.9	4.9
BNL	Cranial Base Length	106.5	4.9	99.8	4.2
BOB	Biorbital Breadth	100.8	4.2	96.1	3.2
BPL	Basion-Prosthion Length	96.8	5.1	90.8	5.0
FC	Frontal Chord	116.4	6.9	111.2	4.2
FMB	Foramen Magnum Breadth	32.0	3.4	30.7	3.0
FML	Foramen Magnum Length	38.4	3.9	36.9	2.9
FMT	Upper Facial Breadth	108.4	4.8	103.3	3.0
GA	Gabellar Angle	126.4	10.2	139.0	9.8
GOL	Max Cranial Length	191.3	7.0	179.8	6.2
IOB	Interorbital Breadth	22.3	3.4	22.0	2.9
MAB	Maxillo-Alveolar Breadth	58.7	6.1	58.0	6.1
MAL	Maxillo-Alveolar Length	51.5	3.5	48.9	3.5
MBB	Mandibular Body Breadth	100.7	4.1	92.9	4.5
MBD	Mastoid Breadth	23.1	4.3	21.0	3.8
MBH	Mandibular Height	55.2	7.1	49.3	6.4
MDH	Mastoid Height	34.5	3.1	30.8	3.4
MNG	Mandibular Angle	118.9	5.4	121.1	4.1
MNL	Mandibular Length	85.1	5.7	80.1	5.1
MiRB	Minimum Ramus Breadth	25.9	2.7	23.6	1.7
MxRB	Maximum Ramus Breadth	25.9	2.7	23.6	1.7
MxRH	Minimum Ramus Heigt	58.5	3.6	50.7	4.1
NAH	Upper Facial Height	60.8	4.2	57.6	3.9
NHH	Nasal Height	52.7	3.0	48.8	3.1
NLB	Nasal Breadth	25.9	2.7	23.6	1.7
OBB	Orbital Breadth	40.2	2.5	38.4	1.7
OBH	Orbital Height	34.6	1.9	34.4	2.1
OC	Occipital Chord	100.6	5.7	97.8	6.8
PC	Parietal Chord	123.0	7.8	116.9	7.1
UFA	Upper Fascial Angle	117.2	8.5	128.2	8.2
WFB	Minimum Frontal Breadth	116.6	7.1	111.2	5.8
XCB	Max Cranial Breadth	145.0	6.5	138.6	4.3
ZYB	Bizygomatic Diameter	133.1	5.0	124.4	3.8

All measurements in mm or degrees

A Pearson's Correlation test was performed to determine which of the variables were the highest predictors of sex. From the correlation study, the seven variables with the highest influence were: biauricular breadth (AUB), bicondylar breadth (BCB), basion-nasion length (BNL), maximum length (GOL), mandibular body breadth (MBB), maximum ramus height (MxRH), and bizygomatic breadth (ZYB). These seven represented a combination of both traditional and non-traditional variables. A binary logistic regression was performed using these seven variables with male coded as 0 and female coded as 1. This regression was used to develop the seven-variable formula for sex estimation. Once the variables were identified, a discriminant function was performed on the seven variables to establish cross-validated classification results.

Fordisc 3.0 Analysis

In order to compare our results to the current field standard, the data was run through the software package, *Fordisc version 3.0* (41). In *Fordisc*, there are 30 variables measured on the skull with published levels of accuracy. They include but are not limited to: cranial length, cranial breadth, bizygomatic breadth, orbital height and width, facial height, and mandibular length and breadth. Results for this portion of the study were compared back to the formula established in the previous section.

Results

3D modeling and virtual measurements

From the import of the DICOM images to output of the data, the time taken for each specimen was dependent on the type of computer used and the observer's experience and familiarity with the software. The import of the images and the making of the model took approximately 45 - 60 minutes per case. The increased time was due to removal of any flair from metallic crowns. The landmarking and measurements took approximately 25 - 30 minutes per case.

Sex Assessment

The Pearson correlation test listed which variables indicated the highest influence on sex estimation. 26 variables of the 35 original variables were determined to be statistically significant at the 0.01 level of a two-tailed test. The variables with the highest loadings were selected and narrowed down to: biauricular breadth (AUB), bicondylar breadth (BCB), basion-nasion length (BNL), maximum length (GOL), mandibular body breadth (MBB), maximum ramus height (MxRH), and bizygomatic breadth (ZYB). The Pearson's test demonstrated strong correlations between measurements that were bilateral.

The binary logistic regression provided a seven-variable formula that was useful for calculating sex from skull. For this formula, each sex was coded as males = 0 and females = 1. The formula for estimating sex from the skull in this

study is listed in Table 4.4. For the calibration sample, the accuracy for the formula was 95.1% in both males (96.7%) and females (94.1%) with a p-value of 0.001 (Table 4.5). The canonical discriminant function run on the calibration dataset had a 92.6% cross-validated group classification accuracy rate also with a p-value of 0.001. Results are shown in Table 4.6.

TABLE 4.4: Seven-variable model for sex estimation

Sex = (-0.455 x AUB) + (0.002 x BCB) + (-0.336 x BNL) + (0.024 x GOL) + (-0.138 x MBB) + (-0.619 x MxRh) + (0.011 x ZYB) + 122.401

Sex, >0 individual is female, <0 is male.

TABLE 4.5: Accuracy of seven-variable method

Accuracy of seven-variable method		
Male	29/30	96.7%
Female	48/51	94.1%
Total	77/81	95.1%

TABLE 4.6: Seven-variable cross validation test

Classification Results[b,c]					
		Sex M=0 F=1	Predicted Group Membership		
			0	1	Total
Original	Count	0	29	1	30
		1	3	48	51
	%	0	96.7	3.3	100
		1	5.9	94.1	100
Cross-validated[a]	Count	0	27	3	30
		1	3	48	51
	%	0	90	10	100
		1	5.9	94.1	100

a. Cross validation is done only for those cases in the analysis. In cross validation, each case is classified by the functions derived from all cases other than that case.

b. 95.1% of original grouped cases correctly classified.

c. 92.6% of cross-validated grouped cases correctly classified.

For the *Fordisc* portion of the study, all of the specimens in the calibration sample were run in the software for all 30 variables that are used in cranial analysis. The results showed that the male specimens were correctly classified 56.57% of the time and the females were classified 98.04% of the time. Overall, the *Fordisc* analysis correctly classified the specimens' sex approximately 82.72% of the time (Table 4.7).

TABLE 4.7: Accuracy of *Fordisc 3.0* method

Accuracy of Fordisc		
Male	17/30	56.6%
Female	50/51	98.0%
Total	67/81	82.7%

Discussion and Conclusions

This study demonstrates that it is possible to estimate sex accurately (95.1% with a p-value of 0.001) in 3D virtual cranial models derived from CT data. With the accuracy of the 3D models for estimating sex established, we are able to explore the benefits of this methodology. The primary goal of this project was to determine if 3D models of cranial anatomy could be made to a high level of anatomical accuracy. These 81 skeletal models provide anatomists and anthropologists with a database of modern, documented specimens with normal anatomy.

In an era of limited anatomical and osteological resources, large collections of virtual anatomy can provide an invaluable resource to both educators and researchers. Many institutions do not have the ability to obtain large skeletal collections due to funding, logistics, or even laws that prevent the collection of human remains. If they do have a collection, the remains are often damaged, incomplete, or of unknown origin. Virtual anatomy databases will allow those institutions to continue to teach anatomy without having to house a collection or to be used to augment their existing one. On the same note, researchers are often unable to analyze remains because they are far too valuable or are reserved for teaching purposes. Virtual specimens allow advanced analyses to be conducted without any damage to the actual specimen.

Another benefit to the virtual osteological collections is that analyses can be conducted remotely for research or even forensic casework. We have tested our methods on several local, state and federal law enforcement agencies with positive feedback from the investigators. Maintaining a chain of evidence is critical in forensics and law enforcement. By using virtual analyses, the researchers never take custody of the actual remains but are still able to conduct their analysis. This also allows law enforcement to use experts beyond their actual geographical location.

Most importantly, the virtual anatomical models are providing more objective results. By 'metricizing' non-metric traits and digitally capturing the anatomy's true geometry, the subjective nature of many anthropological methods is diminished or even removed. Instead of scoring a skull as male or female on a scale of 0-5 with 0 being "undetermined sex" and 5 being "male", we can quantitatively capture the exact nature of the trait, such as supraorbital ridge (glabella). The more quantitative we can be in our data collection, the less subjective our results will be (7).

In *Fordisc 3.0*, skeletal remains are classified using numerous osteological metric variables (3). For the skull, there are approximately 30 variables used to estimate sex. While in our study *Fordisc* classified the skulls correctly 82.72% of the time, the results showed that the males were only classified correctly 56.57% of the time. We suggest that this is due to too much "noise" introduced by the 30

variables or the lack of consideration of non-metric variables. By using the 7 variable formula developed in this study, the authors hypothesize that the estimation of sex in the skull will increase.

While this study has shown that 3D virtual models of skeletal anatomy are useful, in order to increase value of our current dataset more information on the individual's ancestry is needed. Neither the cadavers nor the anonymized patient data included the ancestral background so it is unclear at this time what role, if any, race played in the classification of sex of this calibration sample. Additionally, the cadaver sample's age was highly skewed towards the elderly with a mean age of 79. The clinical cases had a much younger mean (63) and even younger age range (33 - 85). More clinical scans of younger individuals are needed to better determine the effect age would have on our analyses. By collecting more data, we will be able to better understand patterned phenotypic variation in modern human populations

In summary, the establishment of the biological profile (age, sex, stature, and ancestry) from human remains is at the core of the forensic anthropologist's everyday practice. This study demonstrates the value of CT data for making detailed virtual models of the skull that can be analyzed beyond actual contact with the actual bone. From these 3D models, a novel, accurate formula for sex estimation was developed. The proposed method in this study represents a

quick, reliable alternative to traditional anthropological methodologies used in establishing sex in the skull.

Acknowledgements

The researchers would like to thank the administrators and staff of the USF Health Imaging Centers at the USF Morsani Center and USF South for all of their cooperation and support over the past 3 years with our medical imaging project. A special thank you to Melanie O'Brien and Matthew Woods for their numerous hours of help at night and on the weekends. We would also like to thank the developers and staff at Materialise for their assistance and input during the different stages of the project. I would also like to thank my labmate, Jonathan Ford, for his assistance on the various portions of the project.

CHAPTER 5

MAKING FACES: 3D MODELING OF CRANIOFACIAL ANATOMY

Abstract

The value of 3D clinical data from the skull and face of living individuals is the holy grail of forensic and biometric data. In two phases, this study tested making facial approximations from a living individual as well as examined the potential for virtual facial models in forensic analyses. In this study, a series of cadaveric and clinical craniofacial computed tomography (CT) scans with known demographic information were utilized in establishing database of virtual faces for facial approximation and biometrics. The faces were 3D modeled and measured using a combination of traditional soft tissue depths. A series of soft tissue depths were also taken from the same cadavers' actual faces. Comparisons were made between actual depth measurements and those taken virtually. Analyses were also conducted to examine the differences in the scanning quality of cadaveric and clinical tissue. Overall, this study aims to show the usefulness of anatomically accurate virtual 3D models of the face and skull for applications to a variety of fields.

Introduction

The human face is one of the most studied regions of the body. Its geometry is so unique that it can distinguish us from one another, as well as convey our emotions without uttering a word. It is no mystery why facial anatomy is so important in the fields of forensics, biometrics and medicine. People use plastic surgery to electively alter their faces or reconstruct their face to what it used to be prior to some traumatic injury. In biometrics, researchers search for features or traits that are so unique that they distinguish us like a fingerprint. The face is also critical and a critical part in the identification of unknown individuals. Forensic facial approximation is the practice of reconstructing a face on an unknown individual's skull. Each of these fields represent an area where current, relevant modern human craniofacial data is needed.

In our previous studies, we examined the application of 3D bony models to pelvic and cranial identification and the estimation of sex. Computerized soft tissue segmentation and modeling is more difficult due to the variations in the tissue densities. However, with the value of facial data apparent, we began a study into the 3D modeling and virtual analyses of craniofacial anatomy. This study was conducted in two separate phases. In the first phase, we tested national and international experts in forensic facial approximation on creating a reconstruction of an unknown living individual. Their results led to the second phase of this study in which we used a series of cadaveric and clinical computed

tomography (CT) scans to capture the unique geometry of the face. Virtual measurements were undertaken to add to the body of knowledge in soft tissue depths from the face. It was the goal of this study to develop a series of virtual facial models that will be applicable to a variety of fields.

Phase I: Forensic Facial Approximation Challenge

Subsequent to our validation studies of 3D anatomy, our lab began to test the virtual methodologies in forensic settings such as comparing the accuracy of available methods of developing a biological profile (age at death, sex, ancestry and body type) of an unknown individual as seen in Chapters 3 & 4 to facial approximation.

Facial approximation is a common tool utilized in forensic human identification. If human remains are discovered that are unidentifiable, law enforcement agencies will commission a reconstruction from a forensic artist either by photographic projection, clay modeling, or more recently, computerized reconstruction. The success of a reconstruction is determined if there is an identification made based on the model or images. Unfortunately, the agencies are often limited to local artists due to evidentiary concerns. 3D imaging and computer modeling is now allowing facial approximation specialists to go beyond traditional clay models to create virtual computed models of anatomical structures.

Forensic facial reconstruction is used to build an approximation of a face on the skull of an unknown deceased individual for the purposes of eliciting recognition leading to their identification (1 – 4). Traditionally, the soft tissues were reconstructed in plasticine/clay on a plaster cast of the skull. Tissue depth markers are added to the skull at various craniometric landmarks and musculature and facial features are added using the morphology of the skull as a guideline seen in Figure 5.1 (5).

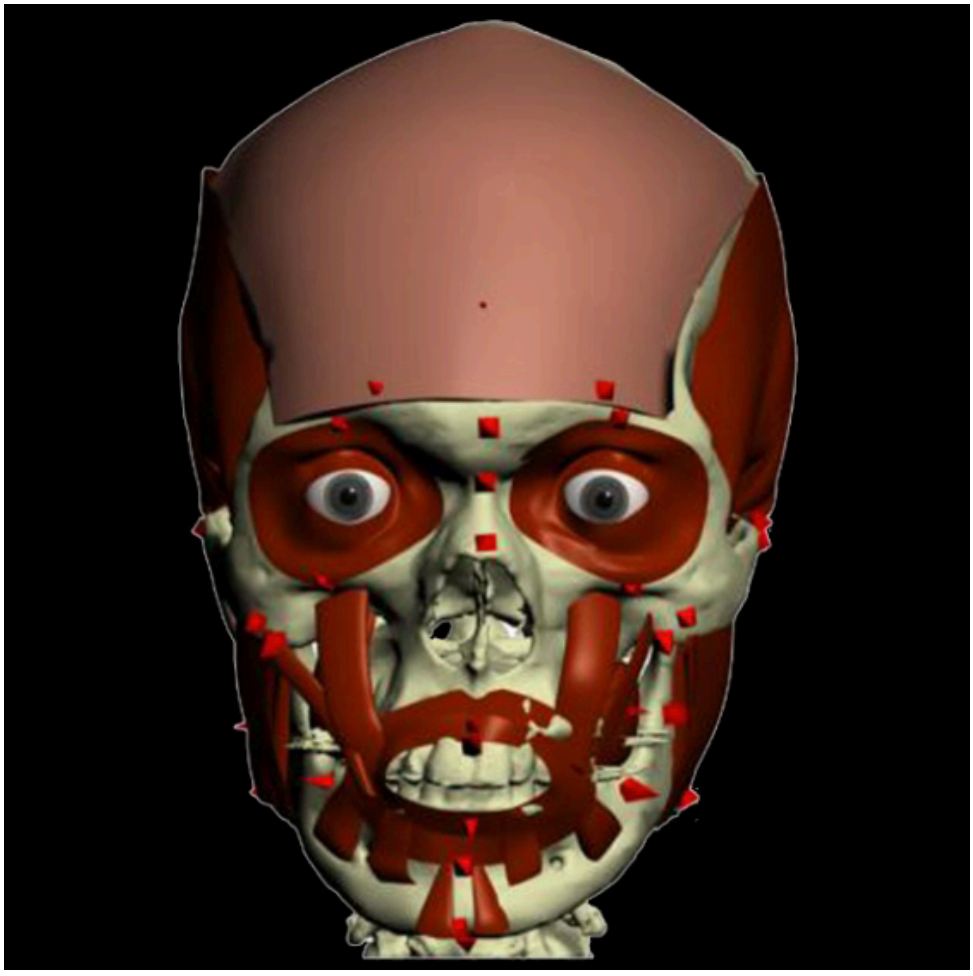

FIGURE 5.1: Virtual facial muscles from the *FaceIT* technique.
(Courtesy S. Davy-Jow)

Materials and Methods

With the goal of developing more objective methods in forensic facial reconstruction, we partnered with leading visualization specialists from the Federal Bureau of Investigation, New York, and the United Kingdom for a unique blind facial approximation study. Using medical imaging, a living individual was CT scanned and anatomically accurate virtual models of both the skull and of the surface contour of the face were computed from CT DICOM data.

The volumetric data from the scan was imported into *Mimics v.13.1*. A floodfill method of seeding the image was done to select only the bone pixels in the data set. This 3D volumetric pixel grouping was then filtered of artifact holes and closed to create one unsegmented structure. The data set was then rendered into a 3D Model and exported as an STL file (Figure 5.2).

The virtual facial approximation participants were provided with the STL files and a standard biological profile determined by a forensic anthropologist.

FIGURE 5.2: Frontal, sagittal and 3/4 views of unknown living individual

An accurate full sized prototype of the skull (Figure 5.3) was then produced from the computed virtual skull model using a 3D ZPrinter 310 (© ZCorp) printer which was then submitted to the clay model specialist.

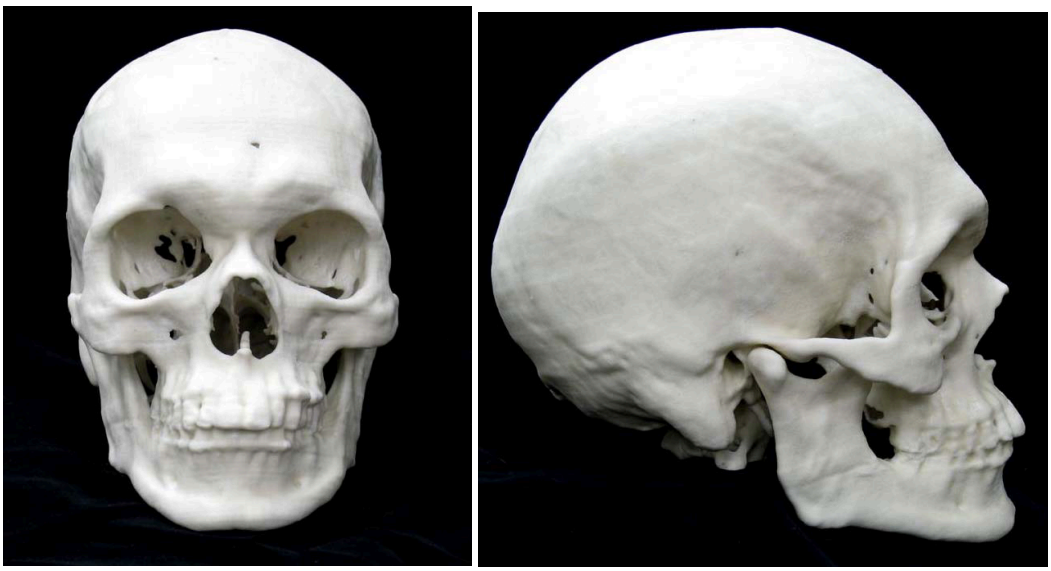

FIGURE 5.3: Frontal and sagittal views of the prototype skull of living individual provided to clay reconstruction artists

Study Results

Clay Modeling

Visualization Specialist Wesley Neville

A face was constructed on the skull prototype by an experienced, professional forensic visual identification specialist from the Federal Bureau of Investigation using traditional clay facial approximation techniques. The reconstruction (Figure 5.4) was completed by Wesley Neville of the FBI and it took approximately 3 weeks to complete. Once the clay model was completed, a laser surface scan of the reconstruction was done and sent to the researchers for comparison to the other reconstructions.

FIGURE 5.4: Frontal, sagittal and 3/4 views of Wesley Neville's clay reconstruction
(Courtesy of W. Neville)

Sculptor Philippe Faraut

Additionally, the FBI requested that renowned artistic sculptor, Philippe Faraut of PCF Studios, Inc., be given the opportunity to complete the same facial approximation challenge. Though his artistic focus is on portraiture sculpting, Mr. Faraut has completed several forensic sculptures for law enforcement in the New York area. Faraut's reconstruction as seen in Figure 5.5 was completed in 3 hours and the entire process was documented on film for the researchers to review.

In his wet-clay method, he completes the reconstruction and if biological profile is male, he will add a mustache and beard for variation. Unfortunately, Philippe Faraut did not have access to a laser scanner so his results could only be visually compared.

FIGURE 5.5: Philippe Faraut's clay reconstruction
(Courtesy of P. Faraut)

Virtual Modeling

FaceIT

Virtual facial approximations were also produced using two computer-based techniques. One method, *FaceIT,* utilized by law enforcement in the United Kingdom and developed by expert Dr. Stephanie Davy-Jow at Liverpool John Moores University, uses the software package, *3dsMax* © (v.9) to create virtual clay models over the skull (2).

A plane was constructed and placed to represent the Frankfurt Horizontal Plane to enable standardization of views. Tissue depth markers, represented by pyramids, were placed at 32 craniometric landmark points on the skull. Based on the anthropologist's biological profile, the depths were taken from previously established data sets for the corresponding individual's profile. A prefabricated facial muscle set was then scaled and deformed to match the morphology of the skull. Other anatomical features such as the eyeballs, lips, and ears were also imported from a feature data bank based on established anthropological characteristics. (Figure 5.6)

FIGURE 5.6: Frontal, sagittal and 3/4 view of virtual reconstruction using the *FaceIT* technique
(Courtesy of S. Davy-Jow)

FBI Virtual Method

The other method in this study tested the FBI's virtual facial approximation technique. A visual information specialist from the Federal Bureau of Investigation was enlisted to test their most current computerized facial approximation software developed in conjunction with General Electric (GE) Medical researchers. The FBI's software imports the STL files and creates a mask over the virtual skull based on a database of standard craniofacial features. The software package allows the user to make adjustments to the mask on a sliding scale for age and weight. (Figure 5.7)

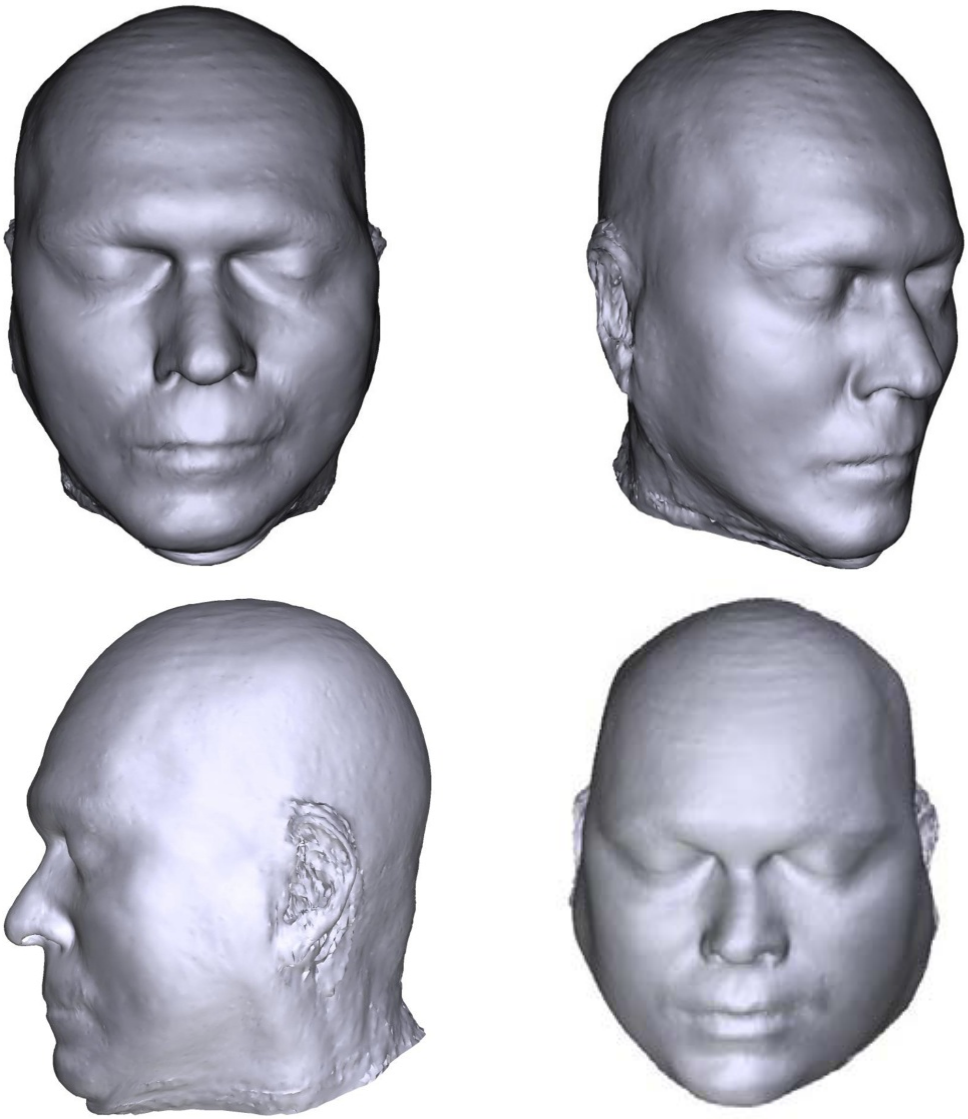

FIGURE 5.7: Frontal, sagittal, ¾, and obese views of virtual reconstruction using the FBI's virtual facial approximation
(Courtesy of C. Adrian)

Final Results

The results from all four attempts (clay and virtual) were compared visually to each other and collectively to the actual features of the living individual (Figure 5.8) to determine the level of accuracy and detail that each provided. While each reconstruction had aspects of the face correct, each approximation had large amounts of variation in specific regions of the face such as the chin area, ears, and nasal region. When the forensic artists were asked why they thought this was, they reported that there is variation in the soft tissue depth literature and more data is needed to improve and objective test facial approximations. Additionally, there is a lack of formal studies into bony- soft tissue relationships so these areas are reliant upon expert experience.

The facial approximation challenge attempted in this study demonstrated the wide range of variation between commonly used facial identification methods. The facial experts who participated in the experiment each commented on the unique nature of the study and opportunity to “practice” on living individuals. Being able to test reconstructing a known, living individual highlighted the strengths and weaknesses of each method and more importantly the weaknesses in the current field data.

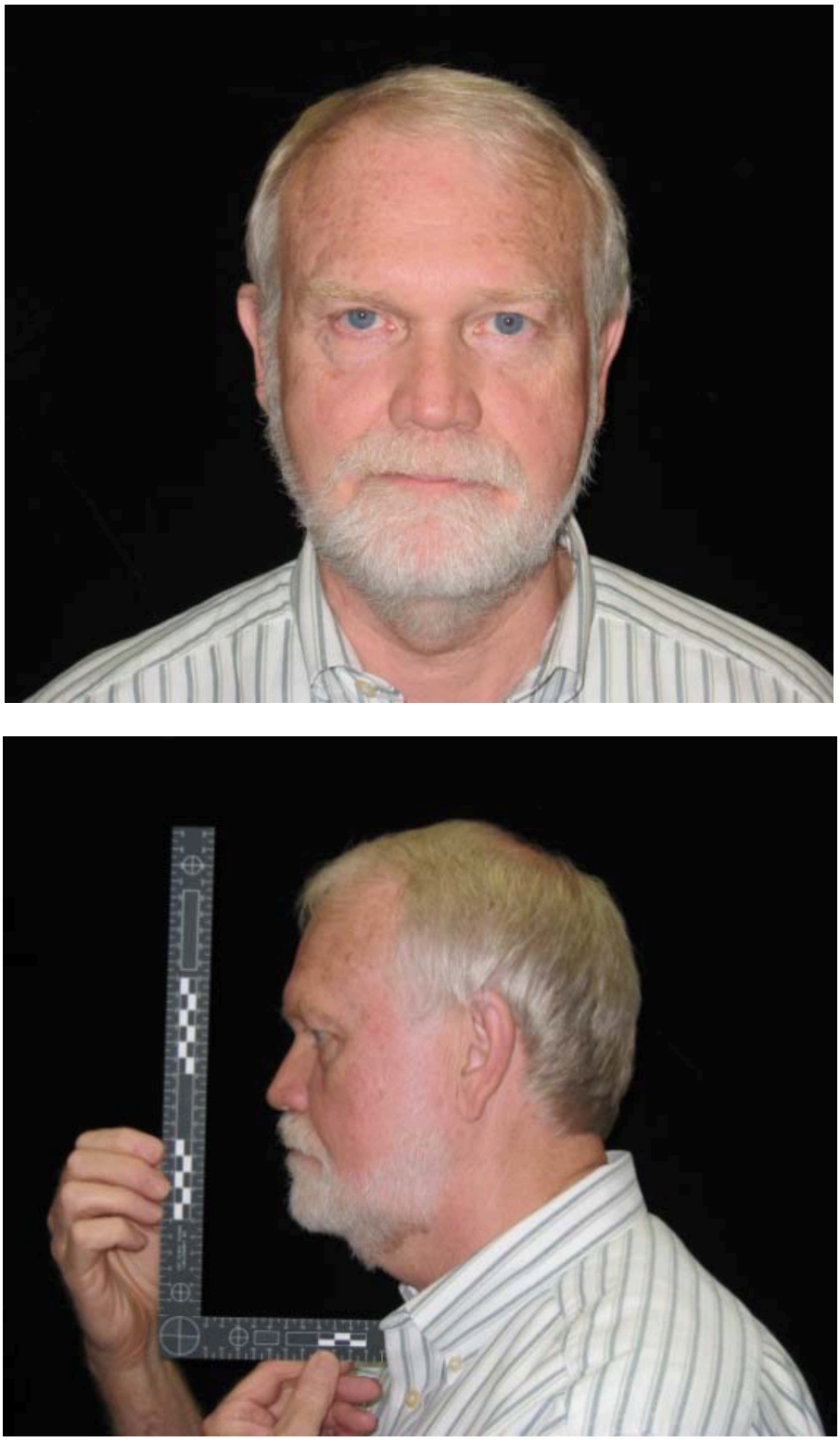

FIGURE 5.8: Frontal and sagittal views of actual living individual

Phase II: Creating Virtual Faces

In order to address the issues raised by the first phase of this project, a second phase was undertaken to duplicate and examine the traditional soft tissue depth methodologies and then test what role virtual models and methods could have in the current data. We began this study with a combination of traditional and unconventional analyses.

Materials and Methods

Cadaveric Soft Tissue Depth Measurements

Soft tissue depth measurements of the face are traditionally used to assist forensic practitioners in understanding the relationship between the skull and the facial soft tissue that lies on top of it. These depths are utilized by forensic researchers, such as facial approximation specialists, to recreate a face of an unknown individual on a skull. The measurements themselves are taken by needle or pin puncture at specific craniofacial landmarks on the cadaver (5). Typically a pin is sooted at the tip and it is placed in the face at a desired landmark. Once the pin reaches bone, it is removed and the amount of soot that has been wiped off, is measured. This measurement is recorded as the depth from the skin to the bone. Numerous studies have attempted to examine alternative methods of depth analyses (6 - 7) such as ultrasound, X-ray, CT and

MRI but it is commonly accepted that the pin method is the most cost efficient and reliable.

In light of the results of our first phase of this project, the researchers decided to replicate the traditional methodologies of facial soft tissue depths and compare those results with virtual depths taken from the same individual. For 2 years (2007-2008), the researchers manually took a series of 30 bilateral soft tissue measurements (3 - 5) from each of the cadavers used in USF's Medical Gross Anatomy course's faces. High-resolution digital images were also taken of each cadaver's face in profile and both lateral sides to document any distortion of the face and angle of the fixed head. This data was used in the morphometric analyses to determine any differences between the actual soft tissue depths manually taken from skull and the virtual soft tissue depths taken from 3D models of the skull and face.

Cadaveric and Clinical Radiological Scans

As previously noted in Chapter 4, in 2007-2008 all of the cadavers obtained for USF's Medical Gross Anatomy course were full-body scanned on GE Multi-Slice Computed Tomography (CT) scanners. In 2007 a total of 38 cadavers were scanned at a 3mm slice thickness and heads at a 1mm slice thickness. Subsequent scans of cadavers have been acquired on a GE LightSpeed VCT 64-slice scanner at a resolution of 0.625 mm slice thickness

from USF Health's South Campus and USF Health's Morsani Center to bring the total to 64.

A total 60 adult individuals with known demographics and complete heads were evaluated to test the usability of computed skulls and faces for virtual soft tissue depth measurements. The age range was 53 – 96, with a mean age of 79.03 (median 85.5). The sex distribution for the calibration sample was 24 males and 36 females. The average age of the males is 78.3 (range 62 - 93) and the average age of the females is 79.5 (range 53 - 96). Cadavers that did not have complete heads or were sub-adult were excluded for this study. The age and sex information was withheld from the observer during the measurement phase.

In this final phase of the project, we also examined the imaging and computer-modeling properties of clinical patient scans compared to cadaveric scans. Recent studies have found that multislice computed tomography (MSCT) and magnetic resonance imaging (MRI) are useful tools in visualizing the relationship between bone and facial geometry (6 - 8). Since researchers have expressed some concerns about the limitations of embalmed and fixed cadaveric material in facial studies (5), clinical scans provide an opportunity to study living tissue without the distortion that sometimes occurs in the cadaver embalming process.

For the purposes of this study, a random selection of craniofacial CT scans taken of patients at the University of South Florida College of Medicine were used per institutional approval. The clinical data was anonymized at the source and collected with informed patient consent. Only age, sex, and scan description were documented beyond the technical meta-data (IRB approved). The deidentified medical scans were from the “Cyberknife” pre-operative scan protocol since they include all facial geometry and the scan terminate beneath the mandible. This scan is usually conducted for patients with brain lesions or tumors, which should not interfere with the craniofacial anatomy. Since the scans for this phase of the project are from clinical procedures, no changes to the scanning protocols were attempted. The Cyberknife surgical pre-operative scans are typically conducted in CT at a slice thickness of 1.25 mm. Any accompanying MRI scans were also reviewed but not used for the analysis.

A total of 21 individuals with known demographics and complete cranial and facial anatomy were evaluated in this study. The age range was 33 - 85, with a mean age of 62.9 (median 70). The sex distribution for calibration sample was 6 males and 15 females. The average age of the males is 59.67 (range 35-80) and the average age of the females is 64.2 (range 33-85). When selecting the study participants, individuals with extensive metallic dental implants such as crowns or partials, were excluded from the study as the implants cause artifacts or “flares” to appear on the DICOM images that occlude portions of the skull and distort other portions of the face.

In total the complete sample for this project with both cadaveric and clinical data was 81 individual CT scans. There were a total of 30 males and 51 females included. The overall mean age was 74.9 (median 79) with an age range of 33- 96. The mean age for the males was 74.6 (range 35 - 93) and the mean age for the females was 75 (range 33 - 96).

3D Computer Models of the Skull and Face

Once the cadaver and clinical data was extracted from the scanner In the lab, the DICOM images were imported into the 3D visualization software package *Mimics* © version 13.1 (Materialise). A mask was created to select for the bone pixels, and the thresholding was adjusted to account for individual variation in bone density. For older individuals with marked osteoporosis, the threshold was manually entered in order to account for individual variation in bone density. The resultant pixel masks from the transverse (axial), coronal, and sagittal planes were converted to voxels by the software to produce a 3D bone model of the selected region(s) of the skeleton. The same process was repeated to select for the soft tissue pixels to isolate the facial tissue and create a 3D model of the face.

The models were cleaned of artifacts in the engineering software package *3Matics* © version 5.01 (Materialise) and saved as Stereolithographic (stl) files for analysis and/or rapid prototyping (FIG 5.9). These models can then be measured in *Mimics* or exported into most other 3D packages for further analyses.

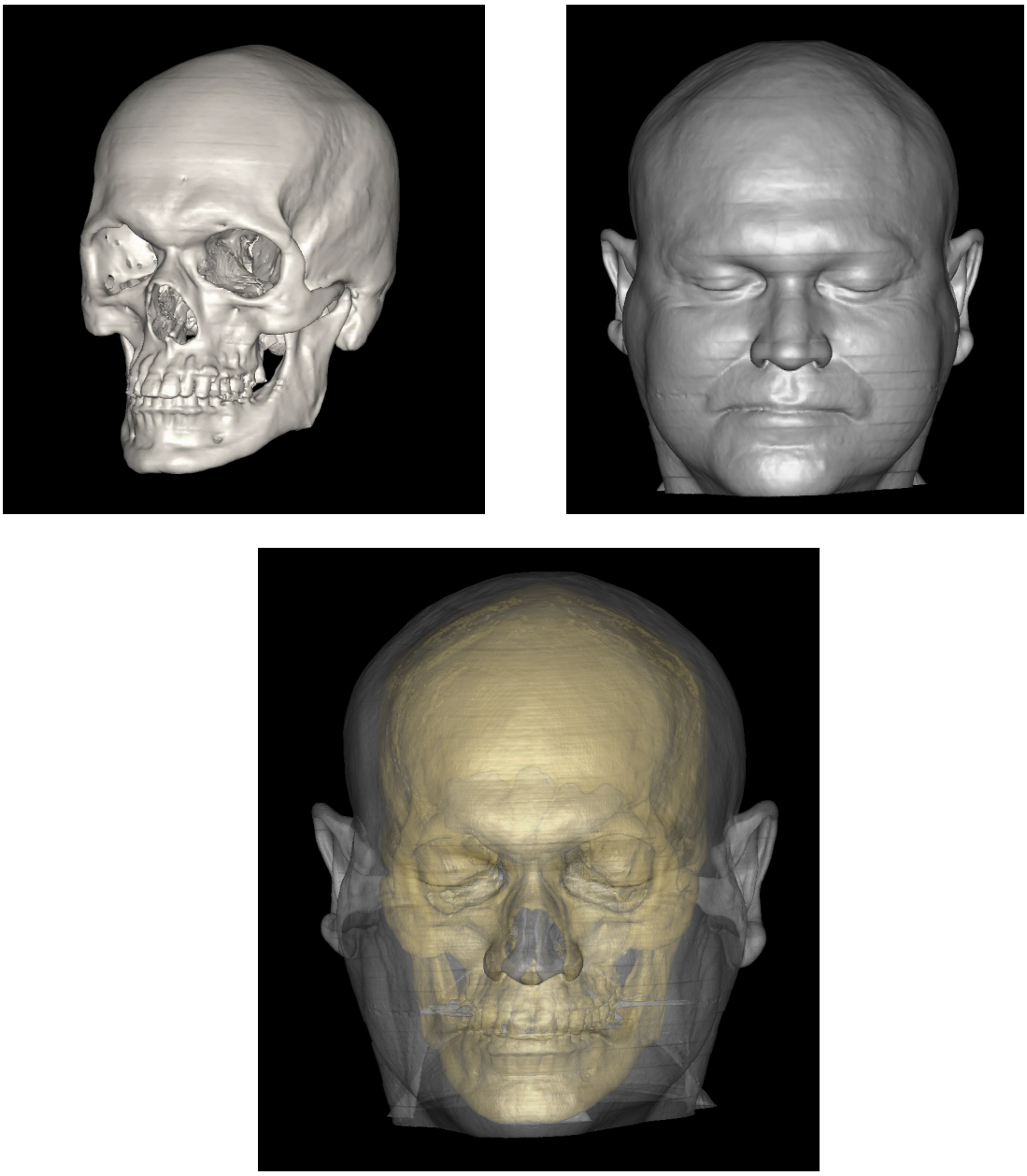

FIGURE 5.9: 3D model of skull and face

Accuracy of the virtual models has been verified in previous studies by the authors and other researchers (3.20).

Virtual Soft Tissue Depth Measurements

A selection of traditional soft tissue measurements was chosen for use in establishing facial geometry (6). For this study, the measurements for the calibration sample were chosen to meet one or more of the following criteria: a commonly used measurement reported in the literature (e.g. beneath the chin) or a 'metricized' version of a traditional non-metric trait (e.g. angle of the glabella or nasal projection). Twenty-five landmarks were placed on each skull (10 midline, 7 bilateral, and 1 projection point) and on the outer face for a total of 50. Landmarks on the face were placed on top of the underlying bony landmarks. Definitions are listed in Table 5.1, below. From these, 22 distances, angles, and anthropological indices were calculated.

An osteometric toolkit was designed for landmark placement in the *Mimics* software package (FIG 5.10) that allowed the researchers to examine the 22 variables. The software then calculates linear distances, angles, and indices between specified points. This data is output in a format ready for use in statistical analysis packages.

TABLE 5.1: List of depth measurements and angles

Landmark	Definition
Midline Depth Measurements (Face to Bone)	
Beneath Chin	Lowest medial landmark beneath the chin
Chin Lip Fold	Midpoint of the labial-mental groove
End of Nasal	Midpoint of the nasal bones at the tip
Glabella	The most prominent midline point between
Lower Lip Margin	Midpoint of the lower vermilion line
Mental Eminence	Most anterior midpoint of the chin
Midphiltrum	Midpoint of the philtral column
Nasion	Midline point of the nasal root
Supraglabella	Midsagittal point superior to the glabella
Upper Lip Margin	Midpoint of the upper vermilion line
Bilateral Depth Measurements (Face to Bone)	
Alare	Most lateral point on the margin of the nasal aperture
Frontal Eminence	Lateral point to supraglabella on right side
Lateral Orbit	Point on the lateral orbital margin on a line with the eye fissure
Mid-Zygomatic	Most anterior projecting point on the body of the malar
Suborbital	Bony prominence below the orbit
Supraorbital	Bony prominence above the orbit
Zygomatic Arch	Most lateral point over the zygomatic arch
Angles	
Glabella-Nasal Angle	Angle from the glabella to the nasion to the end of the nasal
Glabellar Angle	Angle from the supraglabella to the glabella to the nasion
Nasal Projection	Angle from the right alare to the tip of the nose to the left alare
Nasal Cartilage	Angle from the end of the nasal to the tip of the nose to the base of the nose
Vertical Nasal Projection	Angle from the nasion to the tip of the nose to the base of the nose

From Wilkinson 2000, Domaracki and Stephan 2006, Stephan and Simpson 2008

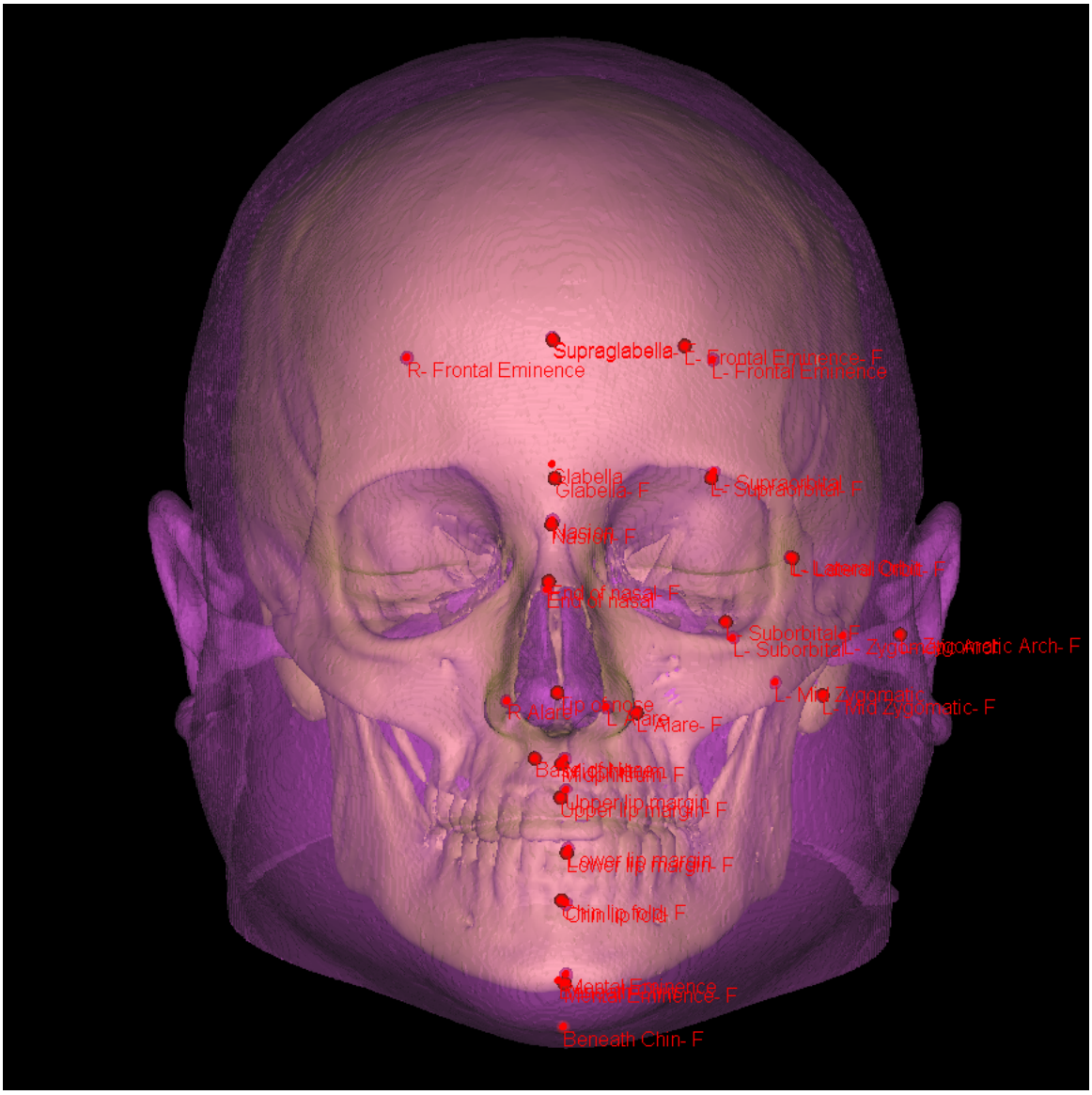

FIGURE 5.10: 3D model with virtual soft tissue depth measurements shown

Statistical Analysis

Data collected for this study was analyzed in the software package, *SPSS* version 18.0. To begin the analysis, measures of central tendency and descriptive statistics (mean, median, standard deviation, etc) were run on the virtual soft tissue depths and then on actual pin depths and to check for any errors in the data. Table 5.2 provides the mean values and standard deviations for all 22 variables across the sample of 81 individuals (male versus female).

Error rates were calculated between the actual pin depths and the virtual soft tissue depths to see what, if any discrepancies there were. Next, a comparison between the cadaveric and clinical 3D faces was calculated using measures of central tendencies and a discriminant function analysis. A Pearson's correlation was performed using all 22 variables with cadaver faces coded as 0 and clinical faces coded as 1. Once the variables with the highest loadings were identified, a discriminant function was performed on the variables to establish cross-validated classification results. It should be noted that while the data was collected bilaterally, there was little measurement variation between the left and right sides of the face and therefore, only the left side was used in the statistical analyses in an effort to not skew the data.

TABLE 5.2: Measures of central tendencies
(Male Virtual vs. Female Virtual)

Variable	Male (Mean)	Male (SD)	Female (Mean)	Female (SD)
Beneath Chin	8.6	3.6	7.0	3.7
Chin Lip Fold	12.3	2.5	11.4	1.5
End of Nasal	3.3	1.5	2.9	1.1
Glabella	5.4	1.5	5.0	1.6
Lower Lip Margin	15.0	4.1	11.0	2.4
Mental Eminence	10.6	3.1	10.2	2.2
Midphiltrum	10.8	3.2	9.1	2.5
Nasion	8.2	3.0	6.9	4.5
Supraglabella	4.0	1.3	3.5	1.5
Upper Lip Margin	9.4	3.6	7.8	3.1
Alare	12.1	2.7	11.0	2.1
Frontal Eminence	5.3	1.9	4.7	2.5
Lateral Orbit	6.6	3.7	6.1	3.2
Mid-Zygomatic	14.2	5.3	13.7	4.1
Suborbital	6.8	3.9	7.4	3.6
Supraorbital	7.8	2.6	6.8	2.2
Zygomatic Arch	12.5	4.7	12.0	4.8
Glabella-Nasal Angle	127.3	8.5	139.4	9.0
Glabellar Angle	150.2	9.5	160.5	8.4
Nasal Projection	43.4	6.5	45.7	5.5
Nasal Cartilage	98.4	6.8	101.8	8.0
Vertical Nasal Projection	96.6	7.7	101.9	9.8

All measurements in mm or degrees

Results

3D modeling and virtual measurements

From the import of the DICOM images to output of the data, the time taken for each specimen was dependent on the type of computer used and the observer's experience and familiarity with the software. The import of the images

and the making of the model took approximately 45 - 60 minutes per case. The increased time was due to removal of any flair from metallic crowns. The landmarking and measurements took approximately 25-30 minutes per case.

Actual pin depths versus virtual depths measurements

Measures of central tendencies were calculated from the actual pin depths taken from the cadaver face and compared to the depths taken from the same cadaver's CT scan. These values can be seen in Table 5.3.

Error rates for 15 of the measurements were calculated (Table 5.4 & Figure 5.11) and they show large discrepancies between the values. Of the 15 measurements, 8 showed greater than 50% difference between the pin method and virtual method. The measurements with the highest variation were left lateral orbit (206%), mental eminence (88.5%), end of nasal (81%), left suborbital (76%), supraglabella (74%), left zygomatic arch (73%), left frontal eminence (67%), and upper lip margin (64%).

TABLE 5.3: Measures of central tendencies (Actual Pin Depth vs. Virtual Depth)

Variable	Measurement Name	Actual (Mean)	Actual (SD)	Virtual (Mean)	Virtual (SD)
Beneath Chin	Lowest medial landmark beneath the chin	7.2	3.6	6.8	2.5
Chin Lip Fold	Midpoint of the labial-mental groove	10.9	2.8	11.6	2.1
End of Nasal	Midpoint of the nasal bones at the tip	3.4	3.1	2.9	1.3
Glabella	The most prominent midline point between	5.0	1.9	4.9	1.6
Lower Lip Margin	Midpoint of the lower vermilion line	10.2	3.3	10.0	2.4
Mental Eminence	Most anterior midpoint of the chin	8.4	2.7	9.6	3.0
Midphiltrum	Midpoint of the philtral column	9.4	3.5	7.2	4.0
Nasion	Midline point of the nasal root	4.9	1.9	3.3	1.3
Supraglabella	Midsagittal point superior to the glabella	3.9	2.3	8.3	3.7
Upper Lip Margin	Midpoint of the upper vermilion line	8.4	3.9	11.4	2.5
Frontal Eminence	Lateral point to supraglabella on right side	4.1	2.3	4.4	2.1
Lateral Orbit	Point on the lateral orbital margin on a line with the eye fissure	13.1	5.9	6.0	3.5
Mid-Zygomatic	Most anteriorly projecting point on the body of the malar	11.5	6.8	14.2	5.0
Suborbital	Bony prominence below the orbit	7.7	5.6	6.5	3.6
Supraorbital	Bony prominence above the orbit	13.3	6.1	7.0	2.4
Zygomatic Arch	Most lateral point over the zygomatic arch	6.1	2.2	12.4	5.1

All measurements in mm

TABLE 5.4: Error Rates Between Actual and Virtual

Variable	Difference (Mean)	Difference (SD)	Percent error (Mean)
Beneath chin	2.3	2.3	47.9%
Chin-lip fold	1.7	2.2	31.9%
End of Nasal	2.2	2.8	80.8%
Glabella	0.9	0.7	30.4%
Lower lip margin	3.6	3.5	50.0%
Left frontal eminence L	2.0	1.3	67.3%
Left lateral orbit L	7.2	4.3	206.2%
Left Zygomatic Arch, mid L	5.0	3.8	73.0%
Left Suborbital L	2.7	2.5	75.9%
Left Supraorbital L	1.5	1.2	37.7%
Mental eminence	2.3	2.2	88.5%
Midphiltrium	2.3	2.4	43.2%
Nasion	2.9	4.2	41.3%
Supraglabella	1.6	1.4	74.3%
Upper lip margin	3.2	2.8	64.2%

All measurements in mm

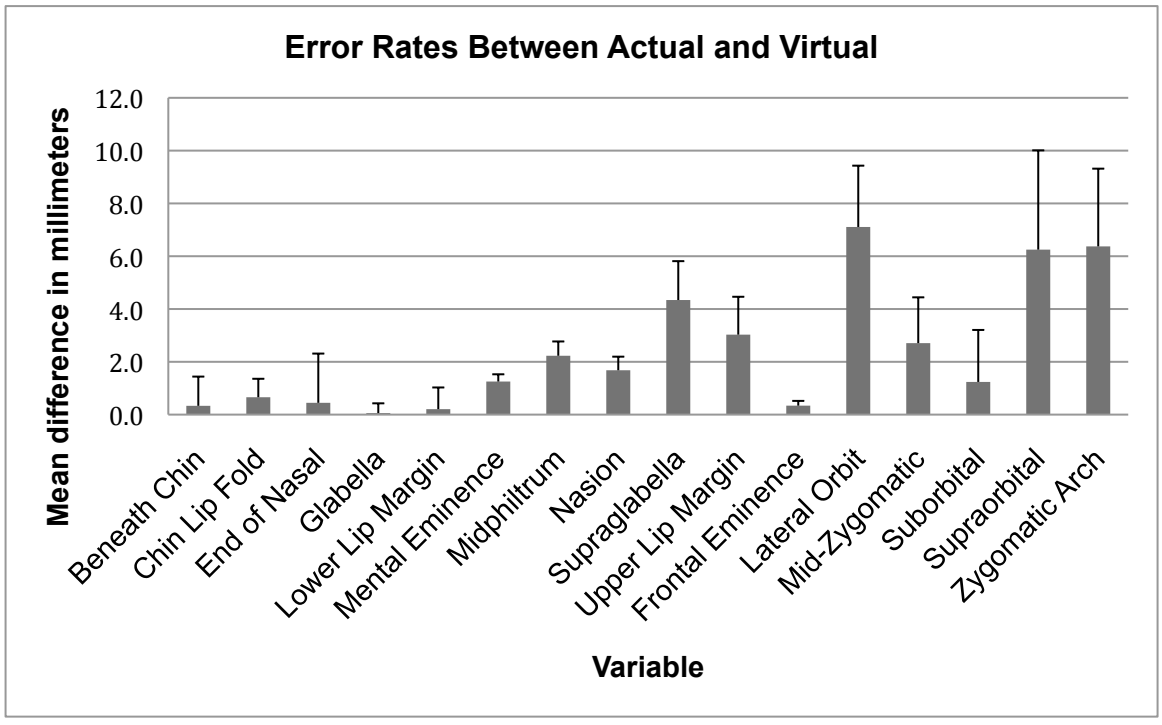

FIGURE 5.11: Error rates between actual and virtual depth measurements

Cadaveric Versus Clinical Facial Data

The Pearson correlation test listed which variables indicated the highest influence on distinction between cadaveric and clinical faces. 7 variables of the 23 original variables were determined to be statistically significant at the 0.01 level of a two-tailed test. The variables with the highest loadings were selected and narrowed down to: beneath the chin, supraglabella, frontal eminence, and vertical nasal projection. The Pearson's test demonstrated weak correlations between measurements that were bilateral and therefore only left sided measurements were included.

TABLE 5.5: Measures of central tendencies (Clinical vs. Cadaver)

Variable	Clinical (Mean)	Clinical (SD)	Cadaver (Mean)	Cadaver (SD)
Beneath Chin	9.8	5.5	6.8	2.5
Chin Lip Fold	12.1	1.6	11.6	2.1
End of Nasal	3.3	1.3	2.9	1.3
Glabella	5.7	1.5	4.9	1.6
Alare	11.0	2.2	13.1	3.9
Lower Lip Margin	11.3	2.7	10.0	2.4
Mental Eminence	10.0	2.6	9.6	3.0
Midphiltrum	7.9	4.0	7.2	4.0
Nasion	4.7	1.0	3.3	1.3
Supraglabella	8.4	2.2	8.3	3.7
Upper Lip Margin	11.4	2.2	11.4	2.5
Frontal Eminence	6.2	2.3	4.4	2.1
Lateral Orbit	7.1	2.9	6.0	3.5
Mid-Zygomatic	12.9	3.0	14.2	5.0
Suborbital	8.9	3.6	6.5	3.6
Supraorbital	7.6	2.4	7.0	2.4
Zygomatic Arch	11.7	3.4	12.4	5.1
Glabella-Nasal Angle	137.6	12.4	133.7	9.7
Glabellar Angle	157.3	13.6	156.4	8.6
Nasal Projection	46.1	6.2	44.4	5.9
Nasal Cartilage	103.1	6.0	99.7	8.0
Vertical Nasal Projection	105.4	6.7	98.0	9.5

All measurements in mm or degrees

The binary logistic regression provided a four-variable formula that was useful for distinguishing a cadaveric face from a clinical face. For this formula, each face was coded as either cadaveric = 0 or clinical = 1. The canonical discriminant function run on the calibration dataset had an 80% group classification accuracy rate with a p-value of 0.001.

The cross-validated group classification from the dataset had a 76.0% accuracy rate also with a p-value of 0.001. Results are shown in Table 5.6.

TABLE 5.6: Four-variable cross validation test

Classification Results[b,c]

		Cad = 0 Clin = 1	Predicted Group Membership		
			0	1	Total
Original	Count	0	46	10	56
		1	5	14	19
	%	0	82.1	17.9	100
		1	26.3	73.7	100
Cross-validated[a]	Count	0	43	13	56
		1	5	14	19
	%	0	76.8	23.2	100
		1	26.3	73.7	100

a. Cross validation is done only for those cases in the analysis. In cross validation, each case is classified by the functions derived from all cases other than that case.
b. 80.0% of original grouped cases correctly classified.
c. 76.0% of cross-validated grouped cases correctly classified.

Discussion and Conclusions

While there are some known drawbacks to cadaveric facial data (5), there is an increasing need for 3D volumetric cranial and facial data in many fields. Recent forensic facial approximation studies (1; 9 - 11) have concluded that there is a critical lack of data and research in this area. Additionally, forensic pathologists (12 - 13) and medical clinicians such as craniofacial, plastic and neuro-surgeons (14) have all expressed needs for more complete studies

conducted on the relationship between the skull and the face. This study's goal was to address that lack of data in the literature by using virtual methodologies.

From the study's results, we have demonstrated that actual pin depth measurements taken from cadaver faces are not a reliable method of soft tissue depth measurements. This is due in large part to the fact that most soft tissue depth locations are based on bony structures or features, such as suture lines, so it can be difficult to visualize through skin. For example, in the sub and supra orbital landmarks researchers attempt to place a pin above and below the eye to hit the orbital ridges which is typically easy to see. However, with the zygomatic arch researchers place the pin at a point along the zygomatic arch on the side of the face. This is often difficult to see and even palpate with fixed cadaveric tissue. Even with a clearly defined orbital ridge in some cases, it is near impossible to replicate, which is the requirement of any accepted technique. With the virtual models from the CT derived data, it is possible to toggle the transparency of the face to see the underlying bone model. This allows the observer to exactly pinpoint the landmark on the bone and track that to the corresponding facial location.

Additionally this study has demonstrated the need for more clinical patient scan data for facial analyses over embalmed cadaveric data. With an 80% distinction rate between the cadaveric and clinical faces, it is clear to see that

cadaveric scans are not representative of living human faces. We hypothesize that there are several reasons for this distinction between the data sets.

First, the embalming process of cadaver involves flushing all blood and other fluids from the body and replacing it with a tissue fixative. Depending on the placement and orientation of the body as well as time since death, the embalming fluid can pool in certain locations causing gross distortion of the anatomical features. Regions that are particularly susceptible are the abdomen, genital region, and face. Ears and facial features are often bloated beyond recognition. This is also due to the body lying down flat for an extended period. Evidence for this distortion was seen in our cadaveric soft tissue depth data in the regions of the supraglabella, beneath the chin, and zygomatic. However, due to lack of resources and medical research approvals, cadavers are the field standard for soft tissue studies.

Embalmed cadavers also scan differently than living tissue. In the gray scale distribution histograms seen in Figures 5.12 and 5.13, at first look they appear very similar because they are both capturing soft tissue and bone. However on the extreme left side of the histograms there is a difference in the threshold level of the soft tissue. The left side of the histogram represents soft tissue or less dense tissue, while the extreme right represents bone or extremely

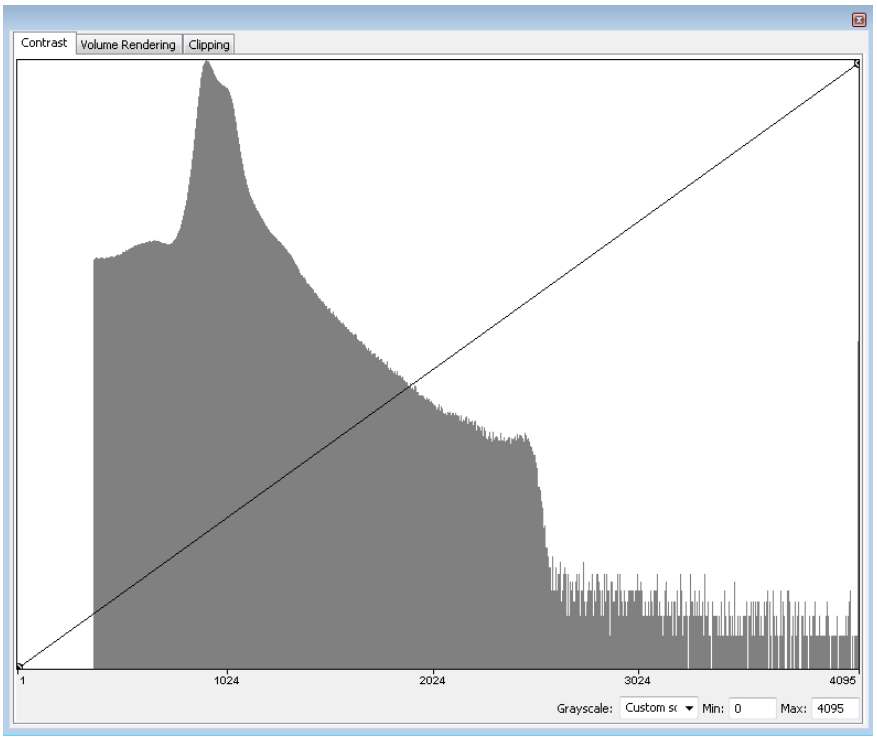

FIGURE 5.12: Histogram of gray scale values of cadaver scan

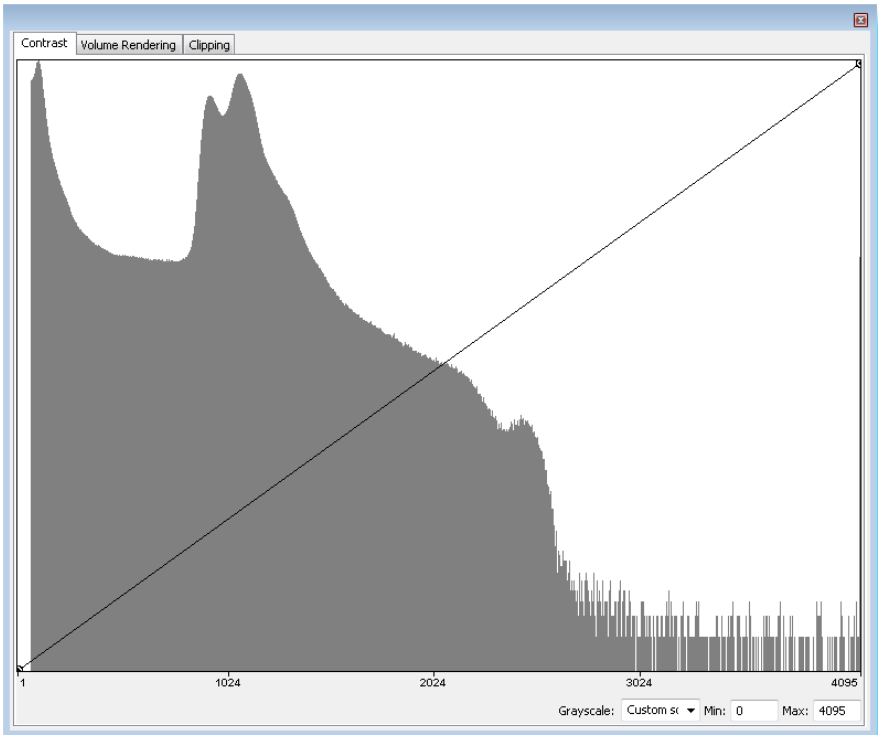

FIGURE 5.13: Histogram of gray scale values of clinical scan

dense tissue. The density in embalmed tissue has increased over that of the living tissue as seen in the peak distribution and rightward skew from the lower soft tissue threshold to more dense tissue (FIG 5.13). This difference between the gray scales means that clinical data is better visualized over cadaveric data because the tissues can be more clearly distinguished.

Lastly, clinical scans are preferred because they provide a snapshot of modern living human data at a wider range of ages. The cadavers were mostly elderly with a mean age of 79. While the clinical scans averaged only 62 years old with a much younger age range. While older adult data is important, it is what is largely documented in the current literature. More young adult and even sub-adult information is needed as they are often the focus of forensic facial approximations.

There are several potential drawbacks to clinical facial data. First, the patients are usually scanned lying down in the scanner albeit only temporarily. It is our recommendation that more upright scanning modalities such as in Cone Beam CT scans and upright CT be explored. As this is a part of our future study, the quality of the resolution of such scans remains to be seen. Another drawback that is often cited is radiation exposure from the CT scan but all of the clinical scans used in this study were conducted for other clinical diagnosis purposes so it is not a concern of this study.

Finally, this study brings to question, if we can use 3D models of the face and skull to capture valuable soft tissue information, are these the only landmarks or depth measurements that we need? Since we have the complete facial geometry, should we capture more information that simple linear landmarks or depth measurements are neglecting? Recent studies in curvature networks (15) are providing interesting alternatives to traditional measurements. We will be exploring that are in our next phases of this continuing project.

It is our belief based on all of our morphometric studies that anatomically accurate 3D models of the skull and face from cadavers and the higher resolution living clinical models will represent a useful dataset to researchers in a variety of fields.

Acknowledgements

We would like to thank all of our collaborators for their work on the facial approximation phase of this project: FBI Visualization Specialist Carl Adrian, Dr. Stephanie Davy-Jow of Liverpool John Moores University (UK), Philippe Faraut of PCF Studios (NY), and FBI Visualization Specialist Wesley Neville. A special thank you to the FBI Forensic Division for allowing their specialists to participate in this study. We would also like to thank Wesley Frusher in USF's College of Engineering for his assistance with the rapid prototyping section of this study. Finally a thank you to the USF Health Imaging Centers, Morsani and South, for

their assistance in the medical imaging portions of this study, particularly Melanie O’Brien and Matthew Woods.

CHAPTER 6

APPLICATIONS, RECOMMENDATIONS FOR FUTURE WORK AND CONCLUSIONS

Applications of Virtual Anatomy

While the development of an anatomically accurate 3D model is valuable, the strength of the 3D imaging and reconstruction lies in the application of the models to different fields. Currently, applications for the various types of 3D data in medicine (1), forensics (2), biometrics (3 - 4), and anatomical education (5 - 6) are expanding.

Medicine

While medical imaging technologies are widely used in clinical medicine for diagnosis, the 3D derivatives such as the anatomical models from those images are largely ignored by practitioners. While mostly used for visualization, the potential to use real anatomical data for medical studies means that the potential for clinical research is limitless. The 3D models developed in these pelvic and craniofacial projects can be used for a variety of clinical applications

such as surgical planning, surgical simulation, biomedical engineering analyses and more. The following is a brief list of current and potential applications of the virtual anatomy dataset that has been developed at the Center for Human Morpho-Informatics Research (CHMR).

Colorectal Surgery

In 2008, the CHMR began a study with the University of South Florida's Division of Colorectal Surgery to 3D reconstruct specific pelvic anatomy such as the pelvic autonomic nerves for use in surgical training.

Colorectal cancer is the third most common cause of cancer and second most common cause of cancer deaths in the United States. It is estimated that nearly 41,000 new cases of rectal cancer were diagnosed in 2008 (7). Radical surgery combined with chemoradiation is regarded as the standard treatment for locally advanced rectal cancer (7 - 9). Moreover, standard surgical therapy for lower rectal cancer includes a total mesorectal excision (TME). This procedure involves removal of the tumor along with the draining lymph nodes.

While potentially curable, rectal cancer treated with surgery is not without complications. Unfortunately, surgery for locally advanced rectal cancer is associated with significant morbidity. The most frequent complications include urinary (7 - 68%) and sexual dysfunction (15 -100%) (10 - 17). The incidence of these complications can be minimized through the proper identification and

understanding of pelvic autonomic structures and their relation to various anatomical and surgical planes. Utilizing the CHMR pelvic data set, a series of cadaveric dissections, and operative experience from our collaborators, we constructed an accurate 3D model of pelvic anatomy. The immediate goal and initial motivation behind this project was to clarify pelvic anatomy for surgeons. Surgeons strive to provide the best technical and oncologic procedures in order to give patients the best possible chance for cure while at the same time maintain their quality of life. An interactive 3D model of the pelvis focusing on the pelvic autonomics and their relation to fascial planes has proven to be an invaluable tool in the operative planning of any pelvic surgery.

This collaboration has won both local and national awards for its application of 3D virtual anatomy for the surgical training and planning for total mesorectal excision. Upon presentation of the study's results at local and national meetings, surgeons are currently reporting a marked reduction in post-operative complications with the new proposed approach.

Obstetrics and Gynecology

In 2009, the CHMR began collaborating with the University of South Florida's Department of Obstetrics and Gynecology and the Division of Uro-gynecology and Pelvic Reconstructive Surgery to explore 3D modeling and reconstruction of pelvic disorders.

The prevalence of female voiding dysfunction increases with age and varies from 2% to 25% (18). Voiding dysfunction may include any or all of the following symptoms: urinary urgency or frequency, poor urinary stream or difficulty with complete emptying, hesitancy, or recurrent UTI (18). Voiding dysfunction may be caused by: surgery, bladder over-distention, inflammation, outflow obstruction, sensory urgency, medications, chronic medical diseases, and psychosomatic factors (18 - 20). Standard therapies for voiding dysfunction include behavior modification with pelvic floor muscle exercises, pharmacologic therapy, biofeedback/external stimulation, or surgical intervention (20). Available surgical interventions include bladder dilation, denervation, botulinum toxin injections, augmentation cystoplasty, and pudendal neuromodulation (20).

Neuromodulation of the pudendal nerve is an FDA-approved, effective and reversible means to addressing chronic voiding dysfunction (20). The pudendal nerve has roots that innervate throughout the pelvic organs, muscles and urethra. Sacral neuromodulation involves placing a lead in the third sacral foramina (S3) to stimulate the pudendal nerve. Placement is usually done through palpation of the posteriorly located SI notch, which is difficult to do in most patients. Using 3D models created by the CHMR from computed tomography scans of the pelvis and a specific pelvimetric toolkit, a series of measurements, angles, and planes were calculated in order to develop a mathematical model for reliable S3 placement that can be replicated via ultrasound imaging pre-operatively.

This collaboration with Division of Uro-gynecological surgery has resulted in several platform presentations at state and national meetings as well as a recently accepted peer-reviewed journal article.

Plastic and Reconstructive Surgery

Another application for the 3D models and data generated by these projects is in the fields of plastic and reconstructive surgery. With the potential of pre-operative medical imaging, plastic surgeons will be able to plan approaches and anatomical modifications on patients (21). In the *Mimics* software, facial implants can be virtually placed and adjusted to test the effect that the implant will have on the face post-operatively. Quantitative comparisons of pre and post-operative modifications will also possible and will provide invaluable research for future surgical training (21).

Additionally with 3D modeling and rapid prototyping, molds of anatomical features such as ears can be created from patient medical scans in cases of traumatic injury such as burns or amputations. Surgeons with the Veterans Administration (VA) hospitals have expressed interest the potential of patient specific models of soldiers with facial trauma for reconstruction. With increased rates of breast cancer in the United States, patients undergoing mastectomies will also be able to have pre-operative 3D models made of their breast anatomy for use later in reconstructive surgery. The applications of 3D modeling and quantitative anatomy for plastic and reconstructive surgery alone are limitless.

Forensic Pathology: Virtopsy

Recent studies have found that Multislice Computed Tomography (MSCT) and Magnetic Resonance Imaging (MRI) can be useful tools in visualizing the internal body for the 3D documentation of disease, injury, and forensic issues (22 - 23). Several forensic researchers have begun to apply these medical imaging modalities to the traditional autopsy. *Virtopsy* (24) is a recent application that uses MSCT, MRI, laser scanning and focused biopsy for a “minimally invasive autopsy”.

The central analysis in any death investigation is the forensic autopsy. Once crime scene evidence has been gathered, bodily remains are removed from the scene and transported to a coroner’s or medical examiner’s office for analysis. There it is the forensic pathologist’s job to document the nature and cause of death. Much of the direction of the forensic case is dependent on the results of pathologist’s final forensic report. The autopsy examination itself is a meticulous study of each organ system beginning with an external inspection of the remains for any signs of trauma or disease. Each bit of evidence is carefully documented and photographed extensively for archival purposes. As the analysis moves internally, every organ is examined grossly, photographed and biopsied for histological sectioning. The entire process can take between one hour and several hours depending on the circumstances of the death, extent of trauma, and amount of physical evidence that has to be logged.

The methodology for the forensic autopsy has changed little in the past 100 years while the demands of modern forensic investigations has changed tremendously in the wake of the Daubert standard (24) and high-profile cases such as the OJ Simpson - Nicole Brown murder trial (25). High crime rates and growing attention on the field have created pressures on the forensic community nationally and internationally to develop alternative methods to assist with standardizing techniques and processing caseloads.

The *Virtopsy* procedure (24) involves a full body CT scan of the remains. CT is used initially because it is the best medical image modality at displaying bone for the documentation of any traumatic injury or metallic implants or fragments (bullets) and overall gross anatomical features quickly. These images are diagnostically reviewed and a list of regions of interest is developed for further study. MRI scans are used more sparingly due to the scan time and the potential of interfering with any metallic objects. MRI, however, is better at examining specific regions of interest shown on CT because it is best for viewing soft tissue and organs. Next, the body is captured in 3D using a laser scanner for the documentation of external pathologies and trauma. Unlike the invasive approach of the traditional autopsy's full body dissection, only select punch biopsies and fluids are taken for histology and biochemical profiles.

One of the biggest benefits of the *Virtopsy* methodology is that it allows for the long-term documentation and archiving of virtual physical evidence. This is

extremely important for use in court for biomechanical studies, the repatriation and timely burial of remains, and simulations or crime scene reconstructions. Further benefits include limited handling of potentially infectious or high-risk cadavers as well as being considerate and observant of concerns held by different cultures and religions. There is momentum amongst the forensic community in support of virtual autopsies, at the very least to augment the traditional exam. As medical imaging costs decline and the methodology is further accepted, *Virtopsy* will likely become a regular essential part of the forensic death investigation.

The CHMR is currently partnered with the Hillsborough County Medical Examiner's Office (FL) to introduce *Virtopsy* procedures to their death investigation cases.

Forensics

Facial approximation or reconstruction, while a useful tool to law enforcement, has long been considered less scientific and more artistic amongst forensic professionals (27). Accurate 3D models of the skull and face are proving useful to forensic artists as well as to law enforcement agencies who have concerns and responsibilities towards maintaining chain of custody of physical evidence. As seen in our studies these models are providing the opportunity to test different facial approximation methodologies (28 - 30).

Results from our studies have been presented at several national conferences such as the American Academy of Forensic Sciences Annual Meetings over the past 3 years with great interest from the forensic community (31 - 35). From our presentations, we have been asked to collaborate on several cases for the Federal Bureau of Investigation and regional Medical Examiner's Offices.

These projects demonstrate the potential for high-end forensic analysis to be conducted remotely without assuming chain of custody of the evidence, which is of great concern in forensic cases. This also allows local law enforcement agencies to have access to experts beyond their geographic location. While there is a wide range of variation between commonly used methods, the benefit of our study findings is that there is an open discussion of the strengths and weaknesses at each stage of the analysis which will in turn increase the understanding and scope of forensic information that can be gleaned from 3D data.

Biometrics

The field of biometrics, or the study of the human form for security or identification purposes, has been growing exponentially over the past few years. Several studies (36 - 38) have expressed the dire need for more 3D data for the study of person specific identification. Much of current biometric research is

focused on facial recognition (39) and therefore large datasets of virtual faces, like the dataset developed at the CHMR are needed to develop mathematical models for identification. Quantitative anatomical models will also be able to provide the opportunity to examine previously unexplored areas in the human anatomy to search for unique patterns in one's body.

Anatomical Education

Anatomists and anthropologists are now able to use the 3D data and models generated in these projects for detecting patterned phenotypic variation between populations (31) and for archival purposes (40). We have also demonstrated the potential for developing new 3D measurement methodologies that test the accuracy of current field standards for osteological analysis.

One unexpected benefit to our studies was the development of a virtual skeletal collection from cadaveric and living CT data. Many universities and research centers have limited access to skeletal material and thus, researchers and students have to travel to institutions such as the Smithsonian Institute for osteological study. These well-known collections are beginning to show their wear from so many researchers handling the remains. It is also increasingly difficult to teach human osteology in labs that have limited resources. Teaching collections are rare as osteological training is becoming more popular. While this project was ongoing, our lab worked with Materialise to test a student version of

the *Mimics Innovation Suite* called Mimics *SE*. It was developed with engineering students in mind, however the CHMR has tested the student edition for virtual osteology laboratories and have created virtual lab exercises for students to become more familiar with our virtual biological profile technique.

With an online global environment expanding daily and a shortage of cadaveric resources for educational purposes, 3D models or virtual anatomy will potentially play a major role in the education of future medical professionals (5). Anatomy, as it has been taught for generations, is in the middle of a forced transition towards computer based learning. 3D virtual anatomy will be able to fill the resource gaps and stimulate a new generation of students.

Recommendations for Future Study

Although we have been successfully demonstrating the effectiveness of applying 3D computer modeling and reconstruction to quantitative anatomical questions, there remain questions still to be answered in our future studies. First, in order to increase the objectivity of our measurement studies we would like to translate all of our 3D models into a fixed Cartesian coordinate system where each model is registered around a specific 0,0,0 (x,y,z) location. This will allow us to further quantify the variation and determine if there are any patterns that can be recognized visually or mathematically. Using this registered data, we intend to conduct more intensive geometric morphometric studies for 3D shape analysis.

While we have extensively duplicated the current field measurements standards for anatomy, physical and forensic anthropology of pelvic and craniofacial anatomy, in light of the results of these studies there is a need to comprehensively review all major bones, especially those used in forensic identification, from a modern human dataset. Additionally, we would like to greatly expand the dataset in order to increase the statistical significance of the studies. This data will help redefine modern standards for the establishment of the biological profile.

Finally, much of our research was focused on traditional landmark based measurements and ‘metricizing’ non-metric indices. One of the major benefits that accurate 3D virtual anatomical models bring is the possibility to expand beyond points or landmarks and examine curves, surfaces, and other data that has not been previously captured. We found in our studies that we were often limited by the lack of comprehensive literature for the pelvic and craniofacial measurements. We would like to explore what type of data can be captured beyond that of point or landmark based data and what that new data tells us about human anatomy.

Conclusions

With exponential increases in computer technology and decreases in medical imaging costs, it is our assertion that there is a transition towards 3D

modeling for research and education and that quantitative virtual anatomy will become a vital tool in anatomical studies. Validated, anatomically accurate 3D models provide for the first time the ability to objectively critique current field standards. With increased pressure on the forensic community to standardize current practices and with malpractice concerns in clinical medicine, methods such as those proposed in these projects will help address these growing issues.

This dissertation set out in the specific aims to address scanning protocols, the development of anatomically accurate computer models, to reexamine morphometric analyses of anatomy, and to apply the results to clinical, research, and educational disciplines. With the 3D transition in mind, this dissertation hopes to contribute to the validation of available technologies, as well as provide additional methodologies for the capture and quantification of 3D volumetric data and 3D anatomically accurate models.

REFERENCES

Chapter 1 References

1. Adams GL, Gansky SA, Miller AJ, Harrell WE, Hatcher DC. (2004) Comparison between traditional 2-Dimensional cephalometry and a 3-dimensional approach on human dry skulls. *American Journal of Orthodontics and Dentofacial Orthopedics*. October; 126:397-409.

2. McLachlan JC. (2004) New Path for Teaching Anatomy: Living Anatomy and Medical Imaging vs. Dissection. *The Anatomical Record (Part B: New Anat.)* 281B:4-5.

3. Tu P, Hartley RI, Lorsnsen WE, Alyassin A, Gupta R, Heier L. (2005) Facial Reconstructions using Flesh Deformation Modes. In Clement JG, Marks MK (Eds.). *Computer-Graphic Facial Reconstruction.* Elsevier Academic Press, MA: 145-162.

4. Turner W, Tu P, Kelliher T, Brown R. (2006) Computer-Aided Forensics: Facial Reconstruction. *Medicine Meets Virtual Reality 14*. J.D. Westwood et al. (Eds.) IOC Press: 550-555.

5. Chang K, Bowyer KW, Sarkar S, Victor B. (2003) Comparison and Combination of Ear and Face Images in Appearance-Based Biometrics. *IEEE Transactions on Pattern Analysis and Machine Intelligence.* Sept; Vol 25 (9); 1160-1165.

6. Patriquin ML, Steyn M, Loth SR. (2005) Metric analysis of sex difference in South African black and white pelves. *Forensic Sci Int*. 14:199-127.

7. Neider GL, Scott JN, Anderson MD. (2000) Using QuickTime Virtual Reality Objects in Computer-Assisted Instruction of Gross Anatomy: *Yorkick—the VR Skull*. *Clinical Anatomy*. 13:287-293.

8. Ciobanu O. (2006) The Use of Computer Aided Design (CAD) Environment in 3D Reconstruction of Anatomic Surfaces. *Medicine Meets Virtual Reality 14*. J.D. Westwood et al. (Eds.) IOC Press: 102 -104.

9. McCraken, Thomas. Ed. (1999) *New Atlas of Human Anatomy*. Barnes & Noble, Inc.

10. Saunders J, O'Malley C. (1950) *The Illustrations from the Works of Andreas Vesalius of Brussels*. Dover Publications, New York.

11. Netter FH. (2006) *Atlas of Human Anatomy*. 4th ed. Philadelphia: Saunders.

12. Keats TE, Sistrom C. (2001) *Atlas of Radiologic Measurement*. 7th edition. Mosby Health Press, MO.

13. Corruccini RS. (1973) Size and Shape in similarity coefficients Based on Metric Characters. *Am J Phys Anthropol*. 38:743-753.

14. Bass WM. (2005) *Human osteology: a laboratory and field manual*. 5th edn. Columbia, MO: Missouri Archaeological Society.

15. King CA, Iscan MY, Loth SR. (1998) Metric and comparative analysis of sexual dimorphism in the Thai femur. *J Forensic Sci*. 43(5): 954-958.

16. Buikstra JE, Ubelaker DH (eds.) (1994) *Standards for Data Collection from Human Skeletal Remains.* Arkansas Archaeological Survey Research Series No. 44.

17. Howells WW. (1937) The Designation of the Principle Anthrometric Landmarks on the Head and Skull. *Am. J. Phys. Anthropol.* 22(3):477-494.

18. Brothwell DR. (1981) *Digging Up Bones* 3rd ed. London: Oxford University Press.

19. Steele DG, Bramblett CA. (1988) *The Anatomy and Biology of the Human Skeleton*. College Station: Texas A&M University Press.

20. Ubelaker DH. (1999) *Human Skeletal Remains, Excavation, Analysis, Interpretation*. 3rd ed., Taraxacum, Washington.

21. Howells WW. (1973) *Cranial variation in man: a study of multivariate analysis of patterns of difference among recent human populations*. Peabody Museum Papers 67:1-259.

22. Howells WW. (1968) Multivariate analysis for the identification of race. In *Personal identification in mass disasters: report of a Seminar, held in Washington D.C. 9-11 December.*:111-121.

23. Howells WW. (1989) *Skull shapes and the map: craniometric analyses in the dispersion of modern Homo*. Peabody Museum Papers 79:1-189.

24. Howells WW. (1995) *Who's Who in Skulls: Ethnic Identification of Crania from Measurements*. Peabody Museum Papers 82:1-120.

25. France, DL. (1994) Observational and Metric Analysis of Sex in the Skeleton. In Forensic Osteology: Advances in the Identification of Human Remains. Kathleen J. Reichs, editors. Charles C. Thomas, Springfield, IL; 163-186.

26. Adams BJ, Byrd JE. (2002) Interobserver variation of selected postcranial skeletal measurements. *J Forensic Sci*;47(6):1193-1202.

27. Ousley SD, Jantz RL. (1996) FORDISC 2.0: *Personal Computer Forensic Discriminant Functions*. University of Tennessee, Knoxville, Tennessee.

28. Ross AH, Williams S. (2008) Testing repeatability and Error of Coordinate Landmark Data Acquired from Crania. *J of Forensic Sci*.; 53(4),1-4.

29. Swennen GR, Schutyser F, Barth EL, De Groeve P, De Mey A. (2006) A New Method of 3-D Cephalometry Pat I: The Anatomic Cartesian 3-D Reference System. *The Journal of Craniofacial Surgery*. Vol 17(2): 314-325.

30. Corruccini RS.. (1987) Shape in Morphometrics: Comparative Analyses. *Am J Phys Anthropol.* 73:289-303.

31. Bookstein FL. (1991) *Morphometric Tools for Landmark Data: Geometry and Biology*. Cambridge University Press, Cambridge.

32. Lestrel, PE. (2000) *Morphometrics for the Life Sciences*. World Scientific Publishing Co., Singapore.

33. O'Higgins P, Strand Vidarsdottir U. (1999) New Approaches to the quantitative analysis of craniofacial growth and variation. In: *Human Growth in the Past: Studies from Bone and Teeth*. Hoppa R, Fitzgerald C, (eds.) Cambridge, Cambridge University Press.

34. Valeri C, Cole T, Lele S, Richtsmeier J. (1998) Capturing data from three dimensional surfaces using fuzzy landmarks. *Am. J. Phys. Anthropol.* 107:113-124.

35. Udupa JK, Herman GT (eds). (2000) *3D Imaging in Medicine* 2nd edition. CRC Press, FL.

36. "Wilhelm Conrad Röntgen - Biography". (2008) Nobelprize.org. Accessed 22 Oct 2008 http://nobelprize.org/nobel_prizes/physics/laureates/1901/rontgen-bio.html

37. Wilhelm Conrad Röntgen (1967) From *Nobel Lectures, Physics 1901-1921*, Elsevier Publishing Company, Amsterdam.

38. Enderle JD, Blanchard SM, Brozino JD. (2005) *Introduction to Biomedical Engineering*. 2nd edition. Elsevier Academic Press, UK

39. Butler P, Mitchell AW, Ellis H (eds). (1999) *Applied Radiological Anatomy*. Cambridge University Press, UK.

40. Schaller S, Wildberger JE, Raupach R, Niethammer M, Klingenbeck-Regn K, Flohr T. (2003) Spatial Domain Filtering for Fast Modification of the Tradeoff Between Image Sharpness and Pixel Noise in Computed Tomography. *IEEE Transactions on Medical Imaging*. July 22(7): 846-853.

41. Vaidyanath S, Temkin B. (2006) Registration and Segmentation for the High Resolution Visible Human Male Images. *Medicine Meets Virtual Reality 14*. J.D. Westwood et al. (Eds.) IOC Press: 556-558.

42. Ackerman MJ. (1998) The visible human project. *Proc IEEE* 86:504-511.

43. Spitzer V, Ackerman MJ, Scherzing AL, Whitlock D. (1996) The visible human male: A technical report. *JAMA* Vol.3: 118-130.

44. Park, JS, et al. (2006) Visible Korean Human: its Techniques and Applications. Clinical Anatomy; 3:216-225.

45. Zhang, SX, et al. (2006) Chinese Visible Human Project. Clinical Anatomy, 19:204-215.

Chapter 2 References

1. Waitzman, A.A., Posnick, J.C., Armstrong, D.C. & Pron, G.E. (1992). Craniofacial, Skeletal Measurements Based on Computed Tomography: Part 1. Accuracy and Reproducibility, *Cleft Palate Craniofacial Journal*, 29(2), 112-117.

2. Nawaratne, S., Fabiny, R., Brien, J.E., Zalcberg, J., Cosolo,W., Whan, A. & Morgan, D.J. (1997) Accuracy of Volume Measurement Using Helical CT, *Journal of Computer Assisted Tomography*, 21(3), 481-486.

3. Schaller S, Wildberger JE, Raupach R, Niethammer M, Klingenbeck-Regn K, Flohr T. (2003) Spatial Domain Filtering for Fast Modification of the Tradeoff Between Image Sharpness and Pixel Noise in Computed Tomography. *IEEE Transactions on Medical Imaging*. July 22(7): 846-853.

4. Buikstra JE, Ubelaker DH (eds.) (1994) *Standards for Data Collection from Human Skeletal Remains.* Arkansas Archaeological Survey Research Series No. 44.

5. Hildebolt CF, Vannier MW. (1988) Three-Dimensional Measurement Accuracy of Skull Surface Landmarks. *Am J Phys Anthropol*. 76:497-503.

6. Molto JE. (1979) The Assessment and Meaning of Intraobserver Error in Population Studies Based on Discontinuous Cranial Traits. *Am J Phys Anthropol.* 51:333-344.

7. Perez-Perez, A. Alesan and L.Roca. (1990) Measurement error: Inter- and Intraobserver Variability. An Empiric Study. *International Journal of Anthropology*. Vol 5, Number 2, 129-135.

8. Rogers T, Saunders SR. (1997) Accuracy of sex determination using morphological traits of the human pelvis. *J Forensic Sci.* ;39:1047-56.

9. Decker SJ. (2004) 'Metricizing' Non-Metric Craniofacial Traits: Application of Three Dimensional Geometric Morphometrics Analysis to Ancestral Identification. [thesis] Las Vegas (NV): University of Nevada, Las Vegas.

10. Decker SJ, Ford JM, Hilbelink DR. (2009) Maintaining Custody: A virtual method of creating accurate reproductions of skeletal remains for facial approximation (abstract). In: *Proceedings of the American Academy of Forensic Sciences 61st Annual Meeting*; 2009 Feb 16-21; Denver, CO: (15)334.

Chapter 3 References

1. Daubert v. Merrell Dow Pharmaceuticals, Inc., (1993) 509 U.S. 579, (113 US S.Ct. 2786)

2. Grivas CR, Komar DA. (2008) Kumho, Daubert, and the nature of scientific inquiry: implications for forensic anthropology. *J Forensic Sci*;53(4):771–6.

3. National Academy of Sciences Website. 'Badly Fragmented' Forensic science system needs overhaul; Evidence to support reliability of many techniques is lacking. Available at: http://www8.nationalacademies.org/onpinews/newsitem.aspx?RecordID=12589 (accessed July 1, 2009).

4. Bass WM. (2005) *Human osteology: a laboratory and field manual.* 5th edn. Columbia, MO: Missouri Archaeological Society.

5. Eliopoulos C, Lagiab A, Manolis S. (2007) A modern, documented human skeletal collection from Greece. *HOMO—J Comp Human Biol*; 58: 221–228

6. Komar DA, Grivas C. (2008) "Manufactured Populations: What Do Contemporary Reference Skeletal Collections Represent?" *Am J Phys Anthropol*;137(2): 224-233.

7. L'Abbe EN, Loots M, Meiring JH. (2005) The Pretoria Bone Collection: A modern South African skeletal sample. *HOMO - J Comp Human Biol*. August; 56(2):197-205.

8. Dabbs GR,Moore-Jansen PH. (2010) A Method for Estimating Sex Using Metric Analysis of the Scapula. *J Forensic Sci.*;55(1):149-152.

9. Bidmos MA, Asala SA. (2003) Discriminant function sexing of the calcaneus of the South African whites. *J Forensic Sci* 48:1213–1218.

10. Cologlu SA, Işçan MY, Yavuz FM and Huseyin S. (1998) Sex determination from the ribs of contemporary Turks, *J Forensic Sci*.; 43:273–276.

11. Oettle AC and Steyn M. (2000) Age estimation from sternal ends of ribs by phase analysis in South African Blacks, *J Forensic Sci*.; 45:1071–1079.

12. Steyn M, _Iscan MY. (1999) Osteometric variation in the humerus: sexual dimorphism in South Africans. *Forensic Sci Int* 106:77–85.

13. Bruzek J. (2002) A method for visual determination of sex, using the human hip bone. *Am J of Phys Anthropol*; 117:157-168.

14. Dar G and Hershkovitz I. (2006) Sacroiliac joint bridging: simple and reliable criteria for sexing the skeleton. *J Forensic Sci*;51(3):480-483.

15. Gonzlez PN, Bernal V, Perez SI. (2009) Geometric morphometric approach to sex estimation of human pelvis. *Forensic Sci Int*; 189:68–74.

16. Buiskstra JE, Ubleaker DH, editors. (1994) Standards for data collection from human skeletal remains: proceedings of a seminar at the Field Museum of Natural History. Fayetteville, AR: Arkansas Archaeological Survey Publications.

17. Moore-Jansen PM, Ousley SD, Jantz RL. (1994) Data collection procedures for forensic skeletal material. Report of Investigations no. 48. Knoxville, TN: University of Tennessee, Department of Anthropology.

18. Decker SJ, Ford JM, Hilbelink DR. (2009) Maintaining Custody: A virtual method of creating accurate reproductions of skeletal remains for facial approximation. Proceedings of the American Academy of Forensic Sciences 61st Annual Meeting; Feb 16-21; Denver, CO: (15)334.

19. Ousley SD, Jantz RL. (1998) The Forensic Data Base: documenting skeletal trends in the United States. In Reichs KJ, editor. *Forensic Osteology: Advances in the Identification of Human remains*. Springfield (IL): Charles C Thomas,: 441-458.

20. Decker SJ, Ford JM, Hoegstrom EJ, Hilbelink DR. **(**2008) Virtual Anatomy: Three-dimensional computer modeling and measurement of human cranial anatomy. Proceedings of the American Academy of Forensic Sciences 60th Annual Meeting; Feb 19-23; Washington, D.C.: (14)312.

21. Ramsthaler F, Kettner M, Gehl A, Verhoff MA. (2010) Digital forensic osteology: morphological sexing of skeletal remains using volume-rendered cranial CT scans. *Forensic Sci Int*;195:148-152.

22. Robinson C, Eisma R, Morgan B, Jeffery A, Graham E, Black S, et al. (2008) Anthropological measurement of lower limb and foot bones using multi-detector computed tomography. *J Forensic Sci*;53(6):1289-1295.

23. Rogers T, Saunders SR. (1997) Accuracy of sex determination using morphological traits of the human pelvis. *J Forensic Sci*;39:1047-56.

24. France, DL. (1994) Observational and Metric Analysis of Sex in the Skeleton. In *Forensic Osteology: Advances in the Identification of Human Remains*. Kathleen J. Reichs, editors. Charles C. Thomas, Springfield, IL; 163-186.

25. Adams BJ, Byrd JE. (2002) Interobserver variation of selected postcranial skeletal measurements. *J Forensic Sci*:47(6):1193-1202.

26. Patriquin ML, Steyn M, Loth SR. (2005) Metric analysis of sex differences in South African black and white pelves. *Forensic Sci Int*;147:119-127.

27. Rissech C, Garcia M, Malgosa A. (2003) Sex and age diagnosis by ischium morphometric analysis. *Forensic Sci Int*; 135:188–196.

28. Steyn M and Iscan MY. (2008) Metric sex determination from the pelvis in modern Greeks. *Forensic Sci Int*; 179:86.e1–86.e6

29. Steyn M and Patriquin ML. (2009) Osteometric sex determination from the pelvis—Does population specificity matter? *Forensic Sci Int*; 191:113.e1–113.e5.

30. Wilson LA, MacLeod N, Humphrey LT. (2008) Morphometric criteria for sexing juvenile human skeletons using the ilium. *J Forensic Sci*;53(2)269-278.

31. Anderson BE. (1990) Ventral arc of the os pubis: anatomical and developmental considerations. *Am J Phys Anthropol*;83:449-58.

32. MacLaughlin, S. M. and Bruce, M. F. (1990) The accuracy of sex identification in European skeletal remains using the Phenice characters. *J Forensic Sci*.;35:1384-92.

33. Phenice TW. (1969) A newly developed visual method of sexing the os pubis. *Am J Phys Anthropol*.;30:297-302.

34. Ubelaker DH and Volk CG. (2002) A Test of the Phenice Method for the Estimation of Sex. *J Forensic Sci*.;47(1):19–24.

35. Vetter JH, Moore-Jansen PH. (2009) Sexual Dimorphism of the Iliac Crest: A Quantitative Approach. Proceedings of the 5th Annual GRASP Symposium, Wichita State University; 64-65.

36. Walker PL. (2005) Greater Sciatic Notch Morphology: Sex, Age, and Population Differences. *Am J of Phys Anthropol*; 127:385-391.

37. Decker SJ. (2004) 'Metricizing' Non-Metric Craniofacial Traits: Application of Three Dimensional Geometric Morphometrics Analysis to Ancestral Identification. [thesis] Las Vegas (NV): University of Nevada, Las Vegas.

38. Cunningham FG, et al. (2009) *Williams Obstetrics*, 23nd edition. New York: McGraw-Hill,.

39. Drake RL, Vogl AW, Mitchell AVM. (2010) *Gray's Anatomy for Students*, 2nd ed. Philadelphia: Churchill Livingstone,.

40. Netter FH. (2006) *Atlas of Human Anatomy*. 4th ed. Philadelphia: Saunders.

41. Ousley SD, Jantz RL. (2005) FORDISC 3.0: Personal computer forensic discriminant functions [computer program]. Knoxville, TN: University of Tennessee.

42. Thali MJ, Dirnhofer R, Vock P. (2009) *The Virtopsy Approach: 3D Optical and Radiological Scanning and Reconstruction in Forensic Medicine.* CRC Press, FL.

Chapter 4 References

1. Ackerman MJ. (1998) The visible human project. *Proc IEEE* 86:504-511.

2. Vaidyanath S, Temkin B. (2006) Registration and Segmentation for the High Resolution Visible Human Male Images. *Medicine Meets Virtual Reality 14*. J.D. Westwood et al. (Eds.) IOC Press: 556-558.

3. Ousley SD, Jantz RL. (2005) FORDISC 3.0: Personal computer forensic discriminant functions [computer program]. Knoxville, TN: University of Tennessee.

4. Bass WM. (2005) *Human osteology: a laboratory and field manual*. 5th edn. Columbia, MO: Missouri Archaeological Society.

5. Holland TD. (1986) Sex determination of fragmentary crania by analysis of the cranial base. *Am J Phys Anthropol*;70:203–8.

6. Meindl RS, Lovejoy CO, Mensford RS, Don Carlos L. (1985) Accuracy and direction of error in the sexing of the skeleton: implication for paleodemography. *Am J Phys Anthropol* 68:79–85.

7. Buikstra JE, Ubelaker DH (eds.) (1994) *Standards for Data Collection from Human Skeletal Remains.* Arkansas Archaeological Survey Research Series No. 44.

8. Decker SJ, Ford JM, Hoegstrom EJ, Hilbelink DR. **(**2008) Virtual Anatomy: Three-dimensional computer modeling and measurement of human cranial anatomy. Proceedings of the American Academy of Forensic Sciences 60th Annual Meeting; Feb 19-23; Washington, D.C.: (14)312.

9. France, DL. (1994) Observational and Metric Analysis of Sex in the Skeleton. In *Forensic Osteology: Advances in the Identification of Human Remains.* Kathleen J. Reichs, editors. Charles C. Thomas, Springfield, IL; 163-186.

10. Clement JG, Marks MK (Eds.). (2005) *Computer-Graphic Facial Reconstruction.* Elsevier Academic Press, MA.

Chapter 5 References

1. Davy SL, Gilbert T, Schofield D, Evison MP. (2005) Forensic Facial Reconstruction Using Computer Modeling Software. In Clement JG, Marks MK (Eds.). (2005) *Computer-Graphic Facial Reconstruction.* Elsevier Academic Press, MA: 183-196.

2. Linney A, Coombes AM. (1998) Computer modeling of facial form. In Clement JG, Ranson DL. *Craniofacial Identification in Forensic Medicine*. Arnold Press, UK: 187-199.

3. Taylor KT. (2001) *Forensic Art and Illustration.* CRC Press, FL.

4. Wilkinson C. (2004) *Forensic Facial Reconstruction*. Cambridge Press, UK.

5. Domaracki M, Stephan CN. (2006) Facial Soft Tissue Thicknesses in Australian Adult Cadavers. *J Forensic Sci* Vol 51 (1): 5-10.

6. Stephan CN, Simpson EK. (2008) Facial Soft Tissue Depths in Craniofacial Identification (Part 1): An Analytical Review of the Published Adult Data. *J Forensic Sci*. Vol 53 (6) 1257- 1272.

7. Stephan CN, Simpson EK. (2008) Facial Soft Tissue Depths in Craniofacial Identification (Part 2): An Analytical Review of the Published Sub-Adult Data. *J Forensic Sci*. Vol 53 (6) 1273- 1279.

8. Shaw RB, Katzel EB, et al. (2010) Aging of the mandible and its aesthetic implications. *Plastic and Reconstructive Surgery* Vol. 125(1)332-342.

9. Clement JG, Marks MK (Eds.). (2005) *Computer-Graphic Facial Reconstruction.* Elsevier Academic Press, MA.

10. Tu P, Hartley RI, Lorsnsen WE, Alyassin A, Gupta R, Heier L. (2005) Facial Reconstructions using Flesh Deformation Modes. In Clement JG, Marks MK (Eds.). *Computer-Graphic Facial Reconstruction.* Elsevier Academic Press, MA: 145-162.

11. Turner W, Tu P, Kelliher T, Brown R. (2006) Computer-Aided Forensics: Facial Reconstruction. *Medicine Meets Virtual Reality 14*. J.D. Westwood et al. (Eds.) IOC Press: 550-555.

12. Linney A, Coombes AM. (1998) Computer modeling of facial form. In Clement JG, Ranson DL. *Craniofacial Identification in Forensic Medicine*. Arnold Press, UK: 187-199.

13. Chang K, Bowyer KW, Sarkar S, Victor B. (2003) Comparison and Combination of Ear and Face Images in Appearance-Based Biometrics. *IEEE Transactions on Pattern Analysis and Machine Intelligence.* Sept; Vol 25 (9); 1160-1165.

14. Swennen GR, Schutyser F, Barth EL, De Groeve P, De Mey A. (2006) A New Method of 3-D Cephalometry Pat I: The Anatomic Cartesian 3-D Reference System. *The Journal of Craniofacial Surgery*. Vol 17(2): 314-325.

15. Razdan A, Bae MS. (2003) A Hybrid Approach to Feature Segmentation of 3-Dimensional Meshes, *Computer Aided Design*, Vol. 35, No. 9, August, pp. 783-790.

16. Decker SJ, Hilbelink, DR, Hoegstrom, EJ, Ford, JM, Adrian, C, Davy-Jow, SL, Faraut, PF. (2008) Who is this Person? A Comparison Study of 3D Facial Approximation Methods (abstract). In: *Proceedings of the American Academy of Forensic Sciences 60th Annual Meeting*; 2008 Feb 19-23; Washington, D.C.: (14)338.

17. Decker SJ, Ford JM, Hilbelink DR. (2009) Maintaining Custody: A virtual method of creating accurate reproductions of skeletal remains for facial approximation (abstract). In: *Proceedings of the American Academy of Forensic Sciences 61st Annual Meeting*; 2009 Feb 16-21; Denver, CO: (15)334.

Chapter 6 References

1. Udupa JK, Herman GT (eds). (2000) *3D Imaging in Medicine* 2nd edition. CRC Press, FL.

2. Linney A, Coombes AM. (1998) Computer modeling of facial form. In Clement JG, Ranson DL. *Craniofacial Identification in Forensic Medicine*. Arnold Press, UK: 187-199.

3. Chang K, Bowyer KW, Sarkar S, Victor B. (2003) Comparison and Combination of Ear and Face Images in Appearance-Based Biometrics. *IEEE Transactions on Pattern Analysis and Machine Intelligence.* Sept; Vol 25 (9); 1160-1165.

4. Turner W, Tu P, Kelliher T, Brown R. (2006) Computer-Aided Forensics: Facial Reconstruction. *Medicine Meets Virtual Reality 14*. J.D. Westwood et al. (Eds.) IOC Press: 550-555.

5. McLachlan JC. (2004) New Path for Teaching Anatomy: Living Anatomy and Medical Imaging vs. Dissection. *The Anatomical Record (Part B: New Anat.)* 281B:4-5.

6. Neider GL, Scott JN, Anderson MD. (2000) Using QuickTime Virtual Reality Objects in Computer-Assisted Instruction of Gross Anatomy: *Yorkick—the VR Skull*. *Clinical Anatomy*. 13:287-293.

7. Cancer Facts and Figures (2008). *American Cancer Society Report* 2008.

8. Adjuvant therapy for patients with colon and rectum cancer. (1990) ACS Consensus Statement; 8:1-25.

9. MacFarlane JK, Ryall RD, Heald RJ. (1993) Mesorectal excision for rectal cancer. *Lancet*; 341:457-60.

10. Enker WE, Thaler HT, Cranor ML, Polyak T. (1995) Total mesorectal excision in the operative treatment of carcinoma of the rectum. *J Am Coll Surg*; 181:335-46.

11. Zaheer S, Pemberton JH, Farouk R, Dozois RR, Wolff BG, Ilstrup D. (1998) Surgical treatment of adenocarcinoma of the rectum. *Ann Surg*; 227:800-11.

12. Balslev I, Harling H. (1983) Sexual dysfunction following operation for carcinoma of the rectum. *Dis Colon Rectum*; 26:785-8.

13. Havenga K, Enker WE, McDermott K, Cohen AM, Minsky BD, Guillem J. (1996) Male and female sexual and urinary function after total mesorectal excision with autonomic nerve preservation for carcinoma of the rectum. *J Am Coll Surg*; 182:495-502.

14. Hojo K, Sawada T, Moriya Y. (1989) An analysis of survival and voiding, sexual function after wide iliopelvic lymphadenectomy in patients with carcinoma of the rectum, compared with conventional lymphadenectomy. *Dis Colon Rectum*; 32:128-33.

15. Longo WE, Virgo KS, Johnson FE, Wade TP, (1998) Vernava AM, Phelan MA, et al. Outcome after proctectomy for rectal cancer in Department of Veterans Affairs Hospitals: a report from the National Surgical Quality Improvement Program. *Ann Surg*; 228:64-70.

16. Neal DE, Williams NS, Johnston D. (1981) A prospective study of bladder function before and after sphincter-saving resections for low carcinoma of the rectum. *Br J Urol*; 53:558-64.

17. Rothenberger DA, Wong WD. (1992) Abdominoperineal resection for adenocarcinoma of the low rectum. *World J Surg*; 16:478-85.

18. Doumouchtsis SK, Jeffery S, Fynes M. Female voiding dysfunction. (2008) *Obstet Gynecol Surv*;63:519-26.

19. Rittenmeyer H. (2008) Sacral nerve neuromodulation (InterStim). Part I: Review of the InterStim system. *Urol Nurs*;28:15-20.

20. Groenendijk PM, Lycklama a Nyeholt AA, Heesakkers JP, et al. (2008) Urodynamic evaluation of sacral neuromodulation for urge urinary incontinence. *BJU Int*;101:325-9.

21. Shaw RB, Katzel EB, et al. (2010) Aging of the mandible and its aesthetic implications. *Plastic and Reconstructive Surgery* Vol. 125(1)332-342.

22. Bolliger S, Thali M, Ross S, Buck U, Naether S, Vock P. (2008) Virtual autopsy using imaging: bridging radiologic and forensic sciences. A review of the Virtopsy and similar projects. *European Radiology*. 18: 273-282.

23. Yen K, Lovblad KO, Scheurer E, Ozdoba A, Thali M, et al. (2007) Post-mortem forensic neuroimaging: Correlation of MSCT and MRI findings with autopsy results. *Foren Sci Int*. 173: 21-35.

24. Thali M, Yen K, Schweitzer W, Vock P, et al. (2003) Virtopsy, a New Imaging Horizon in Forensic Pathology: Virtual Autopsy by Postmortem Multislice Computer Tomography (MSCT) and Magnetic Resonance Imaging (MRI) – a Feasibility Study. *J of Forensic Sci.* Vol 48 (2).

25. *Daubert vs. Merrell Dow Pharmaceuticals* (113 US S.Ct. 2786)

26. Lynch, M. & Jasanoff, S. (1998). Contested Identities: Science, Law and Forensic Practice, *Social Studies of Science*, 28(5-6), 675-686.

27. Davy SL, Gilbert T, Schofield D, Evison MP. (2005) Forensic Facial Reconstruction Using Computer Modeling Software. In Clement JG, Marks MK (Eds.). (2005) *Computer-Graphic Facial Reconstruction.* Elsevier Academic Press, MA: 183-196.

28. Linney A, Coombes AM. (1998) Computer modeling of facial form. In Clement JG, Ranson DL. *Craniofacial Identification in Forensic Medicine*. Arnold Press, UK: 187-199.

29. Wilkinson C. (2004) *Forensic Facial Reconstruction*. Cambridge Press, UK.

30. Taylor KT. (2001) *Forensic Art and Illustration.* CRC Press, FL.

31. Decker SJ. (2004) 'Metricizing' Non-metric Craniofacial Traits: Application of Three Dimensional Geometric Morphometric Analysis to Ancestral Identification. Thesis, University of Nevada, Las Vegas.

32. Decker SJ, Ford JM, Hilbelink DR. (2009) Maintaining Custody: A virtual method of creating accurate reproductions of skeletal remains for facial approximation (abstract). In: *Proceedings of the American Academy of Forensic Sciences 61st Annual Meeting*; 2009 Feb 16-21; Denver, CO: (15)334.

33. Decker SJ, Hilbelink, DR, Hoegstrom, EJ, Ford, JM, Adrian, C, Davy-Jow, SL, Faraut, PF. (2008) Who is this Person? A Comparison Study of 3D Facial Approximation Methods (abstract). In: *Proceedings of the American Academy of Forensic Sciences 60th Annual Meeting*; 2008 Feb 19-23; Washington, D.C.: (14)338.

34. Decker SJ, Davy-Jow SL, Ford JM, Hilbelink DR. (2009) Virtual Forensic Anthropology: applying radiology to the forensic sciences. In: *Proceedings of the Radiological Sciences of North America 2009 95th Scientific Assembly and Annual Meeting*: 2009 Nov: Chicago, IL.

35. Decker SJ, Davy-Jow SL, Ford JM, Hilbelink DR (In Press) Virtual Sex Determination: Metric and non-metric traits of the adult pelvis from 3D computed tomography (CT) models. *J of Forensic Sci.*

36. K. Chang, K. W. Bowyer, S. Sarkar, and B. Victor, (2003) "Comparison and Combination of Ear and Face Images In Appearance-Based Biometrics," *IEEE Transactions on Pattern Analysis and Machine Intelligence*, vol. 25, no. 9, pp. 1160–1165.

37. Tu P, Hartley RI, Lorsnsen WE, Alyassin A, Gupta R, Heier L. (2005) Facial Reconstructions using Flesh Deformation Modes. In Clement JG, Marks MK (Eds.). *Computer-Graphic Facial Reconstruction.* Elsevier Academic Press, MA: 145-162.

38. Turner W, Tu P, Kelliher T, Brown R. (2006) Computer-Aided Forensics: Facial Reconstruction. *Medicine Meets Virtual Reality 14*. J.D. Westwood et al. (Eds.) IOC Press: 550-555.

39. Mohanty PK, Sarkar S, Phillips PJ, Kasturi R, "Subspace Approximation of Face Recognition Algorithms: An Empirical Study," *IEEE Transactions on Information Forensics & Security*, vol. 3, no. 4, pp. 734—748, Dec. 2008.

40. Ousley S, McKeown AH. (2001) Three dimensional digitizing of human skulls as an archival procedure. In *Human remains: Conservation, retrieval, and analysis: Proceedings of a Conference held in Williamsburg, VA.*, 1999. Bar International Series 934.

APPENDICES

APPENDIX A

ARTICLES

Virtual determination of sex: Metric and non-metric traits of the adult pelvis from 3D computed tomography (CT) models. Decker SJ, Davy-Jow SL, Ford JM, Hilbelink Dr. *Journal of Forensic Sciences*. 2010, In Press.

A virtual model for ultrasound guided sacral neuromodulator placement. McCullough M, Decker SJ, Ford JM, Davy-Jow SL, Hilbelink DR, Hart S. *Female Pelvic Medicine and Reconstructive Surgery.* 2010, In Press.

Who is this Person? The application of modern computer technologies to the emerging field of Virtual Forensic Anthropology. Decker SJ, Davy-Jow SL, Ford JM, Hilbelink DR. 2010. *Mimics Innovations Awards*. Last Accessed August 12, 2010. http://www.materialise.com/materialise/view/en/3145574 Mimics+Innovation+Awards+2010.html

APPENDIX B

BOOK CHAPTER

Virtual Forensic Anthropology: Applications of advanced computer graphics technology to the identification of human remains. Davy-Jow SL, Decker SJ, Schofield D. In *Handbook of Research on Practices and Outcomes in Virtual Worlds and Environments.* Harrison Yang and Steve Yuen (editors). 2010, In Press.

APPENDIX C

POSTER AND PLATFORM PRESENTATIONS

July 2010 American Association of Clinical Anatomists: 27th Annual Meeting, Platform Presentation: Cadavers as models: Putting the best face forward? Decker SJ, Ford JM, Hilbelink DR.

American Association of Clinical Anatomists: 27th Annual Meeting, Tech Fair Presentation: Creation of 3D Finite Element Hip Model from the Visible Human Male. Ford JM, Decker SJ, Hilbelink DR.

American Association of Clinical Anatomists: 27th Annual Meeting, Platform Presentation: Cadavers: virtually necessary? Hilbelink DR, Decker SJ, Ford JM.

February 2010 American Academy of Forensic Sciences: 62nd Annual Meeting, Platform Presentation: Virtual Sex: Phenice and Metrics of the Pelvis From 3D Computed Tomography (CT) Models. Decker SJ, Davy-Jow SL, Ford JM, Hilbelink DR

APPENDIX C (Continued)

November 2009 Radiological Sciences of North America 2009 95th Scientific Assembly and Annual Meeting. Educational Session: Detailed 3D male pelvis for Total Mesorectal Excision education and training. Ford JM, Decker SJ, Hilbelink DR, Sanchez J, Krieger B, Marcet J.

Radiological Sciences of North America 2009 95th Scientific Assembly and Annual Meeting. Scientific Session: Virtual Forensic Anthropology: applying radiology to the forensic sciences. Decker SJ, Davy-Jow SL, Ford JM, Hilbelink DR.

April 2009 Federation of American Societies for Experimental Biology 2009 Annual Meeting (American Association of Anatomists) Platform Presentation: Surgical anatomy of the male pelvis: a 3D model based on the Visible Human Project. Sanchez JE, Krieger BR, Marcet JE, Ford JM, Decker SJ, Hilbelink DR.

Federation of American Societies for Experimental Biology 2009 Annual Meeting (American Association of Anatomists) Poster Presentation: Virtual Osteology: Developing the biological profile of the 3D Visible Human Male Skeleton. Ford JM, Decker SJ, Hilbelink DR.

APPENDIX C (Continued)

Mediterranean Society of Pelvic Floor Disorders and Coloprotcology 2009 7th Annual Meeting. Platform Presentation: Defining the Anatomy of Total Mesorectal Excision: An Integrated Approach Using Operative Experience, Cadaveric Dissection, and 3D Modeling. Sanchez JE, Krieger BR, Marcet JE, Decker SJ, Ford JM, Hilbelink DR.

February 2009 USF Health Research Day. Poster Presentation: Surgical anatomy of the male pelvis: a 3D model based on the Visible Human Project. Sanchez JE, Krieger BR, Marcet JE, Decker SJ, Ford JM, Hilbelink DR. * Awarded Best Resident Interdisciplinary Study

American Academy of Forensic Sciences: 61st Annual Meeting, Platform Presentation: SOBER: A virtual collaboratorium for Synchronous Online Biomedical Education and Research. Decker SJ, Ford JM, Davy-Jow SL, Hilbelink A, Hilbelink DR.

American Academy of Forensic Sciences: 61st Annual Meeting, Platform Presentation: Maintaining Custody: A virtual method of creating accurate reproductions of skeletal remains for facial approximation. Decker SJ, Ford JM, Hilbelink DR.

APPENDIX C (Continued)

American Academy of Forensic Sciences: 61st Annual Meeting, Poster Presentation: Three-dimensional computer modeling and anthropological assessment of the National Library of Medicine's Visible Human Male. Decker SJ, Ford JM, Hilbelink DR.

March 2008 International Association of Forensic and & Security Metrology Annual Meeting: Session Symposium: "Who is this Person? Person Specific Identification with Three-Dimensional Anatomy" SJ Decker, DR Hilbelink, EJ Hoegstrom, JM Ford.

February 2008 American Academy of Forensic Sciences: 60th Annual Meeting, Platform Presentation: "Who is this Person? A Comparison Study of 3D Facial Approximation Methods." SJ Decker, DR Hilbelink, EJ Hoegstrom, JM Ford, C Adrian, SL Davy-Jow, and P Faraut.

AAFS Poster Presentation: "Virtual Anatomy: Three-dimensional computer modeling and measurement of human cranial anatomy." SJ Decker, JM Ford, DR Hilbelink, EJ Hoegstrom.

APPENDIX C (Continued)

June 2007 American Association of Clinical Anatomists: 24th Annual Meeting Platform Presentation: "Three-dimensional computer modeling and measurement of human cranial anatomy." Decker, Summer J.,[1] Don R. Hilbelink,[1] and Eric J. Hoegstrom.[2] [1]Department of Pathology and Cell Biology, University of South Florida College of Medicine, [2]Department of Chemical Engineering, University of South Florida College of Engineering, Tampa, FL.

AACA Poster Presentation: "Who is this person? a comparison of facial approximation methods." Decker, Summer J.,[1] Don R. Hilbelink,[1] Eric J. Hoegstrom,[2] Carl Adrian,[3] Stephanie L. Davy-Jow,[4] Wesley W. Neville.[3] [1]Department of Pathology and Cell Biology, University of South Florida College of Medicine, [2]Department of Chemical Engineering, University of South Florida College of Engineering, Tampa, FL. [3]Special Projects Unit, Federal Bureau of Investigation. [4]Department of Archaeology, University of Sheffield, Sheffield, UK.

ABOUT THE AUTHOR

Summer Decker received a Dual Baccalaureate in Anthropology and Spanish in December 2001 from the University of Nevada, Las Vegas (UNLV). She obtained her Master's in Physical Anthropology (Forensics) from UNLV in 2004. After teaching at Florida State College of Jacksonville for several years, she came to the University of South Florida College of Medicine to complete the Master's in Biomedical Ethics and Medical Humanities (2007). In the fall of 2007, she began pursuing her doctorate while working as a teaching assistant and medical researcher in the Center for Human Morpho-Informatics Research (CHMR) where she currently works.

While working at the CHMR, Summer has had opportunities to work on unique research projects with collaborators from around the world in gross anatomy, biomedical engineering, various clinical medical fields, art, biometrics and forensic pathology and anthropology. Several of these projects have won national and international awards and generated numerous peer-reviewed publications. She has continued to work on forensic casework for local, state and federal law enforcements agencies with positive identifications based on her dissertation work.